THE DEVELOPMENT OF SUSTAINABLE HYDROMETALLURGICAL PROCESSES FOR THE RECOVERY OF PRECIOUS METAL

A Thesis Submitted to the College of

Graduate and Postdoctoral Studies

in Partial Fulfilment of the Requirements for

the Degree of Doctor of Philosophy in the

Department of Chemical and Biological Engineering

University of Saskatchewan

Saskatoon, Saskatchewan

By

Afolabi Fatai Ayeni

PERMISSION TO USE

In presenting this thesis in partial fulfillment of the requirements for a Doctor of Philosophy Degree from the University of Saskatchewan, I agree that the libraries of this University may make this thesis freely available for inspection. I further agree that permission for copying of this thesis in any manner, in whole or in part, for scholarly purpose may be granted by the professors who supervised my thesis work or, in their absence, by the Head of the Department or the Dean of the College of Graduate Research and Studies in which the thesis work was complete. It is understood that any copying or publication or use of this thesis or parts thereof for financial gain shall not be allowed without my written permission. It is also understood that due recognition shall be given to me and to the University of Saskatchewan in any scholarly use which may be made of any material in my thesis.

Requests for permission to copy or to make other use of material in this thesis in whole or parts shall be addressed to:

Head of the Department of Chemical and Biological Engineering

University of Saskatchewan, Rm 3B48, Engineering Building, 57 Campus Dr.

Saskatoon, SK S7N 5A9, Canada

OR

Dean

College of Graduate and Postdoctoral Studies

Thorvaldson Building, University of Saskatchewan

116-110 Science Place, Saskatoon, SK S7N 5C9, Canada

ABSTRACT

The study investigates the utilization of cedar wood bark as bioadsorbent for the adsorption and simultaneous precipitation of gold as flakes. This is with a view to establishing the electrochemical study of the adsorption and evaluate pre-treated cedar wood bark as possible adsorbent for gold in various solutions. The research plan for this project is divided into two parts. Part one focuses on understanding the adsorption of gold using the cedar wood bark as adsorbent. The second part focuses on the electrochemical study of the redox reaction during adsorption process using cyclic voltammetry technique. Synthetic solution of gold is prepared with dissolution of gold (III) chloride in hydrochloric acid, sodium thiosulfate and sodium thiourea lixiviants. Cedar wood bark is pre-treated with dilute and concentrated sulfuric acid under various experimental conditions to obtain three bioadsorbents; dilute-air dried (D-AD), concentrated washed-air dried (CW-AD) and concentrated not washed-oven dried (CNW-OD). The gold solutions are electrochemically tested for redox reaction using cyclic voltammetry (CV) techniques. One-point adsorption test is carried out on the various gold solutions to determine the suitable samples for the research. The outcome of the CV experiment indicates that redox reaction of gold in hydrochloric acid medium is easily measured through the anodic and cathodic peak formation. The one-point adsorption test favors the use of D-AD as adsorbent in acidic gold solution with percentage adsorption of 99.999%. Hence, the research is narrowed down to the use of D-AD adsorbent and acidic gold solution. Solid/liquid ratio and hydrochloric acid concentration tests indicate that 1.5 and 0.5 M, respectively, are the best suitable for the research.

For the kinetic study of the adsorption process at temperatures of 298, 303 and 313 K in 96 hours, pseudo-second order model has determination coefficients of 0.988, 0.996 and 0.998, respectively, while the pseudo-first order model has determination coefficients of 0.91, 0.77 and

0.62 at those three different temperatures. Hence, the adsorption process follows the pseudo-second order model. The activation energy from the pseudo-second order rate constant indicates that the process is chemisorption with a value of 59.86 kJ/mol. The adsorption isotherm is found to follow Freundlich isotherm model, which might have favored the formation of gold flakes on the adsorbent. The CV experiment shows the disappearance of anodic peaks as the adsorption of gold progresses, which is an indication of reduction reaction synonymous to adsorption process. X-ray diffractometer (XRD) and Fourier transform infrared (FTIR) instruments were used to determine the presence of gold precipitates and the spectra obtained from the two experiments confirm the presence of gold.

In conclusion, the study established cedar wood bark as a potential source of biomass for adsorption of gold (III) ions from acidic chloride solution, and that cyclic voltammetry (CV) technique was successfully used to examine the adsorption process.

ACKNOWLEDGEMENTS

The successful completion of this thesis was not by my effort alone, but through the grace and wisdom of the Almighty God, and with the encouragement and collaboration of others. The study would not have been possible without the assistance of my supervisor, Prof Shafiq Alam, and co-supervisor, Prof Georges J. Kipouros. Their mentorship and encouragement are highly appreciated.

I would like to thank the members of my advisory committee, Dr. Akindele Odeshi, Dr. Lope Tabil, Dr. Lifeng Zhang and Dr. Oon-Doo Baik for valuable feedback during my GAC meetings. Their comments and suggestions helped to improve the quality of my presentation.

I am grateful to the technical staff of the Department of Chemical and Biological Engineering, University of Saskatchewan, especially Mr. Majak Mapiour, for his assistance in the use of optical microscope. Also, I really appreciate Dr. Ajay Dalai for the permission to use his laboratory shaker. The administrative assistants of the Department are also appreciated, especially Glenda Mooney and Meghan Paul, you are such incredibly wonderful and understandable personalities.

I acknowledge NSERC for providing the fund for this research work and appreciate the other members of Dr. Alam's group for their valuable advice at every stage of this research work. My eternal indebtedness goes to Will Judge of University of Toronto, formerly Ph.D. student in the Department, for his ever-ready assistance in the use of the potentiostat. Prof Richard Evitts, I would always appreciate that moment you came into my rescue when I was having challenges with the use of potentiostat. I thank Dr. Glyn Kennell, in Prof Evitts's lab for giving me orientation on the use of the lab potentiostat.

It is also worthy to mention friends that gave me courage during the difficult period of my studies: Wahab Alabi and Yen Lee, I appreciate and value your contributions toward the completion of this research work. Dr. Ike Oguocha of Mechanical Engineering Department, University of Saskatchewan, I am eternally grateful to you for all you did to assist me during the research study.

DEDICATION

This project is dedicated to Almighty God who permits me to see this day, and to my wife Modupeola for her encouragement and prayers for me throughout this achievement. I will not forget the cooperation of my boys Perez and Penuel without whom this task would have been more cumbersome.

TABLE OF CONTENTS

LIST OF TABLES

LIST OF FIGURES

NOMENCLATURE

A	Frequency constant
C_e	Equilibrium concentration of solute at liquid phase (ppm)
C_f	Final molar concentration (ppm)
C_i	Initial molar concentration (ppm)
E	Measured potential (V)
E^0	Standard electrode potential (V)
E_a	Activation energy
E_{pa}	Anodic peak potential (V)
E_{pc}	Cathodic peak potential (V)
F	Fractional attainment of equilibrium (q_t/q_e)
F	Faraday constant
G^0	Standard Gibbs free energy (kJ/mol)
I	Current (A)
i_{pa}	Anodic peak current (A)
i_{pc}	Cathodic peak current (A)
K	Rate constant
K_l	Langmuir constant (related to energy of adsorption)
K_{eq}	Equilibrium constant
K_F	Freundlich constant (related to adsorption capacity)
k_1	Pseudo-first order rate constant (h^{-1})
k_2	Pseudo-second order rate constant
k_{fd}	Film diffusion rate constant

k_{id}	Intraparticle diffusion rate constant
n	Freundlich constant (related to adsorption intensity)
n	Number of electrons exchanged
Q_m	Langmuir constant (related to adsorption capacity)
Q	Amount of metal ions adsorbed (mmol/g)
q_e	Amount of metal ions adsorbed at an equilibrium (mmol/g)
q_t	Amount of metal ions adsorbed at a time (mmol/g)
R	Gas Constant (8.314 J/mol K)
T	Temperature (K or ^oC)
T	Time (h)
V	Volume of the aqueous solution (cm^3)
V/s	Scan rate
W	Weight of the adsorbent (g)
X/m	Equilibrium concentration of solute on the adsorbent (ppm)
ΔE	Electrical potential difference
ΔG	Gibbs free energy change (kJ/mol)
ΔG^o_f	Standard Gibbs free energy of formation (kJ/mol)
ΔH^o	Standard enthalpy change (kJ/mol)
ΔS^o	Standard entropy change (J/mol . K)

ABBREVIATIONS

CE	Counter electrode
CHNS	Carbon, hydrogen, nitrogen and sulfur
CNW-OD	Concentrated (acid)- not washed – oven dried
CR	Concentration ratio
CV	Cyclic voltammetry
CW-AD	Concentrated (acid) washed-air dried
D-AD	Dilute (acid) -air dried
FTIR	Fourier transform infra-red spectroscopy
FT-IR-ATR	Fourier transform infrared-attenuated total reflection
ICP-OES	Inductively coupled plasma optical emission spectroscopy
IPD	Intraparticle diffusion
PAR	Princeton applied research
PMs	Precious metals
PS/GS	Potentiostat/Galvanostat
RE	Reference electrode
RF	Radio frequency
SCE	Saturated calomel electrode
SHE	Saturated hydrogen electrode
S/L	Solid/liquid
SRC	Saskatchewan research council
STM	Scanning tunneling microscopy
XRD	X-ray diffractometer

WE	Working electrode

CHAPTER ONE

INTRODUCTION

1.1 Research Background

The demand for precious metals such as gold, silver and platinum group metals (PGMs) in the global market has encouraged researchers into their recovery from either ore or waste products of consumer electronics (urban mining). These metals are rare and naturally existing metallic chemical elements of high economic value which are seldomly available and maldistributed. Given the scale of global demand for precious metals to store values, it is important to consider whether adequate resources of mineral metals are present in the earth's crust and technically available to meet the society's future needs; where increase recycling (or secondary recovery) improved material efficiency and demand management will play important roles. Technological progress in exploration, mining and processing minerals raw materials has been the key driver that has enabled supply to keep up with demand.

Metals are considered precious due to their economic importance which has made their production beyond any environmental control in some countries. This has generated interest in the discovery of more hydrometallurgical processes such as leaching process and adsorbent for precious metals adsorption. Recent research shows several techniques, such as, electrodialysis, chemical precipitation, ion exchange and adsorption, being employed for the removal of metals from consumer electronics, wastewater or tailings [1].

This research project is focused on the hydrometallurgical extraction of gold being a metal of importance in the economy of the world. Currently, gold mining industry produces gold metal by leaching with Cyanide (CN), followed by the use of activated carbon as the main adsorbent for

the metal's recovery [2]. However, this method results into poisonous waste generation as cyanide counter ion is mostly used in the leaching process. Recently, biosorption process (biohydrometallurgy), which is the use of biomass based materials as adsorbents for precious and base metal capture, have shown much promise in gold recovery from aqueous solutions. The adsorption process takes advantage of the physiochemical interaction between organic functional groups on biopolymers and charged metal ions [2]. Common functional groups of the materials are amines, hydroxyls and carboxylic acids [3]. Several biopolymers such as chitosan, wheat straw, tannins, lignin and others have shown potential as biosorbents in the recovery of gold and other metals from aqueous solutions. The advantages of these materials are that they occur naturally and in abundance, and some are low-end byproducts from other processes. Sometimes, synthetic solutions are used to study the extraction of gold metals in a preliminary laboratory experiment. Gold III chloride is the auric salts commonly used to achieve this purpose [4], while hydrochloric acid, thiourea and sodium thiosulfate have been the popular lixiviants for the laboratory study [5, 6]. So much work has been done on lignin biosorption and other hydrometallurgical processing of gold; however, the electrochemical study of the mechanism involved was not reported. Few studies have also been reported on the use of wood bark as a source of biomass for adsorption of gold. In previous work, development of some adsorbents such as lignin [7], tannin [8], alfalfa [9], and wheat straw for the adsorption of gold has been widely reported, but there has been no report of prior studies on the use of cedar wood bark as an adsorbent for gold.

Hence, the present research involved these rarely reported cases, and achieved the purpose of contributing to knowledge by developing an environmentally benign adsorbent from wood bark and establish electrochemical procedures for the hydrometallurgical recovery of gold.

In the present work, three test solutions were prepared with gold (III) chloride in hydrochloric acid, ammonium thiosulfate, and sodium thiourea. The adsorbents were pre-treated cedar wood bark with sulfuric acid under various experimental condition, with the goal of finding out if cedar biomass after treatment can adsorb gold, and if the adsorption process is related to electrochemistry. After conducting adsorption test in the three solutions for 24 hours, the percentage adsorption in the acidic solution mixed with adsorbent prepared from dilute acid pre-treatment of the wood bark was higher than that of other mixtures. Hence, the choice is acidic chloride (HCl) solution medium and dilute acid pre-treated wood bark for this research.

1.2 Research Problem

The conventional adsorbent and lixiviants such as activated carbon and cyanide for extraction of gold respectively produce malign wastes and longer process route to produce the metal. Bioadsorbents have been identified as cheap, sustainable and environmentally benign potential substitute for the conventional adsorbents; hence this study.

1.3 Aim and Objectives

The aim of the research work is to develop an environmentally friendly biosorbent, and establish electrochemical procedures for hydrometallurgical recovery of gold, and the specific objectives are to:

i) Develop a suitable bioadsorbent from wood bark for the extraction of gold;

ii) Characterize gold solution and the bioadsorbent;

iii) Determine the percentage adsorption of gold on the bioadsorbent;

iv) Investigate the simultaneous adsorption/reduction process by electrochemical study.

1.4 Scope of the Project

The scope of this work is limited to the bioadsorption of gold using cedar wood bark obtain commercially from Saskatoon as adsorbent in synthetic gold solutions.

1.5 Justification

There is an abundance of cedar wood bark in Canada. Cedar wood bark is a preferred choice because of its rot resistant, insect and water repellant property. This cedar wood bark has not found use in engineering applications especially in extraction process. The outcome of this research provides an avenue for the use of the wood bark in the recovery of gold metal from acidic gold solution. The use of wood bark as bioadsorbent for extraction of gold will provide another means of solving some environmental problems generated by extraction industries. The success of this research will also produce a sustainable bioadsorbent that can serve as potential substitute to the conventional ones.

1.6 Hypothesis

The hypothesis can only be true if the particles of gold metal are formed as layers on the surface of the wood bark and the cyclic voltammogram experiment is successfully used to study the adsorption process.

1.7 Research Questions

Cedar wood bark is historically known to be used for landscape and local fragrance. Its application in adsorption process has never been established. The present research work is first of its kind to use cedar wood bark for metal adsorption, hence, the relevance of the following research questions.

i) Can pre-treated cedar wood bark adsorb gold from solution?

ii) Will the adsorbed gold form flakes on the pre-treated wood bark?

iii) Is the adsorption and reduction process related to electrochemistry?

1.8 Thesis Outline

Chapter one contains background information, research motivation and objectives, research question and outline. Chapter two is devoted to the comprehensive literature review of precious metals, physical mineral processing**,** hydrometallurgy, biomass, chemical pre-treatment, cedar wood bark, electrochemical study, and experimental errors. A brief review of previous research on gold adsorption is also included. Some selected analytical technique and equipment for characterization in the gold adsorption are discussed in chapter three. The electrochemical study of prepared gold solutions is extensively discussed under electrochemical study of redox reaction of various gold III chloride concentrations in acidic solution in chapter four. A publication in the journal of Material Science and Chemical Engineering (MSCE), and a presentation in the Proceedings of Extraction 2018 Conference were extracted from this chapter.

Chapter five of the thesis is dedicated to the adsorption study of gold on pre-treated wood bark in acidic and basic media, and a publication is expected from this. The study of rate of metal uptake (Kinetics), adsorption kinetics models and adsorption thermodynamics are determined in chapter six. The chapter also covered the detection of gold flakes on the pre-treated wood bark after the reduction of gold (III) to elemental gold. A publication is expected to be generated from this chapter.

The summary of research findings, conclusions and recommendations for possible future work are provided in chapter seven. The remaining part of the thesis consists of References and Appendices.

CHAPTER TWO

LITERATURE REVIEW

A brief review on precious metals, physical mineral processing**,** hydrometallurgy, biomass, chemical pre-treatment, cedar wood bark, electrochemical study, analytical technique for characterization and experimental errors is presented in this chapter. Contributions of previous researchers on gold adsorption are also presented.

2.1 Precious Metals

Precious metals are mostly used in industry such as information and communication technology, agriculture and medicine, because of their unique nature in terms of physical and chemical properties. Precious metals have important history of being used as currency, and they are economically important as investment commodities in the global market. Under ISO 4217, gold, silver, and platinum group metals (PGMs for example platinum and palladium) are internationally recognized as forms of currency [10]. Precious metals have some spectacular physical and chemical properties such as lustrous, ductile and non-corrosive, chemically less reactive and high stability. These properties have made them indispensable in high technology industries of the modern world. As a result of their increasing demand and lack of availability, they are very costly. Hence the reason for being termed “precious” [11]. Table 2.1 depicts the position of these metals in the periodic table of elements.

Table 2.1: The periodic table with identified precious metals (including PGMs) [12].

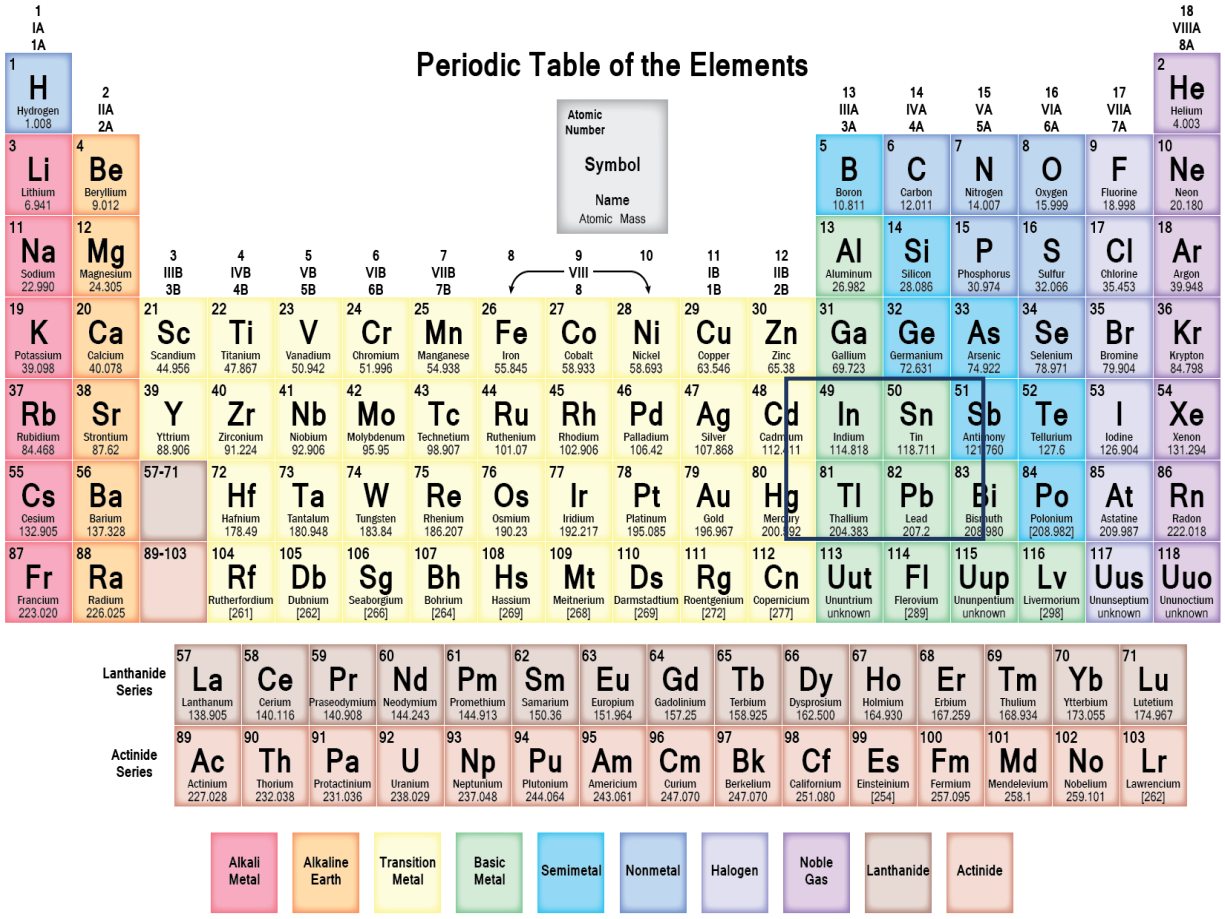

2.1.1 Sources of precious metals

Natural ores of precious metals contain about 1–30 ppm concentration of the metals, and the secondary sources such as electronic and catalytic wastes were reported to have higher concentrations of about 1 - 2000 ppm [11]. The spent catalysts, electronic wastes and other secondary sources are also known as the urban mines of the precious metals. Low concentration of precious metals (PMs) could also be found in the atmosphere as particulate matters which are from the automotive exhausts. The urban sources of precious metals are shown in Table 2.2. The urban mines or sources of PMs are categorised into three: solid wastes, liquid wastes and atmospheric air.

2.1.1.1 Solid wastes

A great amount of various solid materials containing precious metals is generated and considered as wastes. A collection of different solid wastes by municipalities from different household activities for human comfortability is termed municipal solid waste (MSW). Among this category is recyclable material, biodegradable waste, electrical and electronic waste, composite waste like clothing, hazardous waste (paints, spray, chemicals etc.) and medical waste.

Morf *et al.* [13] from their studies reported that about 0.4, 5.3, 0.059, 0.000092 and 0.0005 mg of Au, Ag, Pt, Rh and Ru, respectively could be contained in 1 kg of MSW. This is quite low concentration, however, higher than their natural ores in cases of Au and Pt. The presence of Au, Ag, Pt, Pd and other heavy metals in the incineration bottom ash of MSW was reported by Muchova *et al.* [14], who found out from their studies that 6 mm fraction of the ash contained approximately 100, 1500–4000 and 14 ppm of Au, Ag and Pt, respectively. Similarly, a considerable amount of Ag and Au were found in the MSW melting plants in Japan [11].

Waste electrical and electronic equipment (WEEE), generally known as electronic waste (e-waste) is another solid waste source of PMs. It comprises of a broad range of electronic and electrical products including large household appliances such as air conditioners, refrigerators, vacuum cleaners, television sets, tape recorders and handheld equipment like personal computers, cellular phones, printers and consumer electronics.

Table 2.2: Urban sources of precious metals [11]

Source	Sub-source of the precious metal
Solid wastes	Spent automotive catalysts
	Printed circuit boards (PCB)
	Wastes from electronic and electrical equipment
	Municipal solid wastes
	Sediments of rivers
Liquid wastes	Effluents of precious metals smelting plants
	Jewelry processing plant waste waters
	Run off street water due to rain fall
	Sewage from hospital e.g. X-ray lab
	Municipal wastewaters
Atmospheric air	Automotive exhaust
	Vapour from incineration of precious metals
	Volcanic eruption ashes

The recent economic growth has increased the ownership of diverse kind of electronics, and simultaneously decreases the life span of the electronic goods. This leads to rapid growth in the amounts of unwanted and obsolete electronics. Huismann *et al.* [15] estimated the rate of global WEEE generated as approximately 40 million tonnes per year. The WEEE contains more PMs than their typical metal mines. Many researchers including Cui and Zhang [16] have investigated the recovery of PMs obtained from WEEE. When comparing the amount of Au extracted from the primary and its secondary source, 1 tonne of a scrap of computers has higher gold than that can be extracted from 17 tonnes of ore [17]. Therefore, it is highly recommended to recover PMs from their secondary sources.

The printed circuit boards (PCBs) are another source of precious metals (PMs). It was reported that the worth of Au and Pd recovered from 1 tonne of PCBs was estimated to be $15,200 and $1850, respectively [18].

2.1.1.2 Liquid wastes

Precious metals are also present in the liquid phases as metals in ionic form. Most available liquid wastes containing precious metals are but not limited to spent electroplating and waste solutions from hydrometallurgy processes.

During electroplating process, the washing, rinsing and batch dumps activities generate used electroplating solutions which contain soluble form of various precious and base metals used in coating. The PMs in electronic industries are used as key materials in connectors, switches, relay contacts, soldered joints, connecting wires and connecting strips [16]. During the production of these electronic parts, different stages of electroplating, etching, rinsing and chemical and

mechanical polishing are integrated. The water and other liquids used during these processes contain various PMs which are recycled.

Waste solutions are generated from hydrometallurgical recovery of PMs from the ores and secondary sources. During the recovery processes, a large quantity of secondary waste is generated with low concentrations of dissolved PMs which needed to be recovered [19].

2.1.2 Gold metal

The focus of this project is on gold, hence the need for a brief review of the metal. Gold was discovered in 6000 BCE in the Middle East. It is one of the most popular precious metals, and a chemical element with symbol Au (from the Latin word Aurum), atomic number 79 and atomic weight of 196.967, making it one amongst the upper number components that occur naturally. It is one of the transition metals and can be found on the periodic table in group 11, period 6 and d-block. Gold can be naturally found as free element, alluvial or dust, nuggets and rocks. It can occ -ur in minerals as compound, such as gold sulfide or gold telluride. Figure 2.1 represents typical gold metal nuggets.

2.1.2.1 Properties of gold

Gold is solid at room temperature with density of 19.30 g/cm^3 and 17.31 g/cm^3 at melting point. It melts at 1064.18 ^{o}C and boils at 2970 ^{o}C, heat of fusion of 12.55 kJ/mol, heat of vaporisation of 342 kJ/mol and molar heat capacity of 25.418 J/mol-K. It is an amphoteric oxide at oxidation state, has an electronegativity of 2.54 on Pauling scale and Van der Waals radius of 166 picomet-er (pm). It has a face-centered-cubic structure.

Figure 2.1: Typical nuggets of gold metal as captured by metal detector [20].

2.1.2.2 Chemistry of gold

Gold is one of the most unreactive metals, although, it still forms different kinds of compound with other elements such as chlorine, fluorine at elevated temperature. The oxidation number of gold in its compound is between -1 and +5, however Au(1) and Au(III) are the most influential in gold chemistry. Gold forms an amalgam with mercury at room temperature, and alloys with other metals at higher temperature. Gold does not react with some acids and bases such as hydrofluoric, hydroiodic, sulfuric, and sodium or potassium hydroxide respectively, but dissolve in aqua regia and alkaline solutions of cyanide [21].

2.1.2.3 Gold production

As at the end of 2017, the World Gold Council (WGC) estimated the stocks of gold above the ground to be about 187,200 tonnes. At a price of $1,349 per troy ounce, 187,200 metric tonnes of gold would have a value of $8.9 trillion. The largest producer of gold as of the same period was China with 455 tonnes per year. The second-largest producer was Australia, with 270 tonnes in

the same year, followed by Russia with 250 tonnes [22]. Figure 2.2 shows the time trend of gold production.

2.1.2.3.1 Gold mining and prospecting

Between 1880 and 2006, South Africa recorded the largest mining and ultimate supplier of gold in the world. The country accounted for 50-79% of World gold supply with an average of 1,480 tonnes [23].

As of 2017, China was the world's leading gold-mining country, followed in order by Australia, Russia, the United States, Canada, and Peru, Ghana, Burkina Faso, Mali, Uzbekistan and Indonasia. South Africa, which had dominated world gold production for most of the 20th century, had declined to sixth place [24]. Other major producers are the African countries, such as Ghana, Burkina Faso, Mali, Indonesia and Uzbekistan.

Today about one-quarter of the world gold output is estimated to originate from artisanal or small-scale mining [25].

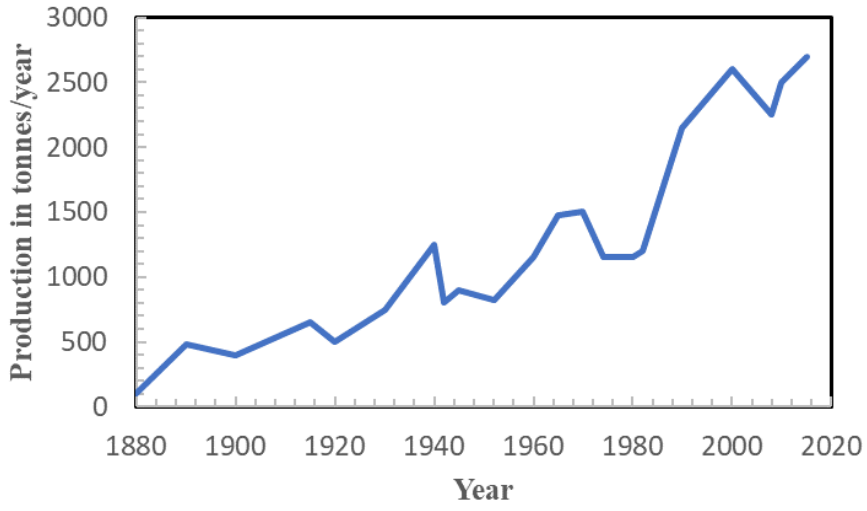

Figure 2.2: Time trend of gold production [26].

2.1.2.3.2 Gold extraction, refining and consumption

Gold ore grades as little as 0.5 parts per million (ppm) can be economical for extraction in large and easily mined deposits. Ore grades in open pit mines are in the range of 1–5 ppm and ore grades in underground or hard rock mines are reported to be at least 3 ppm. Ore grades of about 30 ppm are usually needed before gold is visible to the naked eye, in most gold mines the gold is invisible [27]. The industrial methods of refining gold after initial production are Wohlwill and Miller processes. The former is based on electrolysis while the latter is chlorination in the gold melt. Although, Wohlwill process results in higher purity, it is more complex and can easily be applied to small scale installation only [28, 29].

Other ways of assaying and purifying smaller amounts of gold embody parting and inquartation yet as cupellation, or processing ways supported the dissolution of gold in aqua regia [30].

The estimated world consumption of gold is about 50% in jewelry, 40% in investments, and 10% in industry [31, 32]. China is reported to be the largest single consumer of gold in 2013 with an increase of 32 percent in a year. While other countries used gold primarily for jewelry, China uses gold for manufacturing and retail [33]. Tables 2.3 and 2.4 list the top gold producing countries and the highest gold consuming countries on the globe respectively.

Production of gold is usually associated with hazardous pollution [34, 35]. Deposit of low-grade gold ore may contain less than 1 ppm gold metal with ore ground and dissolved in sodium cyanide. Spillage of cyanide from gold industries has been reported in both developed and developing countries, and this has resulted to loss of lives of riverine animals and in some cases human lives. These are considered as major environmental disasters [36, 37]. The presence of many heavy elements such as cadmium, lead, zinc, copper, arsenic, selenium and mercury in the

surface and ground water have been traced to gold ore dumps. It was once common to use mercury to recover gold from ore, but today the use of mercury is largely limited to artisanal miners [38]. Very little quantities of mercury compounds can reach water bodies, causing heavy metal contamination. Mercury can then be up taken by plants thereby enter human food chain in the form of methylmercury. Mercury poisoning can cause incurable brain function damage and severe retardation in humans (Minamata disease).

In terms of energy consumption, gold extraction is very energy intensive. Extracting ore from deep mines and grinding the large quantity of ore for further chemical extraction requires about 25 kWh of electricity per gram of gold produced.

2.1.2.4 Applications of gold

Gold has been in use historically as a gold coinage which represented currency. It also finds application in the production of jewelry and award medals. The price of gold in Canada as at November 3, 2018 is CA$1,613.92 per ounce (31.1 g) [41]. The most necessary industrial use for gold is in fabrication of corrosion-free electrical connectors in computers and different electrical devices. For example, gold is used in the connectors of the more expensive electronics cables, such as audio, video and USB cables, certain computers, communications equipment, spacecraft, jet aircraft engines [42]. Gold metal and its compounds have long been used for medicinal purposes. Gold metal is perhaps the most anciently administered medicine and known as Dioscorides, introduced by a Greek physician in 40 – 90 AD [43, 44].

Table 2.3: A list of countries by gold production in 2017 (Note the figures are for primary production) [39].

Rank	**Country**	**Gold production (metric tonnes)**	**Reserves (metric tonnes)**
	Rest of the world	845	12,000
	World (rounded)	3,150	54,000
1	China	440	2,000
2	Australia	300	9,800
3	Russia	255	5,500
4	United States	245	3,000
5	Canada	180	2,200
6	Peru	155	2,300
7	South Africa	145	6,000
8	Mexico	110	1,400
9	Uzbekistan	100	1,800
10	Brazil	85	2,400
11	Ghana	80	1,000
11	Indonesia	80	2,500
13	Papua New Guinea	60	1,300

Table 2.4: Gold consumption by country (in tonnes) [40].

Country	**2009**	**2010**	**2011**	**2012**	**2013**
India	442.37	745.70	986.3	864	974
China	376.96	428.00	921.5	817.5	1120.1
United States	150.28	128.61	199.5	161	190
Turkey	75.16	74.07	143	118	175.2
Saudi Arabia	77.75	72.95	69.1	58.5	72.2
Russia	60.12	67.50	76.7	81.9	73.3
United Arab Emirates	67.60	63.37	60.9	58.1	77.1
Egypt	56.68	53.43	36	47.8	57.3
Indonesia	41.00	32.75	55	52.3	68
United Kingdom	31.75	27.35	22.6	21.1	23.4
Some other Persian Gulf Countries	24.10	21.97	22	19.9	24.6
Japan	21.85	18.50	−30.1	7.6	21.3
South Korea	18.83	15.87	15.5	12.1	17.5
Vietnam	15.08	14.36	100.8	77	92.2
Thailand	7.33	6.28	107.4	80.9	140.1
Total	**1508.70**	**1805.60**			
Other Countries	*251.6*	*254.0*	*390.4*	*393.5*	*450.7*
World Total	**1760.3**	**2059.6**	**3487.5**	**3163.6**	*3863.5*

In the 19th century gold had a reputation as a therapy for nervous disorders. There was a report made by Keeley in 1897 that gold could be used to treat alcoholism, depression, epilepsy, migraine, and glandular problems such as amenorrhea and impotence [45].

Gold alloys are used in tooth restorations (restorative dentistry), such as crowns and permanent bridges. Colloidal gold is employed in analysis applications in medication, biology and materials science. Colloidal gold particles coated with specific antibodies are utilized as probes for the presence and position of antigens on the surfaces of cells [46].

Gold, or its alloys, find applications when sputtered as conducting coat with argon plasma on biological specimens and other non-metallic materials like plastics and glass to be viewed under a scanning electron microscope (SEM).

Gold is applied because of the reflective layer on some high-end CDs. It is also used in automobile for heat shielding. Gold has been reported to be an electric conducting material for de-icing in some aircraft cockpit windows. The heat produced by the resistance of the gold prevents ice from forming [47].

Gold cyanide is that the solution utilized in industrial electroplating of gold onto base metals and electroforming. Gold, when dispersed in nanoparticles, can act as a heterogeneous catalyst for chemical reactions [48].

2.2 Mineral Processing

Mineral processing or physical mineral beneficiation (also known as ore dressing), is the practice of beneficiating valuable minerals from their ores. Industrial mineral treatment processes typically mix many unit operations to liberate associate degreed separate minerals by exploiting the variations in physical properties of the various minerals that conjure an ore [49].

In general, the values and gangue materials can be differentiated from each other by several differences in physical properties [50]. Recovery and concentrate grades during extraction are subjected to many factors among which are grain size ranges of the liberated minerals, the portion of natural fines in the ore and constraints imposed by concentrate end-users [51]. Several auxiliary handling operations also are thought-about a branch of extraction like storage (as in bin design), conveying, sampling, weighing, slurry transport, and pneumatic transport [49]. There are two fundamental operations in mineral processing, namely the release, or liberation, of the valuable minerals, and separation of these values from the gangue, this latter process being known as concentration.

Liberation of the precious minerals from the gangue is accomplished by comminution, which involves crushing, and, if necessary, grinding, to such a particle size that the product is a mixture of relatively clean particles of minerals and gangue. Grinding is commonly the best energy client, accounting for up to five hundredth of a concentrator's energy consumption. Effective process development of an ore body depends on an understanding of the mineral characteristics of the deposit, ore characteristics such as mineral abundance and texture, control the liberation and concentration of values, and thus the economics of the deposit [52]. Valuable information regarding the response of ore to treatment can be revealed by viewing tailing particles under microscope and subsequently analyse the result.

The most important physical methods which are used to concentrate ores are dependent of difference in specific gravity, magnetic, optical and radioactive, floatation and electrostatic properties of the minerals in the ore. The basic operations in mineral processing are comminution, concentration, screening, classifying, dewatering and drying [49, 53].

2.2.1 Liberation

Liberation is defined as the release of the valuable minerals from the gangue at the possible coarsest particle size, and it is a very important objective of comminution [54]. A successfully achieved liberation of minerals could lead to energy saving, easier and cheaper separation stages. Although, complete liberation size is hardly achieved in operations, even if the ore is grinded to the finest grain size of the valuable mineral particles [49, 54].

2.2.2 Ore characterization

The effective development of a treatment process of a mineral depends on a thorough of the characteristics of the materials being treated. If the properties of ores are better understood and reliably measured, then efficient processes can be designed, and the mineral treatment can be optimized [55]. Improved characterization has several aspects. It can mean better ways of measuring mineral characteristics of ores and process products using modern, automated equipment [56] . It can also mean a better understanding of the influence of these measured parameters on process performance [57]. Finally, it can mean improved methods for manipulating and presenting mineralogical data [55]. Considerable advances have been made in each of these aspects of characterization.

2.2.3 Concentration

The objective of mineral processing, regardless of the methods used, is always the same, i.e. to separate the minerals into two or more products with the values in the concentrates, the gangue in the tailings, and the locked particles in the middling. Middling is in fact, misplaced particles, i.e. those particles which ideally should have reported to either concentrate or the tailings. The recovery, in the case of the concentration of a metallic ore, is the percentage of total metal

contained in the ore that is recovered in the concentrate; a recovery of 75% means that 75% of the metal in the ore is recovered in the concentrate and 25% is lost in the tailings. Normally the term, recovery, refers to the amount of metal recovered in the concentrates-the valuable products [58].

The ratio of concentration is the weight of the feed (or heads) to the weight of the concentrates, and it is a measure of the efficiency of the concentration process and grade.

There is an approximately inverse relationship between recovery and grade of concentrate in all concentrating processes [59].

2.3 Pyrometallurgy

Pyrometallurgy is the thermal treatment of minerals and metallurgical ores and concentrates to recover valuable metals due to changes in the physical and chemical properties of the materials [60]. The products of pyrometallurgical treatment or process such as pure metals may be sold to end user. Other products include intermediate compounds or alloys which can serve as feed for further processing. Gold, iron, copper is examples of elements that are extracted by pyrometallur -gical processes [61].

2.4 Hydrometallurgy

Hydrometallurgy could be described as technique that the sector of extractive science makes use of solution for the recovery of metals from ores, concentrates, and recycled or residual materials [62]. The hydrometallurgy process can be complemented by mineral processing such as froth flotation, pyrometallurgy, vapour metallurgy and molten salt electrometallurgy.

Hydrometallurgy process involves the following major three steps: Leaching Purification and/or Concentration of the solution (adsorption, solvent extraction and ion exchange), and recovery or reduction of the metal from its solution (biosorption and electrowinning).

Additional steps are physical separation, such as, washing, clarification, thickening, filtering, drying or evaporation. Figure 2.3 shows the sequence of hydrometallurgical process of refractory gold ore.

2.4.1 Leaching

Leaching is a widely used extractive metallurgy technique which converts metals into soluble salts and impurities insoluble in aqueous media. Leaching is generally described as a process of extracting a soluble constituent from a solid by means of a solvent either naturally or by industrial process. It is a hydrometallurgical process, where the solid to be separated consists of insoluble constituent and soluble constituent. The liquid/solvent is added to the solid to selectively dissolve it. In other words, the constituent of interest is dissolved and separated from other constituent parts [63].

Some terms in the process flowsheet (Figure 2.3) can be described as:

ROM: This stands for run-off-mine, which can simply be defined as the gold ore delivered from the mine site to the beneficiation plant. This is the raw material for gold processing plant, and contains gold, rocks, middlings, associate minerals and gangue (contamination).

Elution: This is otherwise known as striping and it describes the process of extracting or removing trapped gold ion from the adsorbent (activated carbon) by washing with solvent.

Leaching occurred naturally by weathering, and in chemical processing industry, leaching has a variety of applications, such as separation of metal from its ore using acid. In this respect, either one of two purposes can be achieved:

i. Opening of ores, concentrates, or metallurgical products to solubilize the metal values.
ii. Leaching easily solubilized constituents (usually gangue minerals) of an ore or a concentrate to have it in a more concentrated form.

For a good leaching, the reaction must be selective and fast, the solvent inexpensive and easily regenerated. The leaching of a solid in an aqueous phase depends primarily on the nature of the solid, whether it is ionic, covalent or metallic. Various types of leaching process are physical, chemical, electrochemical or electrolytic processes.

When compare to pyrometallurgical process, leaching is easier to perform and much less harmful, because no gaseous pollution occurs. Drawbacks of leaching are the highly acidic and, in some cases, toxic residual effluent such as cyanide waste from gold leaching, and its lower efficiency caused by the low temperatures of the operation, that dramatically have an effect on reaction rates.

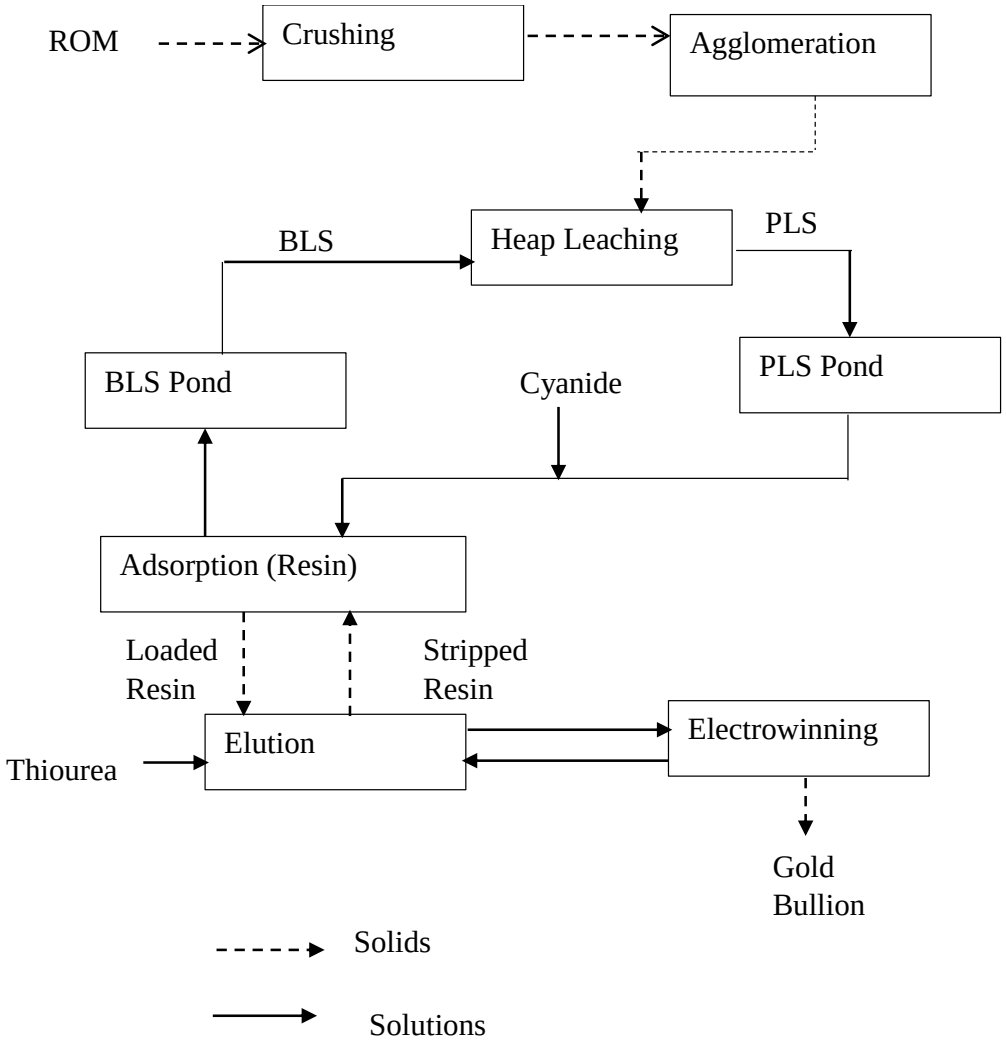

Figure 2.3: A typical flowsheet for hydrometallurgical process of refractory gold ore [64].

2.4.1.1 Theory of leaching

The leaching of an aqueous material relies on the material formation. This can be metallic, ionic and covalent. Various types of leaching process are physical, chemical, electrochemical or electrolytic processes.

a) Physical process

This process applied mainly to ionic solids such as NaCl in aqueous phase of water where there is no chemical transformation. This could further be explained using reaction R_1.

$$Na^{+}Cl^{-}_{(s)} + (a+b)H_2O \rightarrow Na(H_2O)^{+}_{a(aq)} + Cl(H_2O)^{-}_{b(aq)} \qquad R_1$$

b) Chemical process

Chemical process applied to solid which is either majorly covalent or partly ionic and covalent. Examples of these solids include oxides, hydroxide, sulfide and sulfates, some halides and carbonate, silica and silicates. Generally, the rate of dissolution increases with concentration of the reagents and with increased temperature. Ore containing valuable metals and gangue are either completely dissolved or selectively dissolved in an acidic/basic solution yielding either a homogeneous solution or a heterogeneous solution respectively. Group of leaching agents and corresponding soluble minerals are depicted in Table 2.5 [65].

The success of leaching process depends on some general principles such as: recovery, rate of leaching process (recovery/time), particle size, concentration of leaching agent, temperature, pulp density and agitation intensity [65]. Various methods have been identified with leaching, and these include heap, agitated, in-situ, bio-leaching, and autoclave leaching.

2.4.2 Adsorption (solution concentration and purification)

The leach liquor or pregnant solutions (PS) normally undergo concentration of the metal ions that are to be recovered and sometimes required removal of undesirable metal ions [62]. Adsorption is a post leaching process of purifying or concentrating metals in aqueous solution prior to metal recovery or precipitation. It could also be described as an increase in the

concentration of a substance at the interface of a condensed and a liquid or gaseous layer owing to the operation of surface forces [66].

Adsorption is a surface concept in which adsorptive (gas or liquid) molecules bind to a solid surface. In practice, adsorption is performed either in batch or continuous operation in a column packed with porous sorbents. The complete course of adsorption includes mass transfer and comprises three steps: film diffusion (external diffusion), which is the transport of adsorptive from the bulk phase to the external surface of adsorbent; pore diffusion {intraparticle diffusion (IPD)}, which is the transport of adsorptive from the external surface into the pores; and surface reaction, which is the attachment of adsorptive to the internal surface of sorbent [67].

Adsorption could be achieved through adsorption on activated charcoal, sorption on ion exchange resins, extraction by organic solvents, and biosorption. Common operation for the methods is, loading, washing, unloading or stripping/elution. The amount of metal ions adsorbed (q, mol/kg), could be determined via equation 2.1 [7]:

$$q = \frac{C_i - C_f}{W} \times V \qquad (2.1)$$

Where, W – weight of the adsorbent (g), V – Volume of the aqueous solution, C_i and C_f are the initial and final molar concentrations of ions respectively.

The concentration ratio (CR) is used to evaluate the overall concentration effectiveness of the whole sorption-desorption process (equation 2.2):

$$CR = \frac{\text{Eluate Metal Concentration}}{\text{Feed Metal Concentration}} \qquad (2.2)$$

Percentage metal adsorption is calculated using equation 2.3:

$$\% \text{ adsorbed } = \frac{C_i - C_f}{C_f} \times 100\% \quad (2.3)$$

Where, C_i and C_f are the initial and final molar concentrations of ions respectively.

The intraparticle diffusion (IPD) control can be calculated using the following equations [68]:

$$q_t = k_{id} t^{0.5} \quad (2.4)$$

Where q_t is the amount of metal ion adsorbed at time t. The linear plot of q_t versus $t^{0.5}$ infers that the kinetics of the adsorption is controlled by intraparticle diffusion, and the slope is the rate constant, k_{id} with intercept at approximately zero.

The film diffusion (external diffusion) control can be determined by equation [69]:

$$\ln(1 - F) = -k_{fd} t \quad (2.5)$$

Where F is the fractional attainment of equilibrium, and can be expressed as q_t/q_e, k_{fd} is the rate constant. On linearization, the plot of –In (1-F) against t with approximately zero intercept would infer that liquid film diffusion is responsible for the control of the adsorption.

Physical and chemical interactions are possible between adsorbent and adsorbate [70, 71], and these are known as physisorption and chemisorption respectively. Physisorption is attributed to the attractive forces between sorbent and adsorbate molecules [72], while the chemisorption provides a stronger bond as it involves the transfer or sharing of electrons between adsorbent and adsorbate species. As a guideline, an isosteric heat of adsorption with magnitude between 5 and 40 kJ/mol indicates physisorption as the dominant adsorption mode, while one between 40 and 125 kJ/mol indicates chemisorption [73]. For small values of adsorption of propane on active carbon supersorbon, Sedlacek reported that the activation energy of transfer is equal to the adsorption isosteric heat [74].

Table 2.5: The summary of some reagents for leaching [65].

Group	Reagent(s)	Examples
Water	H_2O	Cl, SO_4, NO_3
Acids	HF	N_2O_5 and T_2O_5
	HCl	Processing of $FeTiO_3$
	HNO_3	Uranium concentrates from ores
	(dil. /conc.) H_2SO_4	CuO, ZnO, PO_4, Laterites, Cerium ore
Bases	NaOH, NH_4OH	Limestone, dolomite, iron carbonate
Aqueous Salt Solutions	Na_2CO_3,	Tungsten and Uranium from Ores
	NaCN	Gold and Silver from Ores

2.4.2.1 Adsorption kinetics models

Adsorption is one of the most widely used methods to explain technologies for removing metals from aqueous media. It is due to the relatively simple design, operation, cost effectiveness, and energy efficiency of the process [75]. Adsorption kinetics can be represented by a plot of metal uptake against time, and this plot is known as a kinetic isotherm. The plot forms the basis of all kinetics studies because the generated curve represents the kinetics of the process. The kinetics are dependent on factors such as types of adsorbent and adsorbate, and experimental conditions, such as temperature and pH [76, 77].

The basis for kinetics studies is the kinetic isotherm, which is obtained experimentally by tracking the adsorbed amount against time. However, through kinetic investigations, model has also been developed to describe the adsorption rate. Ideally, the model should, with minimal complexity, (i) reveal the rate-limiting mechanism and (ii) extrapolate to operating conditions of interest. Achieving these two objectives enables the identification of operating conditions with minimum mass transfer resistance, and the prediction of performance of adsorbent [78]. Many models have been developed to predict the uptake rate of the adsorbate into the adsorbent [79, 80]. Pseudo-first order and pseudo-second order models are the two most common empirical models for the adsorption studies in aqueous solution. Several works have compared these two empirical models and find the theoretical differences between them [81, 82, 83, and 84]. The applications of second order models to adsorption systems were reviewed by Ho [85]. Liu and Liu [86] in their work summarized the useful kinetic models for biosorption, and Plazinski *et al.* [87] reviewed the adsorption kinetic models that had been theoretically associated with surface reaction mechanism.

The pseudo-first order (PFO) equation which could be derived from liquid film diffusion model [87], was proposed by Lagergren in 1898 for adsorption of oxalic and malonic acid onto charcoal [88], and can be represented in a differential form:

$$\log(q_e - q_t) = \log q_e - \frac{k_1}{2.303} t \qquad (2.6)$$

Rearranging equation 2.6 into linearized form,

$$\mathrm{In}(1 - \frac{q_t}{q_e}) = -k_1 t \qquad (2.7)$$

Where q_t and q_e are the quantity of adsorbed material (mmol/g) at any time t and equilibrium respectively, and k_1 (h^{-1}) is the pseudo-first order rate constant, while t is the adsorption time. Plotting $In(1- q_t/q_e)$ versus t gives a straight line that passes through the origin with a slope of rate constants ($k_{1)}$ for a system that obeys this model.

The pseudo-second order (PSO) assumes that the uptake rate is second order with respect to the available surface sites and can be written in the form of:

$$\frac{dq_t}{dt} = k_2(q_e - q_t)^2 \qquad (2.8)$$

Rearranging equation 2.8 into linearized form:

$$\frac{t}{q_t} = \frac{1}{k_2\, q_e^2} + \frac{t}{q_e} \qquad (2.9)$$

Where q_t and q_e are the amount of materials adsorbed at any time t (mmol/g) and equilibrium (mmol/g) respectively, k_2 is the pseudo-second order rate constant of sorption. A plot of t/q_t versus t gives a straight line for PSO-compliant kinetics.

2.4.2.2 Adsorption isotherms

The process of adsorption is usually studied through adsorption isotherm, that is, the relation between the amount of adsorbate adsorbed on the adsorbent and its pressure (if gas) or concentration (if liquid) at constant temperature. There are about 15 different isotherm models developed till date [65], however, 2 are the most commonly used in hydrometallurgical study of adsorption. The 2 most commonly used isotherm models are Freundlich and Langmuir.

Freundlich isotherm describes associate empirical relation between the concentrations of a substance on the surface of an associate adsorbent to the concentration of the substance within

the liquid with which it is in contact [89]. The Freundlich isotherm is mathematically expressed as

$$\log\frac{X}{m} = \log K_F + \frac{1}{n}\log C_e \qquad (2.10)$$

Where, K_F is the Freundlich constant (related to adsorption capacity) and n is Freundlich constant (related to adsorption intensity). The Freundlich isotherm is based on multiple layer of solute concentration on the surface of adsorbent with uniform energy.

The Langmuir isotherm is a theoretical construct and assumes that at maximum coverage, there is only a monolayer of adsorbate on the surface of the adsorbent. This means that there is no stacking of adsorbed molecules [90]. The isotherm model is represented mathematically as

$$\frac{C_e}{X/m} = \frac{C_e}{Q_m} + \frac{1}{Q_m K_l} \qquad (2.11)$$

Where, Q_m is the Langmuir constant (related to adsorption capacity), K_l is the Langmuir constant (related to energy of adsorption), C_e is the equilibrium concentration of solute in liquid phase and X/m is the equilibrium concentration of solute on the adsorbent, in both models.

2.4.3 Metal recovery

Metal recovery is the final step in a hydrometallurgical process, where the metals suitable for sale as raw materials to end users are often directly produced. The primary types of metal recovery processes are electrowinning and electrorefining. For example, a major target of hydrometallurgy is gold, which is conveniently obtained by electrowinning.

Electrowinning or electroextraction is the electrodeposition (extraction by passing electric current) of metals from their sources (ore, residual or e-waste) that have been subjected to

leaching and adsorption. Electrorefining is a post electrowinning process that involves direct purification of non-ferrous metals such as gold, silver and copper.

Both processes use the principle of electroplating where electric current is passed through dissolved metal solution with substrate (metal to be coated) acting as cathode. Some electrons from the cathode are transferred to the positively charged metal ions in solution, setting them free as atoms, which are then transfer to the surface of the substrate, thereby plating it [90].

2.4.4 Kinetics study

Kinetics study is the rate at which chemical reactions occur. It is very important as it provides a more effective indication of the actual rate of a reaction [65]. Kinetics generally studies homogeneous, heterogeneous and electrochemical reactions, with their rates depending on factors such as concentration, temperature and sometimes interface, pressure, particle size, and catalyst [65, 91, 92].

2.4.4.1 Homogeneous reactions

Homogeneous reactions include reactions in which there exist no interface between reactants, and for this reason they are far less complex. The rate of such reactions is influenced by concentration, temperature and catalysts.

Concentration

The rate of reaction between miscible reagents [A] and [B], and the formation of products [C] and [D] is:

$$A + B \rightarrow C + D \qquad R_2$$

For example, if the concentration of [A] is relatively high compared to [B], then the reagent B will be rate limiting.

$$-d[A]/dt \text{ (Rate of Consumption of A)} = K[A]^{\alpha}\,[B]^{\beta} \quad (2.12)$$

$$-d[A]^2/dt^2 = 0 \text{ (maximum rate)} = K\alpha\,[B]^{\beta} \quad (2.13)$$

K = specific rate constant, αand β= order of reaction, (α+ β) = overall order

Temperature

Reaction rates generally increase with increasing temperature and the way reactions respond to changes in temperature can be measured in terms of activation energy.

$$K = Ae^{-\frac{E}{RT}} \quad (2.14)$$

Therefore, as $T \rightarrow \infty$, $e^{-E/RT} \rightarrow 1$, and when $T \rightarrow 0$, $e^{-E/RT} \rightarrow 0$

K = Rate Constant, A = Frequency Constant, E = Activation Energy, R = Gas Constant (8.314 J/mol. K), T = Temperature (K)

Catalyst

Catalysts are often only tiny amounts of substance added to a chemical system which affect the rate of reaction, but which are not themselves consumed in the reaction. In general, reactions occur quicker with a catalyst as a result of they need less energy of activation. Catalyst can be classified as homogeneous and heterogeneous. A homogeneous catalyst has molecules that are dispersed in the same phase as the molecules of reactant, usually gaseous or liquid phase, while a heterogeneous catalyst is one whose molecules are not in the same phase as the reactants, which are typically gases or liquids that are adsorbed onto the surface of the solid catalyst [93].

$$-d[A]/dt = K[A]^{\alpha}[B]^{\beta},\ K = Ae^{-E/RT} \quad (2.15)$$

Therefore, as $E \rightarrow \infty$, $e^{-E/RT} \rightarrow 0$, and when $E \rightarrow 0$, $e^{-E/RT} \rightarrow 1$

K = Rate Constant, A = Frequency Constant, E = Activation Energy, R = Gas Constant (8.314 J/mol. K), T = Temperature (K)

2.4.4.2 Heterogeneous reaction

Heterogeneous reactions respond to the same variables/factors as homogeneous reactions; however, the presence of a reaction interface usually exerts a significant effect on the kinetics, and this may override the variables completely (rate limiting). In heterogeneous reaction, everything must be transferred across this interface. i.e. Mass, heat, and electrons (oxidation/reduction).

Heterogeneous reactions involving solid and liquid proceed through the following steps:

i. Reactants absorption in form of gases by solution.

ii. Diffusion across boundary layer as a result of reactant being transported from the bulk of the solution to the interface.

iii. Reactants adsorption to the solid surface

iv. Surface reactions

v. Soluble products desorption from the solid surface.

vi. The bulk of the solution accepts transported desorbed products.

During the transportation of the reactants from the bulk of the solution to the interface, if diffusion across the boundary layer is rate determining, then the reaction rate can be modified by the operating conditions; such as increasing surface area, agitation, and bulk concentration.

2.4.4.3 Electrochemical reaction

A basic understanding of the kinetics is highly useful in studying electrochemical reactions because these reactions are very common in leaching process. The thermodynamic drive for electrochemical reactions to proceed can be measured in terms of standard electrode potential (Volts), while the rate of the reaction can be measured in terms of current flow (Amperes) [65].

Using Ohm's law, the relationship between potential and current is as follows (ideal linear resistance):

V = IR, at low currents, the resistance is negligible.

When an electrochemical reaction is made to proceed at faster rates, forces come into play (Polarization) which tend to resist the progress of the reaction and this polarization can be anodic or cathodic [94].

2.4.4.4 Kinetics in hydrometallurgical process (leaching/adsorption)

The importance of kinetics in the investigation of dissolution reaction during leaching has prompted the unreserved interest of researchers to work more on the subject. Abdel-Aal [95] studied the kinetics of sulfuric acid leaching of low-grade zinc silicate ore obtained from eastern desert of Egypt. In the study, particle size, acid concentration, reaction temperature was varied. He reported that rate of reaction decreases with time due to reduction of the reactant surface and the increase in path length for the diffusion of ions. From the result obtained, the extraction

efficiency was 94% at a particle size of -200+270 mesh, temperature of 70℃, duration of 180 min, acid concentration of 10% and solid: liquid ratio (S/L) 1:20 g/mL. The activation energy of the reaction was 3.2 kCal/mol, making the process a diffusion-controlled reaction (Figure 2.4)

Santos *et al.* [96] have also reported the kinetics of zinc silicate leaching in sodium hydroxide. In their work, an irreversible and heterogeneous reaction of zinc silicate ores in sodium hydroxide solutions was assumed. Shrinking particle model was employed to study the leaching kinetics due to reduction in both mass of solid and particle size during leaching. The process was found to be chemically controlled having obtained activation energy of 67.8± 9.0 kJ/mol (Figure 2.5).

The kinetics of leaching chalcocite in acidic oxygenated sulfate-chloride solutions was widely reported by Cheng *et al.* [97]. In their work, dissolution of chalcocite in oxygenated acidic sulfate-chloride solution was found to occur in two stages and the first stage was confirmed to be having a rate-limiting step due to the diffusion of oxygen through the liquid boundary layer around the particle to the reaction surface. The first stage was diffusion-controlled process with activation energy of 33.5 kJ/mol (8 kCal/mol) and second stage was a chemically controlled reaction (activated energy of 59.0 kJ/mol) due to the introduction of chloride ion. The effects of agitation, temperature, partial pressure, reaction concentration on the kinetics of the leaching process were adequately studied. Figure 2.6 shows graphical representation of temperature dependence during chalcocite leaching, as reported by Cheng *et al.*

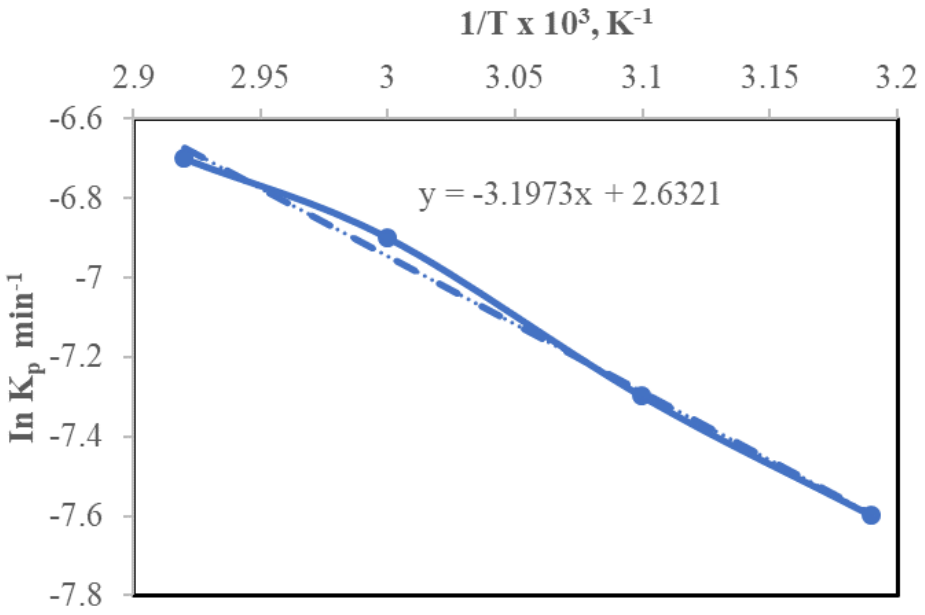

Figure 2.4: Arrhenius plot for the leaching of zinc silicate ore in acid solution [95].

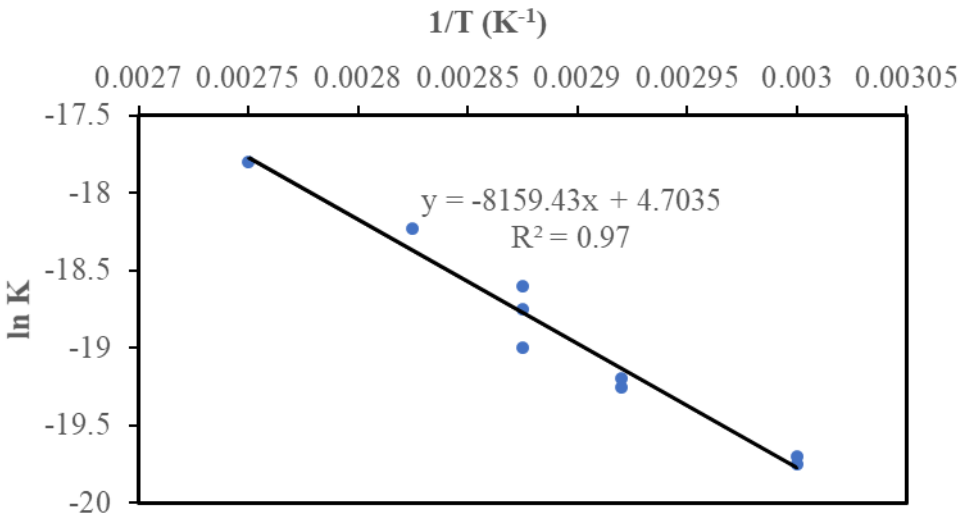

Figure 2.5: Arrhenius plot of ln rate constant versus 1/T for leaching zinc silicate ore in base solution [96].

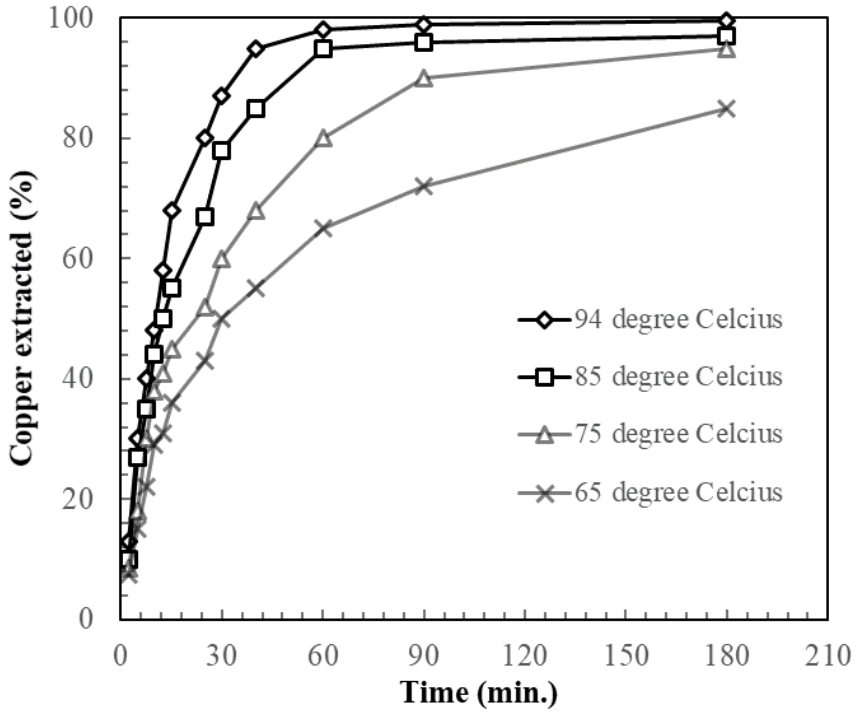

Figure 2.6: Temperature dependence during chalcocite leaching [97].

Another research of note was the kinetic study of gold and silver leaching in ammonia-thiosulfate solutions reported by Jeffrey [5]. The work was based on electroplated gold/silver material being leached by prepared solution of thiosulfate containing copper and ammonia. The effects of thiosulfate concentration, ammonia concentration on the kinetics of the leaching process were studied using rotating electrochemical quartz crystal microbalance (REQCM). Silver leaching was found to occur very rapidly, and was rate limited by the mass transfer of copper to the silver surface, and at high copper concentrations, the reaction was found to be chemically controlled, hence the rate increases with temperature.

On the other hand, it was also reported in the work that the leaching of gold was found to be much more complex, with the reaction being initially hindered by a transient film, which when

broken or dissolved allowed the reaction rate to reach a steady state. The steady state leaching rate was found to be dependent on thiosulfate, ammonia, and copper concentration [5].

Kinetics of gold leaching has been studied in various solutions by Qi and Hiskey [98] on the dissolution kinetics of gold in iodide solutions, and Breuer and Jeffrey [99] on the thiosulfate leaching kinetics of gold in the presence of copper and ammonia. Birloaga *et al.* [100] studied the various factors affecting recovery of copper and gold from hydrometallurgical processing of waste printed circuit boards, and Jeffrey *et al.* [101] reported the kinetic aspects that compares the leaching of Gold in the cyanide, thiosulfate, and chloride systems.

2.4.5 Thermodynamics of hydrometallurgy

Thermodynamics provides an indication of the tendency of a chemical reaction to proceed under specific conditions. Measurements can be made using free energy change (ΔG), equilibrium constant (K_{eq}), and electrical potential difference (ΔE) data. In hydrometallurgy, these measurements serve to determine the feasibility of such chemical processes. Thermodynamics of a reaction at equilibrium follows both Le Chatelier's principle (Principle of equilibrium shift due to change in conditions) and Hess's Law (Energy change independent on pathway or number of steps), oxidation and reduction processes, electrical and electrochemical potentials.

The Le Chatelier's principle or law states that: "If a chemical system at equilibrium experiences a change in concentration, temperature, volume, or partial pressure, then the equilibrium shifts to oppose the effects of the imposed change and a new equilibrium is established". This can also be explained as, if a system in equilibrium is interrupted, it will adjust itself in such a way that the effect of the change will be cancelled. The system can also be disturbed using catalyst. In a nutshell, Le Chatelier's principle can be used to indicate the direction of equilibrium (reactants

or products favored) resulting from changes in concentration, temperature, and pressure. Habashi [102] in his review mentioned that Le Chatelier's principle was used for the pressure leaching of bauxite with NaOH solution to obtain sodium aluminate solution. It was also reported by Marsden and House [103] that, countercurrent leaching using the effect of concentration in line with Le Chatelier's principle, can be exploited by performing intermediate solid-liquid separation steps during leaching to remove high-grade gold solutions, and re-diluting the solids leading to greater driving force for gold dissolution.

2.4.5.1 Gibbs free energy change (ΔG)

The value of Gibbs free energy change is determined by the reacting species, their activities, the temperature and pressure. The reaction will be at equilibrium when the ΔG is zero. If ΔG is negative value, the reaction is driven in the forward direction and the reduction of metal ions occurs. This leads to decrease in the activities of the reactants and increase in the activities of the product with a corresponding decrease in ΔG, and this moves the reaction towards equilibrium. However, if ΔG is positive then the reverse is the case and a similar decrease in the value of ΔG [104]. The following equation R_3 can be used to explain this statement:

$$M^{2+} + H_2 = M + 2H^+ \qquad R_3$$

With negative value of ΔG, more M^{2+} are reduced to M by H_2, while the activities of the reactants (left side of the equation) are reduced, and to move the reaction forward more M are produced stirring up activities of the product side. However, when ΔG is positive, the reaction tends to shift backward, and M is oxidized leading to more M^{2+} being released into solution.

2.4.5.2 Free energy and electrochemical potential

Free energy and electrochemical potentials are interrelated. Leaching is a chemical process that involves oxidation and reduction, which can be carried out in an electrochemical cell, so that the oxidation takes place at the anode of the cell and reduction at the cathode. Reduction and oxidation (Redox) process involves transfer of electrons. Current can flow between the electrodes and the electrical characteristics of this electron flow such as voltage and current can be measured. At equilibrium, i.e., no net current is flowing, the voltage is a measure of the thermodynamic potential of the cell reaction. It is related to the free energy change for the reaction by the equation:

$$\Delta G = -nFE \qquad (2.16)$$

Where, n represents the stoichiometric number of electrons, and F is the Faraday constant.

Using the SHE electrode as a reference electrode, the electrochemical potential of many common metals has been acquired and tabulated in electromotive force tables Table 2.6.

Under standard thermodynamic conditions of $0^{o}C$ and 101.325 kPa, Equation 2.16 becomes Equation 2.17:

$$\Delta G^{0} = -nFE^{0} \qquad (2.17)$$

Generally, if

$\Delta G < 0$, the reaction is spontaneous

$\Delta G > 0$, the reaction is non-spontaneous

$\Delta G = 0$, the reaction is in equilibrium

Table 2.6: Electromotive force (EMF) series [65].

Reaction	**E^0 (V)**
$Au^{3+} + 3e^- = Au$	1.498 Noble (cathodic)
$ClO_3^- + 6H^+ + 6e^- = Cl^- + 3H_2O$	1.451
$Cl_2 + 2e^- = 2Cl^-$	1.358
$Cr_2O_7^{2-} + 14H^+ + 6e^- = 2Cr^{3+} + 7H_2O$	1.232
$O_2 + 4H^+ + 4e^- = 2H_2O$	1.229
$Pt^{2+} + 2e^- = Pt$	1.118
$NO_3^- + 4H^+ + 3e^- = NO + 2H_2O$	0.957
$Pd^{2+} + 2e^- = Pd$	0.951
$Ag^+ + e^- = Ag$	0.800
$Hg_2^{2+} + 2e^- = 2Hg$	0.797
$Fe^{3+} + e^- = Fe^{2+}$	0.771
$I_2 + 2e^- = 2I^-$	0.536
$O_2 + 2H_2O + 4e^- = 4OH^-$	0.401
$Cu^{2+} + 2e^- = Cu$	0.342
Cu^{2+} (sat) $+ 2e^- = Cu$ ($CuSO_4$)	0.316 Reference electrode
$AgCl + e^- = Ag + Cl^-$ (0.1 M KCl)	0.288 Reference electrode
$Hg_2Cl_2 + 2e^- = 2Hg + 2Cl^-$ (sat KCl)	0.241 Reference electrode
$2H^+ + 2e^- = H_2$	0.000
$Pb^{2+} + 2e^- = Pb$	−0.126
$Sn^{2+} + 2e^- = Sn$	−0.138
$Mo^{3+} + 3e^- = Mo$	−0.200
$Ni^{2+} + 2e^- = Ni$	−0.257
$Co^{2+} + 2e^- = Co$	−0.277
$Cd^{2+} + 2e^- = Cd$	−0.403
$Fe^{2+} + 2e^- = Fe$	−0.447

For example, the reduction of Au (E^0=1.498 V) is spontaneous, while the reduction of Fe (E= -0.447 V) is non-spontaneous, thus metal will undergo oxidation. The electrochemical potential varies with temperature and concentration of the dissolved species in equilibrium with the electrodes as described by Nernst Equation:

$$E = E^0 - \frac{RT}{nF} \ln K \qquad (2.18)$$

Where, E – measured potential, E^0 – standard electrode potential, R – gas constant, T – temperature (K), K – reaction equilibrium constant, n – number of electrons exchanged, and F – Faraday's constant

2.4.6 Pourbaix diagram (E_H – pH)

Pourbaix diagram is used widely in hydrometallurgy (especially leaching process) to describe the state of substance (dissolved or solid) under equilibrium conditions. This diagram is created by applying the Nernst equation for various reactions and plotting the resulting voltage against pH. This allows one to identify whether an acidic or basic solvent should be used to leach an ore. Example of the diagram is shown in Figure 2.7.

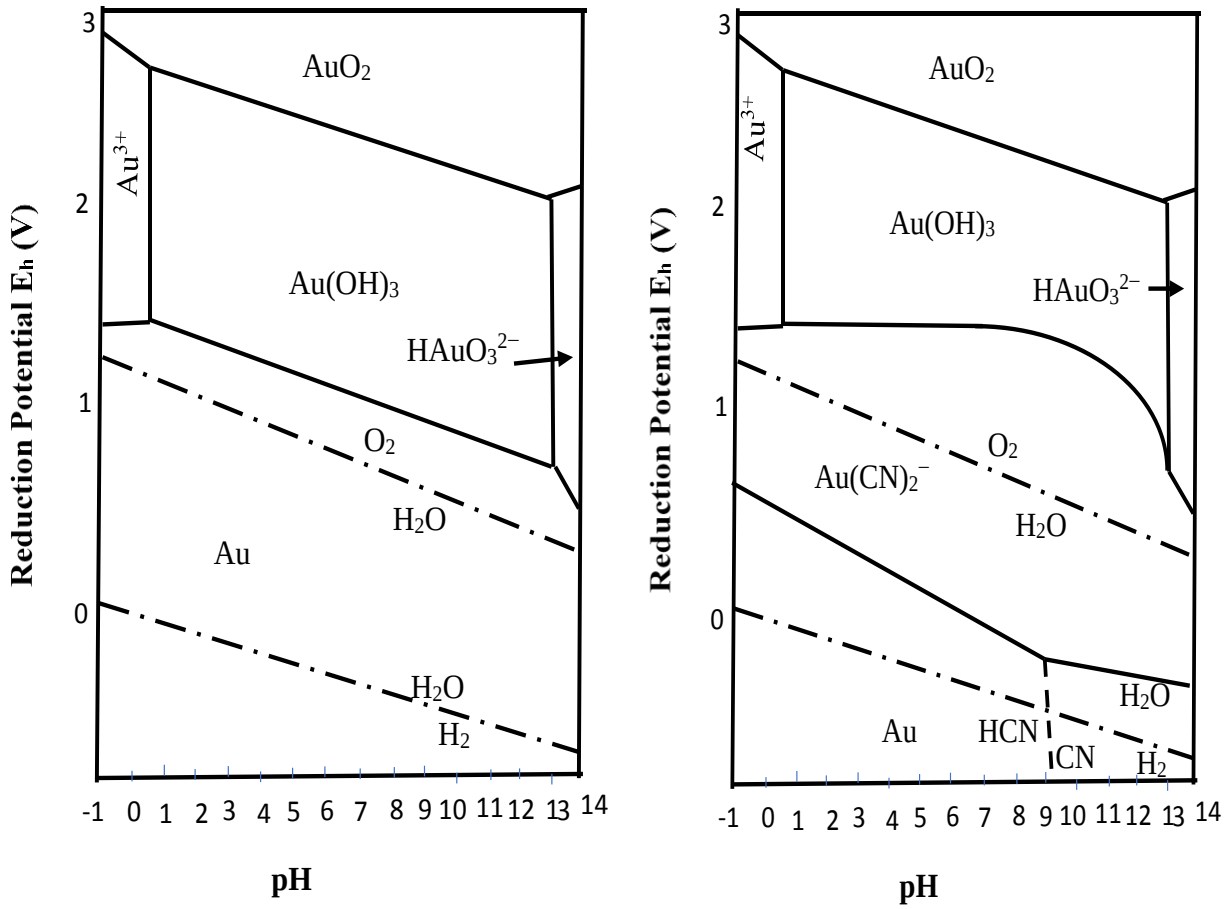

Figure 2.7: Pourbaix diagram for (a) Au –H_2O System and (b) Au –CN –H_2O System [65].

The leaching of gold can be represented in an equation R_4 thus:

$$2Au_{(s)} + 4(CN)^-_{(aq)} + 2H^+_{(aq)} + 0.5O_{2\,(g)} \rightarrow 2Au(CN)_2^-{}_{(aq)} + H_2O \qquad R_4$$

Under standard conditions, the free energy change for a chemical reaction is calculated from the tables of standard Gibbs free energy of formation ΔG^o_f, for all reacting species.

Considering Figure 2.7, a reaction such as R_5 can be deduced:

$$Au^{3+} + 3e = Au \qquad R_5$$

The standard Gibbs free energy change for the reaction can be given as

$$\Delta G^o = \Delta G^o_f\,(Au) - \Delta G^o_f\,(Au^{3+}) \qquad (2.19)$$

Where ΔG^o_f, represents the standard Gibbs free energy of formation.

From the table of standard Gibbs free energy of formation, the value of ΔG^o = -433 kJ mol^{-1}

Therefore, from Equation 2.18

$$E^o = -\frac{433 \times 10^3}{3 \times 96487} = 1.5V$$

This value that is larger than 0 indicates that Au^{3+} is thermodynamically not stable and can easily be reduced to Au.

Considering standard Gibbs free energy of water formation, the ΔG^o = -237 kJ mol^{-1}. The standard reduction potential for the reaction R_6 is 1.23V

$$O_2 + 4H^+ + 4e = 2H_2O \qquad R_6$$

The implication of this is that Au^{3+} can never dissolve or oxidized in water, so it becomes unstable and spontaneously reduced to Au since the standard potential of Au^{3+} is greater than that of water. Water will rather oxidize to oxygen.

In Figure 2.7b, the addition of complexing agent such as cyanide shifted the standard electro-potential value of Au^{3+} from positive to negative, thereby making Au^{3+} to be stabled in solution within a large range of pH.

2.5 Biomass

Biomass is a renewable and sustainable energy source which contain a wide range of biological materials that can be used as fuels (or processed into fuel), and as main source for the production of other industrial chemicals. Among the biomass, lignocellulosic which is the most abundant of all the biomass on earth seems to be of low cost. It is composed of heterogeneous complex carbohydrate polymers (cellulose, hemicellulose and lignin), with 40-60% by weight cellulose, 20-40% by weight hemicellulose, and 10-30% by weight lignin [105]. In general, biomass can be sourced from purpose-grown energy crops such as miscanthus and coppice, and waste materials from barley, canola, oat and wheat straw [105].

Pre-treatment is an early stage process of converting biomass to a commodity product. Pre-treatment processing of biomass is necessary for the enhancement of its quality by modifying the structure of cellulose-hemicellulose-lignin matrix [106]. For pre-treatment to be considered a successful process, it must meet the following requirements: (1) improve the formation of sugars or the ability to subsequently form sugars by hydrolysis, (2) avoid the degradation or loss of sugar, (3) avoid the formation of by-products that are repressive to the next chemical reaction and fermentation processes, and (4) be efficient.

Pre-treatment processing could be classified into physical, thermochemical, chemical, biological, and electrical or combination of these [107]. For the scope of this study, physical, thermochemical, chemical and biological pre-treatment would be reviewed.

2.5.1 Physical pre-treatment

This could be termed the mechanical pre-treatment. Parveen *et al.* [108], reported the reduction of cellulose crystallinity by the combined operation of crushing and grinding/milling of

lignocellulosic biomass. It was found that the size of the materials was reduced to 10-30 mm after chipping and 0.2-2 mm after milling or grinding. Vibratory ball milling was found to be more effective than ordinary ball milling in reducing cellulose crystallinity and eventual increase in digestibility [107].

2.5.2 Thermochemical pre-treatment

Steam explosion, microwave and radio frequency (RF) heating are some examples of this method.

Steam explosion is one of the most applied pre-treatment process due to its limited energy consumption. In the method, high-pressure saturated steam of between 2.5 and 7.0 MPa is injected into a biomass filled reactor (batch or continuous) at a temperature between 180 and 280°C. With sudden reduction of pressure, the biomass goes through an explosive decompression with hemicellulose disintegration and disruption of lignin matrix. The crucial parameters to be monitored during steam explosion pre-treatment process are the residence or soaking time, temperature, particle size and moisture content [108]. The advantages of the process are high yield and little or no corrosion problems, with disadvantage of having possible undesirable products.

Microwave and radio frequency (RF) heating are based on dielectric heating which is volumetric and rapid heat transfer. This technique is about placing biomass materials in an electrical field for the electric heating pre-treatment, dipole molecules like water or other dielectric materials rotate vigorously to orient within the field. More polar components will absorb more energy, resulting to hotspot being created in the non-homogeneous materials, leading to disruption of the lignocellulosic structures. Microwave spectrum (1 mm wavelength) lies between the infrared and radio frequency radiation and has the advantage of penetrating material and heat quickly and

uniformly and can create thermal and no-thermal effect. Radio frequency heating follows the same procedure as microwave with deeper heat penetration of material than microwave [106].

All these thermal methods can be improved by the addition of chemicals such as alkaline before or during the process.

2.5.3 Chemical pre-treatment

Acids, alkaline, oxidizing agents and ozone have been reportedly used for chemical pre-treatment of biomass. For lignin removal, alkaline, ozonolysis, peroxide and wet oxidation pre-treatments have been found to be more effective [106].

Inorganic acids such as H_2SO_4 and HCl are commonly used for both concentrated and dilute acid hydrolysis. High dose of concentrated acid is a powerful agent used to treat biomass at ambient temperature resulting to conversion. However, toxicity, corrosion, hazard and cost of maintenance are the disadvantages of this method. The use of dilute acid to treat biomass at high temperature results into high reaction rate and improved cellulose hydrolysis. The demerit is the high rate of equipment corrosion.

Alkaline that are commonly used for biomass pre-treatment are NaOH, KOH, $Ca(OH)_2$, and NH_4OH. They can be used at lower temperature and pressure than acid (though process time is longer), and their effectiveness depends on the lignin content of the biomass. Oxidizing agents such as H_2O_2, CH_3CO_3H (per acetic acid) and ozonolysis (using ozone for hydrolysis) are used to disrupt the lignocellulosic structure [106].

2.5.4 Biological pre-treatment

The pre-treatment process in this group makes use of microorganisms such as brown, white and soft rot fungi to degrade lignin and hemicellulose in lignocellulosic biomass. Brown rot fungi attack cellulose while white and soft rots degrade both the lignin and cellulose. This process requires no expensive instruments or equipment; hence, it does not require high energy. It is safe and environmentally friendly. However, the rate of the process is very slow, so, long process time is expected [108].

2.5.5 Brief review of biomass as a source of adsorbent

Preliminary investigation of lignin bioadsorption of gold has been carried out, and so much work has also been done on other hydrometallurgical processing for gold. Figure 2.8 depicts the chemical structure of lignin [109].

Recently, research attention has been targeted at biosorption, a cost efficient biological technique which has been shown to possess great potential to succeed typical technique for recovery of precious metals using various biosorbents. Some researchers have investigated the recovery of gold using biosorbents such as algae [110, 111], fungi [112, 113] and yeasts [114]. Traditionally, activated carbon is generally used in the industry for adsorption of gold from aqueous solution. However, its manufacturing and regenerating poses several constraints and represents a major portion of the operating cost in a mining operation [115].

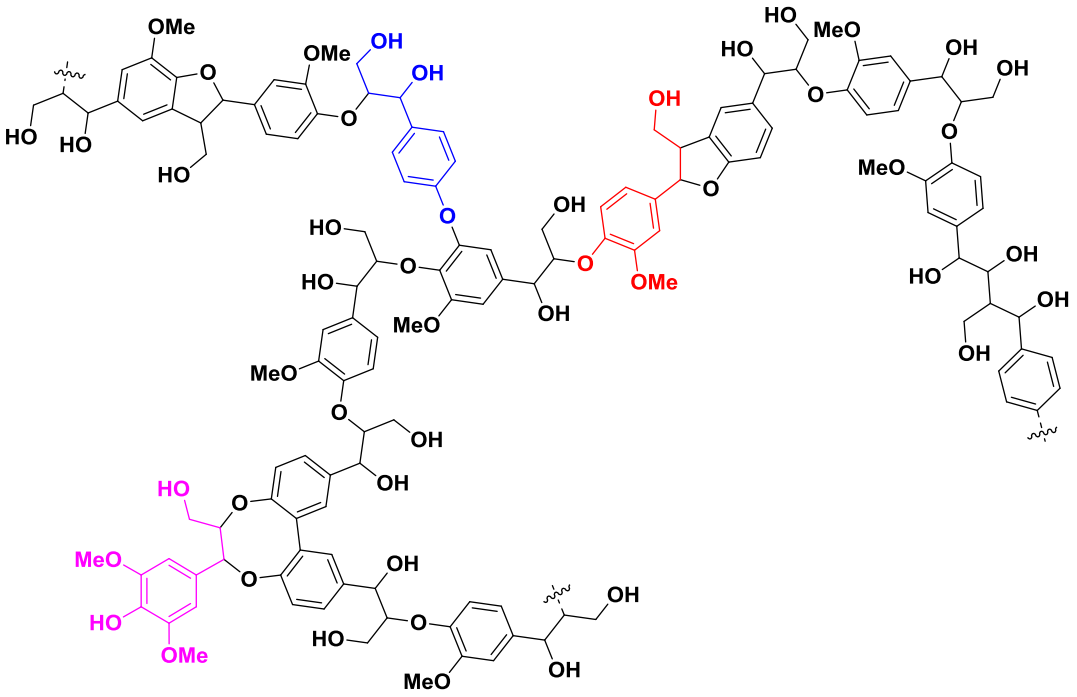

Figure 2.8: Chemical structure of lignin biomass [109].

An alternative to the utilization of activated carbon might include the employment of cot efficient biosorbents for the recovery of gold ions from aqueous solutions. Algae have been proved to be efficient and economical biosorbent for the recovery of gold from aqueous solution. Au(III) was successfully recovered as metallic gold nanoparticle using dead biomass of the brown alga, *Fucus vesiculosus* [116]. Chlorella vulgaris, a green alga was capable of removing more than 90% of the gold from very dilute solution [110, 117]. The brown marine alga *Sargassum natans* was also found to be highly selective for gold [118, 119].

The fungal cells of *Aspergillus niger*, *Mucor rouxii* and *Rhizopus arrihus* were found to take up precious metals like gold [120, 121]. Two strains of a fungus, *Cladosporioum cladosporoides* 1 and *C. cladosporoides* 2 showed preferential sorption of gold [122]. The plant organ of a bracket fungi *(Fomitopsis carnea)* immobilized in polyvinyl alcohol was used as biosorbent and also the gold (III) recovery was found to be 94 mg/g [123]. It has been reported that *A.oryzae*,

Chaetomium globosum, Giberella fujikuroi, Mucor hiemalis,Penicilium chrysogenum and *P. lilacinum* have good biosorption capacity of gold [124].

Among the 19 *actinomycetes* strains, *Strptomyces phaeochromogenes* HUT6013 has demonstrated maximum biosorption of gold at 282 μmol/g dry wt cells. Gold biosorption capacities of 14 strains of various yeast species viz. *Candida krusei, C. robusta, C. utilis, Cryptococcus albidus, C. laurentii Debaromyces hansenii, Endomycopsis fibigera, Hansenula anomala, H. saturnas, Kluyveromyces Pichia farinose, Saccharomyces cerevisiae, Sporobolomyces salmonicolor* and *Torulopsis aeria* were also reported [124]. Au(III) biosorption by waste biomass of Saccharomyces cerevisiae have been reported by Lin *et al.* [125].

High capacities of gold biosorption by gram negative microorganism strains viz. *Acinetobacter calcoaceticus, Erwinia herbicola, Pseudomonas aeruginosa and P. maltophilia* from a solution containing hydrogen tetrachloroaurate have been reported by Tsuruta [124]. Magnetotactic bacteria (MTB) are investigated by Huiping *et al.* [126] as biosorbent for the adsorption of Au(III) from aqueous solution. Other researchers have evaluated hen eggshell membrane ability to recover gold ions, Au(I) and Au(III) from solutions and electroplating wastewater [127]. The plant biomass like alfalfa biomass which was able to reduce gold (III) to Gold (0) was reported by Gardea-Torresdey *et al.* [128]. Gold (III) recovery from multi-elemental solutions was also reported by Gamez *et al.* [9]. Chemically modified hop biomass was evaluated for binding and reduction of Au(III) by López *et al.* [129]. The use of persimmon peel gel for the recovery of Au(III) from aqueous chloride medium has been investigated by Parajuli *et al.* [130]. Recently, selective adsorption of gold by discarded agro-waste materials such as rice husk carbon and barley straw carbon has been reported by Chand *et al.* [131]. Biopolymer, chitosan is a deacetylated derivative of chitin, the second most abundant biopolymer on earth after cellulose.

Chitosan can be easily modified by grafting new functional groups onto the polymer backbone to increase its range of properties and functionalities [2]. Glutar-aldehyde-cross-linked and sulfur grafted chitosan were reported as sorbent of Au(III) by Arrascue *et al.* [132]. Chemically modified chitosan was used, and uptake value of gold was reported at 3.4 mmol/g [133]. Chemically modified cross-linked chitosan resin with l-lysine has been used to examine the adsorption of Au(III) from aqueous solutions [134], and the maximum adsorption capacity was 70.34 mg/g. Activated hard shell of Iranian apricot stones has been proved as a promising adsorbent for gold recovery [135]. The results showed that under the optimum operating conditions more than 98% of gold ions were adsorbed onto activated carbon just after 3 h. Tasdelen *et al.* [136] demonstrated that gold recovery using DEAE-cellulose was effective for recovering gold from diluted gold chloride solutions.

2.5.6 Cedar wood

Cedarwood is lightweight, soft, resinous, and durable, even when in contact with soil or moisture. It is a crucial structural timber in native regions however is occasionally used elsewhere.

Cedar belongs to Pinaceae family *genus cedrus*. It is of four species of evergreen timber, the atlas cedar (*C. atlantica*), the cyprus cedar (*C. brevifolia*), the deodar (*C. deodara*), and the cedar of Lebanon (*C. libani*). These are called the true cedars and have a common feature of being tall trees with large trunks and massive, irregular heads of spreading branches. The trees are covered with smooth, dark gray bark that becomes brown and scaly with age. Many varieties of the Atlas cedar are popular ornamentals in Canada, especially in the province of British Columbia [137].

The process of harvesting cedar can cause some damage to the tree; hence, harvesters use methods that ensure the survival of the tree as a species. The harvesting of the cedar bark requires careful skill and knowledge to protect the tree from being killed by infestation or stunted growth. The cedar bark harvester de-bark only portions of the tree to ensure its survival [138]. Shindo *et al.* reported that pyrolyzed cedar bark at 773 K has microporosity of 0.07-0.1 mL/g, mean pore diameter of 0.46-0.77 nm and specific surface area of 80-448 m^2/g. At this high temperature, it was observed that there was significant decay of morphology of the cedar bark [139].

Cedar wood bark is aromatic, decay resistant and insect repellant, these can explain the reason for its use in heating homes and landscaping.

2.6 Electrochemical Reduction

This is part of redox reaction where electrons are transferred directly between ions when connected by an external electric circuit and an intervening electrolyte/solution. This principle has been adopted by researchers to separate or deposit metals from their solution.

In understanding/predicting the effect of reactant on spontaneity of electrochemical reaction, Nernst Equation (equation 2.18) is applied.

Few studies have been carried out on electrochemical reduction in metallic solution: i) electrochemical reduction of silver iodide [140]. Fourcade and Tzedakis [140] used computerized potentiostat as the electrochemical apparatus with silver disk working electrode, saturated calomel reference electrode and platinum counter electrode to measure all the electrode potentials during the adsorption experiments. They carried out voltammetric studies in the transient state to confirm the resulting signal which was attributed to the reduction of the

adsorbed silver iodide and the reaction rate controlled simultaneously by the adsorption kinetics and electrochemical kinetics. They also determined the adsorption isotherm of silver iodide on silver in order to examine the influence of the duration of electrode immersion in the suspension and the mass concentration of the silver iodide. The Langmuir isotherm (monolayer adsorption) shows a satisfactory agreement with experimental results. ii) adsorption and electrochemical activity [141]. Tao *et al.* [141] extensively reported scanning tunneling microscopy (STM) and electrochemical study of redox properties, adsorption, and self-assembly processes of porphins on Au surfaces. The electrochemical cell was made of Teflon, silver wire reference electrode, platinum wire counter electrode and gold working electrode. Cyclic voltammetry (CV) was performed using potentiostat/galvanostat under inert condition. The combined CV and STM investigation revealed a complex play between redox reactions and the adsorbed state of porphins.

2.6.1 Cyclic voltammetry technique

Cyclic voltammetry (CV) is a type of electrochemical measurement in which the electrochemical properties of an analyte in solution is studied [142, 143, and 144]. In cyclic voltammetry, the electrode potential inclines linearly with time in cyclical phases (Figure 2.9a) [145]. The rate of change in voltage over time throughout every of those phases is referred to as the experiment's scan rate (V/s). The potential is measured between the working electrode (operating conductor) and the reference electrode, whereas the current is measured between the working electrode and the counter electrode. These data are plotted as current (*i*) versus applied potential or potential (E) as depicted in Figure 2.9b. In Figure 2.9a, during the initial forward scan (from t_0 to t_1) an increasingly reducing potential is applied; thus, the cathodic current will, at least initially, increase over this time period if there are reducible analytes in the system.

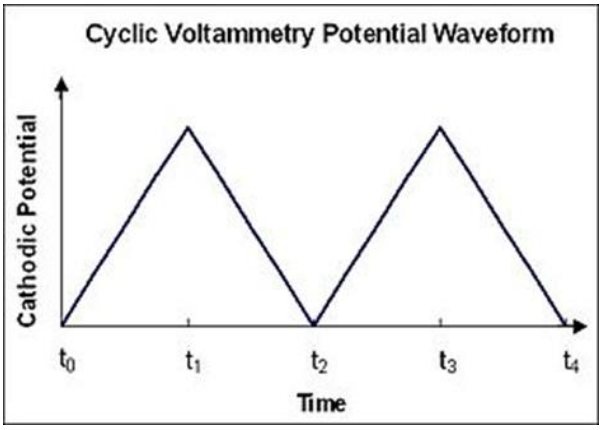

(a)

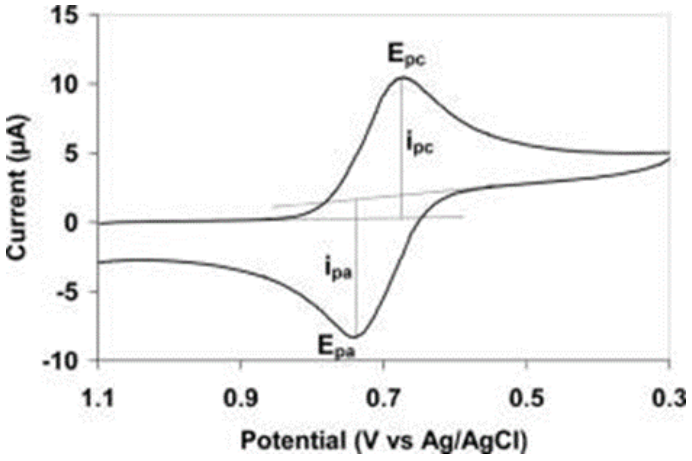

(b)

Figure 2.9: CV curves showing (a) cyclic voltammetry waveform, (b) the cathodic and anodic peak current (i_{pc} and i_{pa} respectively for a reversible reaction) [145].

When there is depletion of reducible analyte concentration, there will be simultaneous decrease in the cathodic current and at this point the reduction potential of the analyte is reached.If the redox reaction couple is reversible then throughout the reverse scan (from t_1 to t_2), the reduced analyte can begin to be re-oxidized, giving rise to a current of reverse polarity (anodic current) to before [145].

For a reversible redox reaction, the shape of oxidation peak is very similar to that of the reduction peak. Hence, CV information will give adequate knowledge about redox reaction potentials and electrochemistry of the reaction rates.

The cyclic voltammetry technique is mostly reliant on the analyte being studied. The analyte needs to be oxidation-reduction active inside the potential window to be scanned. Often the analyte displays a reversible CV wave, which is observed when all the initial analyte can be recovered after a forward and reverse scan cycle.

Focusing on current, reversible couples are characterized by [143]:

$$\frac{i_{pa}}{i_{pc}} = 1 \qquad (2.20)$$

Many redox reaction processes determined by CV are quasi-reversible or non-reversible. The irreversibility is indicated by:

$$\frac{i_{pa}}{i_{pc}} \neq 1 \qquad (2.21)$$

Electrochemical cell filled with solution and electrodes is usually used to conduct CV experiments. The species to be studied and electrolytes are dissolved in a solvent to prepare the solution. The electrochemical cell is fitted with three electrodes: working, reference and counter or auxiliary electrodes. The electrodes are static and placed in unagitated solutions throughout the cyclic voltammetry experiment. This still solution technique provides cyclic voltammetry's characteristic diffusion-controlled peaks. This technique permits a little part of the analyte to stay after reduction or oxidation, so it can show any redox activity.

Common materials for the working electrode include glassy carbon, gold and platinum. The counter electrode, referred to as the auxiliary or second electrode, may be any material like platinum that conducts current without reacting with the bulk electrolyte.

Reactions occurring at the counter electrode surface are not important if it continues to conduct current well. To maintain the detected current, the counter electrode can typically oxidize or reduce the solvent or bulk solution.

In various field of chemistry, cyclic voltammetry (CV) is a widely acceptable technique for electrochemical analysis. CV is used for electrochemical study of various redox reaction processes, thus in the determination of products stability, the reaction reversibility, existence of intermediates, and kinetics of electron transfer in the reaction [146 – 148].

2.7 Sampling Error

Many scientific measurements are made on populations. Such as final value that is reported for melting point is from a population, albeit rather a small one. It is intuitively understood that the more samples are used from a given population the less the error is likely to be.

These errors are related to samples that are not well represented. Suppose that a chemist wishes to time a reaction in a certain hood that is situated near a drafty vent in lab. The rate of this reaction can rely on how the space leaks, if the heating or cooling is on, the ambient temperature of the lab during busy and slow periods. It does not matter how many samples one takes – if the sampling method is this biased, a true picture cannot be obtained. The bias in this example is obvious. This is not always so, even to experienced investigators [149].

It is noteworthy that when assessing possible experimental errors, the importance of any error on the result should be determined and only errors which cause a significant impact on experimental data should be listed.

Error

$$\text{error} = \text{experimental value} - \text{known value} \tag{2.22}$$

Relative error

$$\text{relative error} = \frac{\text{error}}{\text{known value}} \tag{2.23}$$

Percentage error

$$\%\ \text{error} = \text{relative error} \times 100\% \tag{2.24}$$

2.8 Previous Research on Gold Bioadsorption

Table 2.7 depicts various researches conducted for adsorption of gold bioadsorbents.

Table 2.7: Adsorption of gold (Au^{3+}) using various bioadsorbents.

Bioadsorbents	pH	Q_{max} (mmol/g)	Reference
Algae			
Dealginated Seaweed Waste	3.0	0.4	[150]
Sargassum fluitans	2.0	0.0032	[151]
Chlorella vulgaris	6-7	0.5	[152]
Sargassum natanss	2.5	2.1	[153]
Ascophyllum nodosum	2.5	0.15	[153]
Chlorella vulgaris	2.0	0.5	[154]
Fungi			
Saccharomyces cerevisiae	5.0	0.026	[155]
Cladosporium cladosporioides	4.0	0.5	[156]
Cladosporium cladosporioides	4.0	0.18	[157]
Aspergillus niger	2.5	1.0	[158]
Rhizopus arrhizus	2.5	0.8	[159]
Bacteria			
Streptomyces erythraeus	4.0	0.03	[155]
Spirulina platensis	4.0	0.026	[155]
Others			
Bisthiourea derivative of resins	2.0	3.63	[157]
Condensed-tannin gel	2.0	40.0	[158]
Hen eggshell membrane	3.0	0.67	[159]
(ESM)	3.0	0.4	[159]
Dealginated Seaweed Waste			

2.9 Summary of the Literature Review

The literature review has revealed various research works on the extraction of gold through different methods of hydrometallurgical processes. These include the use of activated carbon and biomass as adsorbents in cyanide and acidic solutions respectively, the post adsorption process such as elution and electrowinning.

After all findings, the following need further examination:

- Effect of pre-treated wood bark on the adsorption and simultaneous precipitation of gold from its solution; thereby nullify the post adsorption process. This results into less processing time and cost.
- The study of the mechanism of the adsorption and precipitation
- The electrochemical study of the adsorption/reduction

All these led to the objectives of this present study as stated in Chapter one.

CHAPTER THREE

EXPERIMENTAL

The experimental procedures of the research are adequately explained in the subsequent relevant chapters of this thesis. The focus of this chapter is on the equipment for characterization employed at each step involved in the gold adsorption study. The equipment includes inductively coupled plasma optical emission spectrophotometer (ICP-OES); carbon, hydrogen, nitrogen and sulfur (CHNS) analyzer; Fourier transform infra-red (FTIR) spectroscopy; X-ray diffractometer (XRD); and potentiostat/galvanostat for cyclic voltammetry (CV) measurement.

3.1 Characterization Techniques

3.1.1 Inductively coupled plasma optical emission spectrophotometer (ICP-OES)

Elemental composition of gold sample (gold solution) was determined using ICP-OES at Saskatchewan Research Council (SRC), Saskatoon. The equipment is made up of light source unit, spectrophotometer, a detector and a data processing. The samples before and after adsorptions were poured from the sample bottles into labeled test tubes and sampled. The samples were then pumped into a nebulizer which sent sample mists to the touch (argon plasma). The plasma atomizes the molecules and excites them at a very high temperature. The excited atoms return to low energy position which in turns emits spectrum rays that correspond to the photon wavelength. The gold element is characterized by wavelength and the intensity of light corresponds to the quantity of the element. The report is transferred to a data system.

3.1.2 Carbon, hydrogen, nitrogen and sulfur (CHNS) analyzer

Elemental analyses of total carbon, hydrogen, nitrogen and sulfur were performed to provide the composition of the cedar wood bark adsorbent. This was carried out to determine any substantial increase in the sulfur content of wood bark after pre-treatment with H_2SO_4, since sulfur has high affinity for gold. For this purpose, the Vario EL III CHNS elemental analyzer (Elementar Americas Inc., Mt. Laurel. NJ, USA) in the department was used. About 10 mg of dried wood bark was combusted in a reactor at 850^{o}C. The products obtained were passed over heated copper which removed oxygen and converted oxides of nitrogen to nitrogen gas. All analytical results were automatically calculated and complete operating conditions for each sample were stored. All instrument parameters were controlled through Windows PC.

3.1.3 Fourier transform infra-red (FTIR) spectroscopy

For the purpose of determining characteristic functional groups present in cedar wood bark adsorbent before and after adsorption, Fourier transform infrared spectroscopy (FTIR) was performed in the laboratory using a Fourier Transform Infrared-Attenuated Total Reflection (Vertex 70 FTIR-ATR, Bruker Optics Inc., Billerica, MA, USA). The sample was directly inserted in the optical path, infrared radiation was focused on the sample to scan and observe its chemical properties.

The concept of the instrument is to transmit infrared radiation frequency between 10,000cm^{-1} and 100 cm^{-1} through a test sample. This results into partial absorption of the radiation in the sample while some penetrates through. The sample molecules form either rotational or vibrational energy after absorbing the radiation. The outcome of which is the formation of spectrum of the sample's molecular fingerprint with frequency from 4000 cm^{-1} to 400 cm^{-1} on the detector.

The particular “peak” of energy at a certain wavenumber was correctly used to characterize the functional groups present in the sample.

3.1.4 X-ray diffractometer (XRD)

XRD was used to determine the crystallinity and bulk phase of the adsorbent and adsorbed gold. The diffraction pattern was studied using Rigaku rotaflex Cu rotating anode X-ray diffraction instrument (RU-200, Rigaku Americas Corporation, Woodlands, Texas, USA), equipped with generation voltage of 40 kV and tube current of 40 mA. For each study, each sample of the adsorbent and adsorbed gold was powdered and mixed with methanol to form a mud which was loaded to the coarse side of a glass plate and placed under ambient drying condition. The dried sample plate was then loaded in the analysis chamber. Each sample of adsorbent and adsorbed gold was scanned at a rate of 4^{o} min^{-1} with 2θ varying between 10^{o} and 90^{o}.

3.1.5 Potentiostat/galvanostat

Potentiostat/galvanostat (PAR 283, AMETEK, Inc., Cassatt road, Berwyn, PA 19312, USA), was the instrument used to study the cyclic voltammetry (CV) measurement of the gold solutions, gold solution with adsorbent before and after adsorption. Each sample was contained in the electrochemical cell. Before use, the potentiostat was calibrated for accuracy. Three electrodes; glassy carbon (working electrode), saturated calomel (reference electrode), and platinum wire (counter electrode) were attached correspondingly to the potentiostat which was set on cyclic voltammogram mode with applied potentials of -1.25 to 1.25 V, scan rate of 5 mV/s in 1 cycle. The electrodes were immersed in the electrochemical cell containing the sample. The CV mode was switched on and the plot of potential versus current was generated.

CHAPTER FOUR

ELECTROCHEMICAL STUDY OF THE ADSORPTION PROCESS

A version of this chapter has been published in the Journal of Material Science and Chemical Engineering, a subsidiary of Journal of Minerals and Materials Characterization and Engineering (JMMCE), Scientific Research Publishing (h5-index: 16, Google-based impact factor at the time of publication: 1.2)

- Ayeni, A., Alam, S. and Kipouros, G. (2018) Electrochemical Study of Redox Reaction of Various Gold III Chloride Concentrations in Acidic Solution. Journal of Materials Science and Chemical Engineering, 6, 80 – 89.

The following conference presentation was also derived from this chapter:

- The Cyclic Voltammetry Measurement of Redox Reactions for Gold in Acidic and Basic Media, Extraction 2018, 1st Global Conference on Extractive Metallurgy, Ottawa, ON, August 26 – 29, 2018.

Contribution of the Ph.D. candidate

The laboratory potentiostat/galvanostat for the cyclic voltammetry measurement of the test solutions was set-up and calibrated by Afolabi Ayeni, in line with the advice from Professor Georges J. Kipouros. The test solutions and experimental conditions were respectively prepared and selected by Afolabi Ayeni. The electrodes used for the CV study were selected by Afolabi Ayeni with assistance from Professor Georges J. Kipouros and Mr. Ding of Dalhousie University, Halifax. The CV experiment was conducted by Afolabi Ayeni. All data generated were analysed and interpreted by Afolabi Ayeni. All experiments were discussed with Profs S.

Alam and G. J. Kipouros. The text was written by Afolabi Ayeni and vetted by Profs S. Alam and G. J. Kipouros.

Contribution of this chapter to the overall study

In order to find a suitable electrochemical technique for redox reaction of gold in acidic and basic solutions, it was necessary to test the cyclic voltammetry (CV) technique on these gold solutions. In this part of research, the main focus was on the suitability of cyclic voltammetry technique for the study of adsorption of gold from its solutions, since adsorption in this research work is a redox process. This chapter meets the electrochemical study of adsorption/reduction process as stated in specific objective (iv) of the research work.

4.1 Electrochemical Study of Redox Reaction of Various Gold III Chloride Concentrations in Acidic Solution

Abstract

The redox reaction of gold III chloride in acid solutions has been electrochemically investigated using a cyclic voltammetry technique. This work emphasizes the current and potential sites at which gold III chloride is reduced in hydrochloric acid that is vital to electrochemical evaluation of gold recovery. The solutions were prepared by reacting HCl with $AuCl_3$ in various concentrations thus 30 and 60 mg/L $AuCl_3$ in 0.1 and 0.5 M HCl, respectively. Solutions of 0.1 and 0.5 M HCl containing 0, 30 and 60 mg/L $AuCl_3$, respectively were tested for possible reduction and oxidation reactions by cyclic voltammogram experiment using a glassy carbon, a saturated calomel and a platinum wire mesh as working, reference and counter electrodes, respectively. The results showed no peak in the case of the absence of $AuCl_3$ in the solutions, but appreciable cathodic and anodic peaks for the reduction and oxidation of various concentrations

of $AuCl_3$ in acid solutions. The reaction between $AuCl_3$ and HCl was found to be reversible because the ratio of oxidation peak current and reduction peak current was 1. The concentration of $AuCl_4^-$ on the surface of the working electrode at the reduction site for each $AuCl_3$ concentration using Nernst equation was 1.22×10^9 ppm and 2.44×10^9 ppm. The reduction potentials were independent of concentration, while the current was highly dependent of concentration.

4.1.1 Introduction

The demand for gold in the global market has jolted researchers into gold recovery methods from either a lean ore or waste products of consumer electronics (urban mining). Sometimes, synthetic solutions are used to study the extraction of gold in a preliminary laboratory experiment. Gold III chloride is the auric salts commonly used to achieve this purpose [4]. Hydrochloric acid has been the popular leachant for precious metals from secondary sources [7]. Hence, in this study, solutions of gold III chloride in HCl were prepared to investigate reversible and redox reactions using a cyclic voltammetry technique.

Few studies have been carried out on the electrochemical reduction to metal, such as the electrochemical reduction of silver from iodide solutions [140]. Fourcade and Tzedakis [140] used a potentiostat as the electrochemical apparatus with a silver disk working electrode, a saturated calomel reference electrode and a platinum counter electrode to measure all the electrode potentials during the adsorption experiments. Tao *et al.* [141] reported scanning tunneling microscopy (STM) and electrochemical study of the interplay between redox properties, adsorption, and self-assembly processes of porphins on Au surfaces.

Cyclic voltammetry technique is generally used to study the electrochemical properties of an analyte in solution [142 – 144]. The theory of voltammetric methods is based on the solution of the Nernst equation. Voltammetry is a method in which information about an analyte is obtained by measuring the current generated as the applied potential to the working electrode is varied. Potential is measured between the working electrode and the reference electrode, while current is measured between the working and the counter electrode [160 and 161]. The Nernst equation (equation 2.18) is expressed in terms of potential at the working electrode.

$$E = E^0 - \frac{RT}{nF} \ln Q$$

Where, E = measured potential, E^0 = standard electrode potential, R = gas constant, T = temperature (^oK), Q = reaction quotient, n = number of electrons exchanged, and F = Faraday's constant.

The redox reaction and half-cell reaction of gold III chloride in HCl are represented in reactions R_7 and R_8 respectively thus,

$$AuCl_3 + HCl \rightarrow [AuCl_4]^- + H^+ \qquad (R_7)$$

For half-cell reaction,

$$AuCl_3 + e^- \rightarrow AuCl_4^- \qquad (R_8)$$

The result from the experiment showed no reasonable cathodic or anodic peak for hydrochloric acid solution without the presence of gold III chloride, while peaks were observed during the measurement of various concentrations of the gold III chloride in hydrochloric acid solution. It could be deduced from the experiment the reaction of gold III chloride with HCl is a redox and reversible reaction.

The objective of this work was to investigate the reaction processes in gold III chloride acid solution using cyclic voltammetry.

4.1.2 Experimental

4.1.2.1 Materials and instrumentations

Glassware, analytical grade hydrochloric acid, gold (III) chloride, and de-ionized water were used for the preparation of the solutions. The electrochemical equipment consisted of a PAR 283 Potentiostat/Galvanostat (PS/GS) and a Solartron 1260 Frequency response analyzer, Glassy carbon electrode was used as working electrode (WE), a platinum mesh served as counter electrode (CE), while a saturated calomel electrode (SCE) was the reference electrode (RE).

4.1.2.2 Experimental procedure

4.1.2.2.1 Preparation of solutions

Solutions of 30 ppm and 60 ppm of $AuCl_3$ in 200 mL of 0.1 and 0.5 M HCl were prepared. The reaction between $AuCl_3$ and HCl is a redox as shown in R_8. $AuCl_3$ was reduced to $[AuCl_4]^-$ and HCl was oxidized to H^+. This redox reaction was electrochemically measured by subjecting the gold chloride solution to cyclic voltammogram experiment, in which the cathodic and anodic current peaks were determined relative to applied potentials. This was achieved with a core driven software PAR 283 Potentiostat/Galvanostat (PG/GS) and a Z-plot driven Solartron instrument [140]. Cleaning of the electrodes was done prior to the experiment, for the purpose of revealing the surface of the electrodes which might have been covered by impurities and conditioned them for the experiment as reported by Feng *et al.*, [162]. The 0.5 M HCl was prepared, and the electrodes were immersed in the diluted solution. The electrodes were then connected to the Potentiostat which was set at cyclic voltammogram experiment mode for

cleaning. The vertex potential 1 and 2 were set at -0.25 and 1.25 V respectively at a scan rate of 5.0 mV/s. The cleaning was done for 1 h.

Subsequently, about 100 mL of 30 ppm $AuCl_3$ (in 0.1 M HCl) was poured into a 250 mL beaker. The electrodes were immersed into the solution and connected with connecting cables to the Instrument accordingly.

4.1.2.2.2 Cyclic voltammetry measurement

The cyclic voltammogram experiment was performed with a PAR potentiostat/galvanostat. The schematic of the setup is as shown in Figure 4.1. The applied potential was set between -0.25 V and 1.25 V. The scan rate was set at 5 mV/s, and the No. of cycles was maintained at 1 mV/point. During the measurement, the scanning of the potential was from -0.25 to 1.25 V, and then back to -0.25 V at a rate of 5 mV/s for 1 cycle. This procedure was performed on all the prepared solutions and the measurement of peaks was recorded via the plot of current density as a function of the potential. The experiment was carried out at a room temperature of $25^{o}C$.

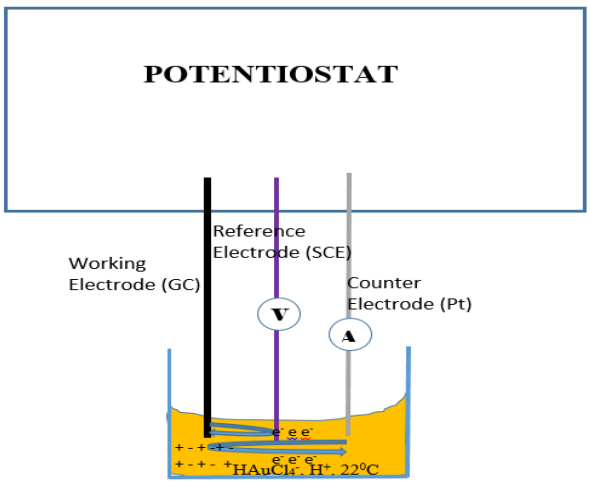

Figure 4.1: Schematic of CV experimental setup.

4.1.3 Results and discussion

The experimental results are depicted in Figures 4.2 – 4.7. The system moved through the various dynamic regime (start – finish), and the oxidation and reduction peaks could be observed through the voltammogram. The figures represent the current generated by applied cyclic potentials on 30 ppm, 60 ppm, 0 ppm $AuCl_3$ in 0.1 and 0.5 M HCl, respectively. Where, E_{pa} and E_{pc} were oxidation and reduction potential peaks, respectively, and I_{pa} and I_{pc} were the corresponding current at the peak of oxidation and reduction in that order. There are reports on the formation of these asymmetry peaks during voltammetric measurements [140, 162 and 163].

In Figure 4.2, oxidation peak was reached at about 1 V (E_{pa}), and 0.0028 A/cm^2 current density (I_{pa}) was generated. At this point the HCl was oxidized completely to H^+. On the other hand, the complete reduction of $AuCl_3$ to $AuCl_4^-$ was achieved at a potential E_{pc} and current I_{pc} of 0.55 V and 0.0028 A/cm^2, respectively. Khunathai *et al* reported the standard reduction potential E^0 of $AuCl_4^-$ to be 1.0 V [164]. The Nernst equation (2.18) was employed to determine the concentration of reduced auric chloride ion ($AuCl_4^-$) at the surface of the working electrode in 30 ppm solution, thus:

$$E = E^0 - \frac{RT}{nF}\ln Q$$

From the half-reaction depicted in reaction $R_{8,}$

$$InQ = In\frac{concentration\ of\ AuCl_4^-}{concentration\ of\ AuCl_3} = (E^0 - E)\frac{nF}{RT}$$

$$= (1 - 0.55) \times \frac{1 \times 96500}{8.314 \times (273 + 25)}$$

$$= 17.52$$

$$Concentration\ of\ AuCl_4^- = 30 \times e^{17.52} = 1.22 \times 10^9\ ppm$$

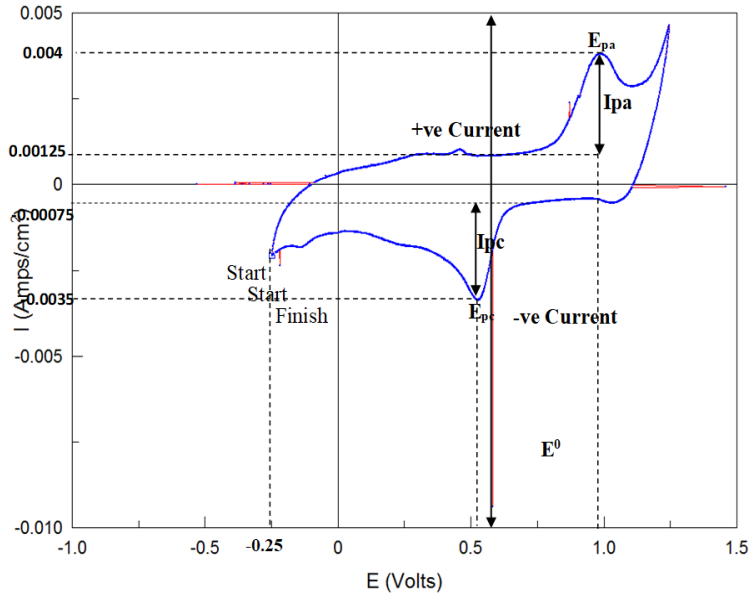

Figure 4.2: Cyclic voltammetry measurement of 30 ppm $AuCl_3$ in 0.1 M HCl at room temperature (25℃).

For a reversible reaction, equation 2.20 applies [142],

$$\frac{i_{pc}}{i_{pa}} = 1$$

In Figure 4.2, i_{pc} = 0.0035 – 0.00075 = 0.00275

i_{pa} = 0.004 – 0.00125 = 0.00275.

Hence, I_{pc}:I_{pa} = 0.00275:0.00275 = 1.

From this experiment, 30 ppm of $AuCl_3$ would be reduced to $AuCl_4^-$ at the reduction peak on the surface of the working electrode at a concentration of 1.47×10^9ppm. The reaction was also a reversible reaction, considering the ratio of I_{pc} to I_{pa} which was found to be 1 [143].

Figure 4.3 shows voltammetry measurement of 60 ppm $AuCl_3$ in 0.1 M HCl solution, with the E_{pc} and E_{pa} obtained at 0.55 V and 1.23 V, respectively. The corresponding cathodic and anodic peak current density (I_{pc} and I_{pa}) were 0.0022 and 0.0024 A/cm^2. From equations 2.18 and 2.20 respectively, the concentration of the $AuCl_4^-$ at reduction peak on the surface of the electrode was 2.44×10^9ppm, and the ratio of i_{pc} to i_{pa} was 1. Hence, the reaction was also a reversible one.

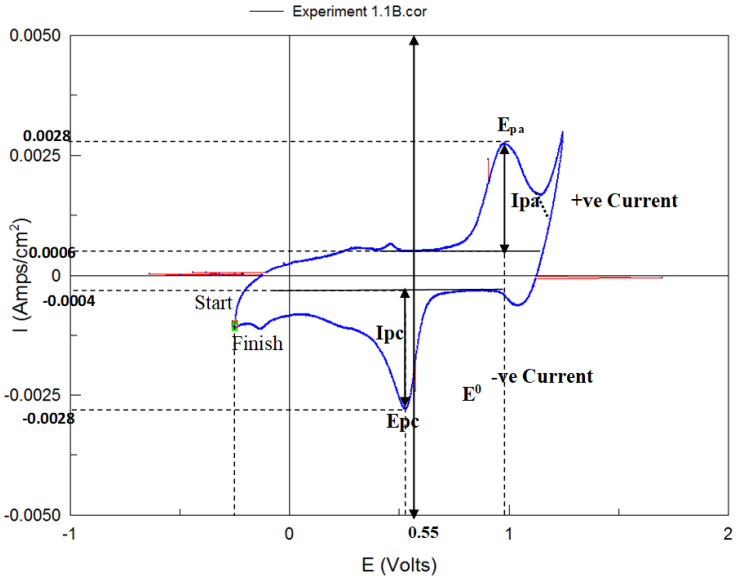

Figure 4.3: Cyclic voltammetry measurement of 60 ppm $AuCl_3$ in 0.1 M HCl solution at room temperature (25℃).

Figure 4.4 depicts the voltammetry measurement of 0.1 M HCl without $AuCl_3$ (0 ppm $AuCl_3$), no peak was feasible either at the oxidation zone or reduction zone.

This confirmed electrochemically, that the reaction between HCl and water was not a redox reaction but a dissociation.

$$HCl + H_2O \rightarrow H_3O^+ + Cl^- \qquad R_9$$

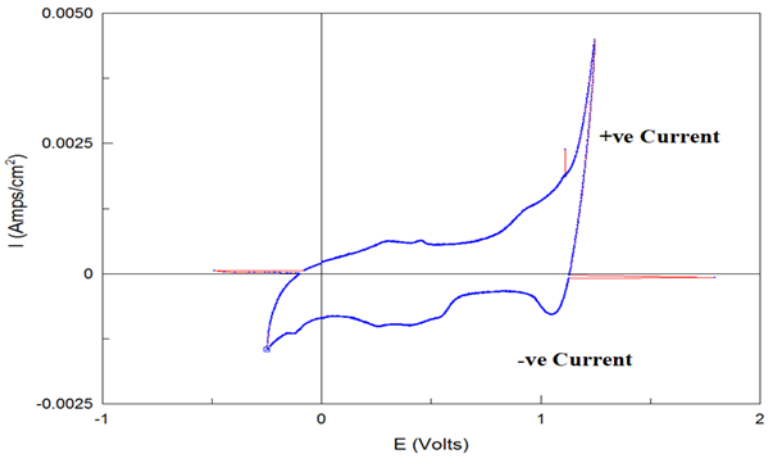

Figure 4.4: Cyclic voltammetry measurement of 0 ppm $AuCl_3$ in 0.1M HCl solution at room temperature (25℃).

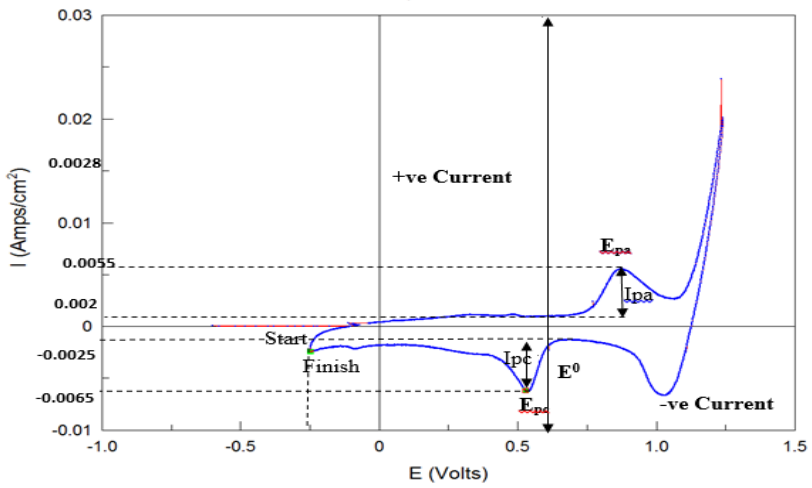

Figure 4.5: Cyclic voltammetry measurement of 30 ppm $AuCl_3$ in 0.5 M HCl solution at room temperature (25℃).

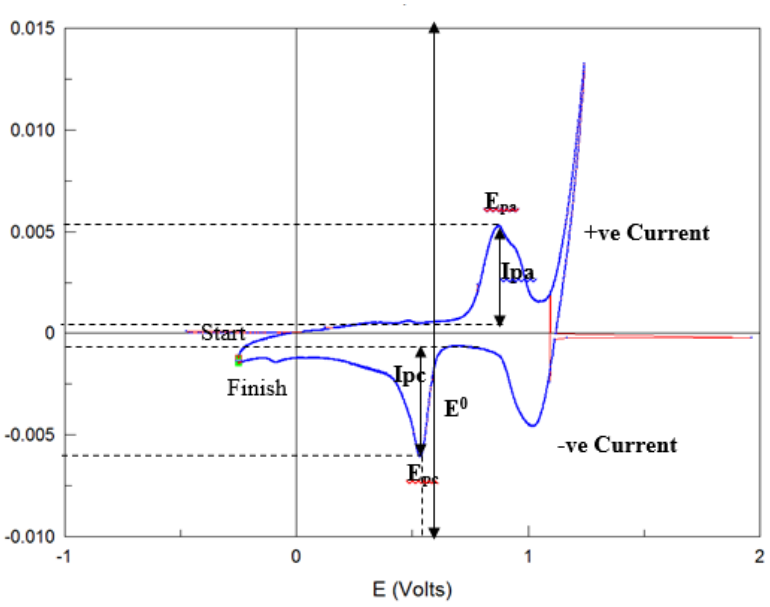

Figure 4.6: Cyclic voltammetry measurement of 60 ppm $AuCl_3$ in 0.5 M HCl solution at room temperature (25℃).

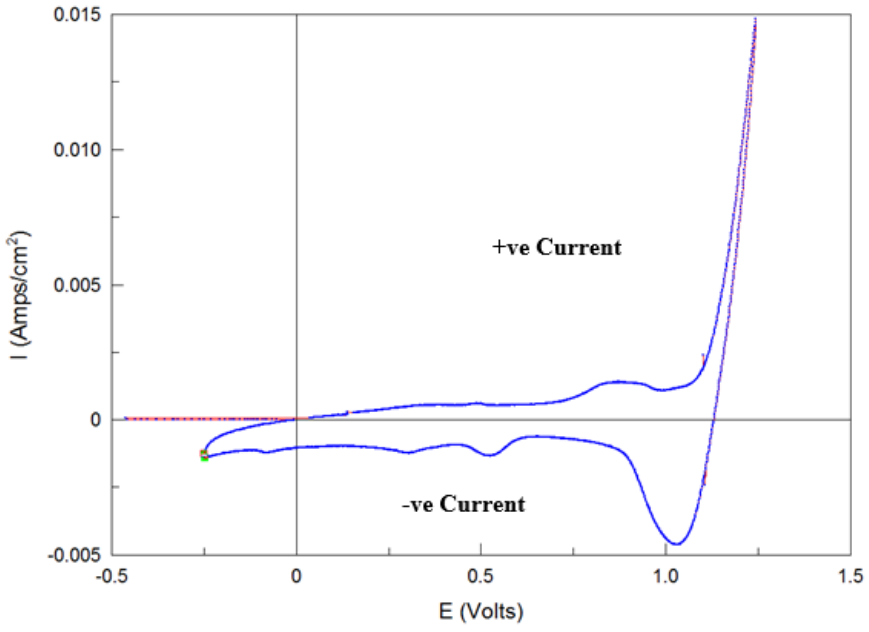

Figure 4.7: Cyclic voltammetry measurement of 0 ppm $AuCl_3$ in 0.5 M HCl solution at room temperature (25℃).

Figures 4.5 and 4.6 represented the higher concentration of $AuCl_3$ and HCl, however the values of E_{pc} was the same as that of Figures 4.2 and 4.3 (0.55 V), indicating evidence that the standard potential and reduction potential peaks did not change with concentration. The reduction peak current varied with concentration as shown in Figures 4.2 and 4.5 and were - 0.0035 and -0.0065 A /cm^2, respectively. Figure 4.7, just like Figure 4.4, had no peak because it was not a redox reaction.

4.1.3.1 Summary of cyclic voltammetry (CV) curves for various concentration

The form of CV curves as depicted in Figure 4.8 are like those published in various literature under similar experimental conditions.

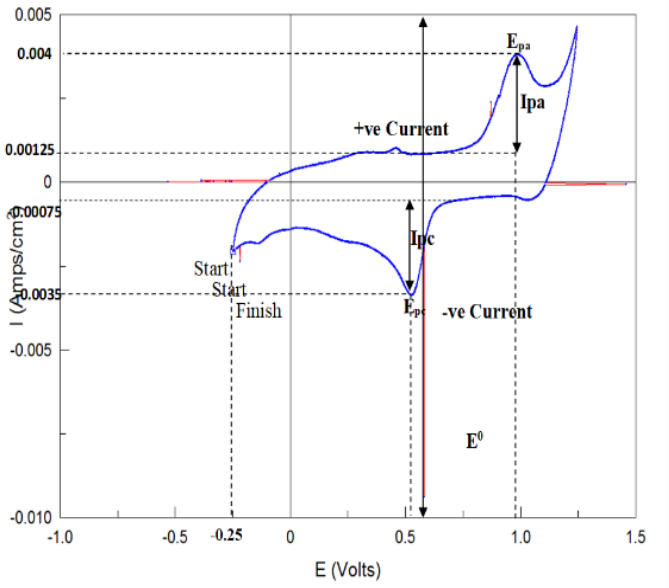

(a)

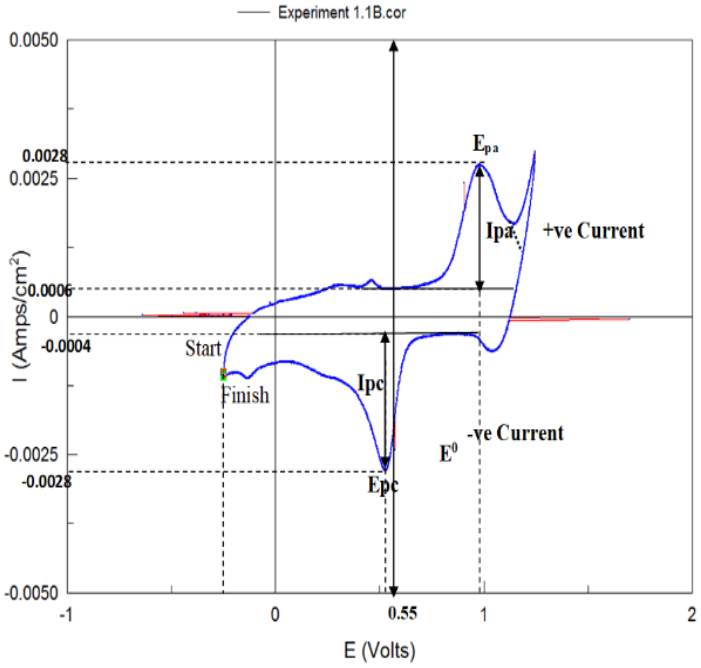
Experiment 1.1B.cor
0.0050
0.0028
0.0025
0.0006
0
-0.0004
-0.0025
-0.0028
-0.0050
I (Amps/cm²)
Epa
Ipa
+ve Current
Start
Finish
Ipc
-ve Current
E⁰
Epc
-1
0
0.55
1
2
E (Volts)

(b)

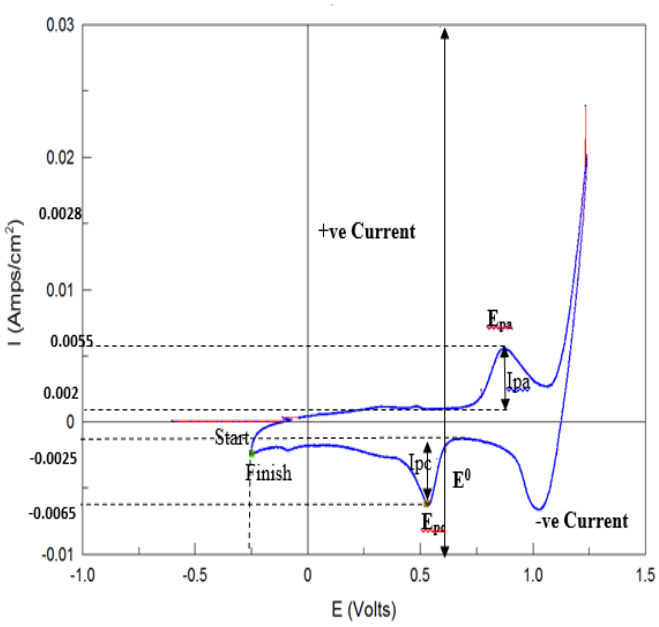
0.03
0.02
0.0028
0.01
0.0055
0.002
0
-0.0025
-0.0065
-0.01
I (Amps/cm²)
+ve Current
Epa
Ipa
Start
Finish
Ipc
E⁰
Epc
-ve Current
-1.0
-0.5
0
0.5
1.0
1.5
E (Volts)

(c)

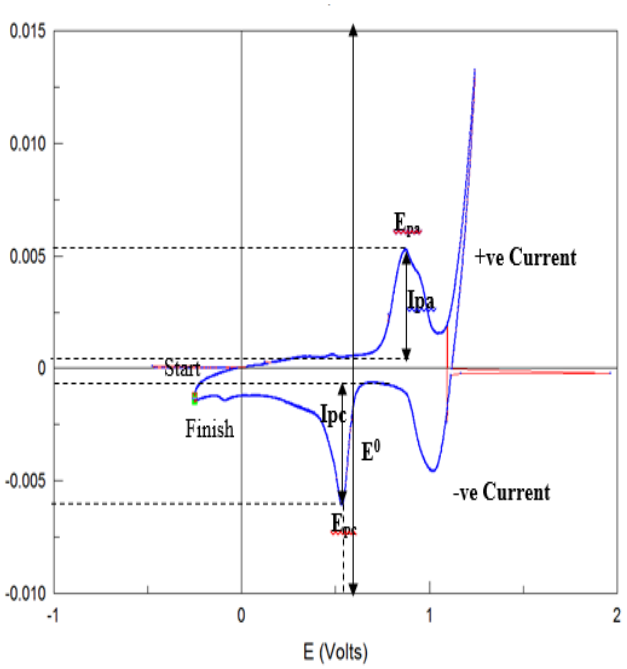
0.015
0.010
0.005
0
-0.005
-0.010
-1
0
1
2
E (Volts)
E_{pa}
+ve Current
Ipa
Start
Finish
Ipc
E^0
-ve Current
E_{pc}

(d)

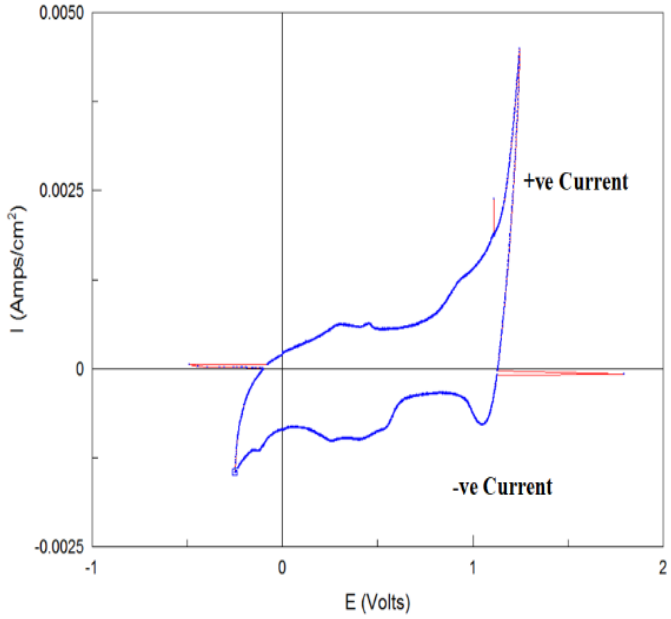
0.0050
0.0025
0
-0.0025
-1
0
1
2
I (Amps/cm^2)
E (Volts)
+ve Current
-ve Current

(e)

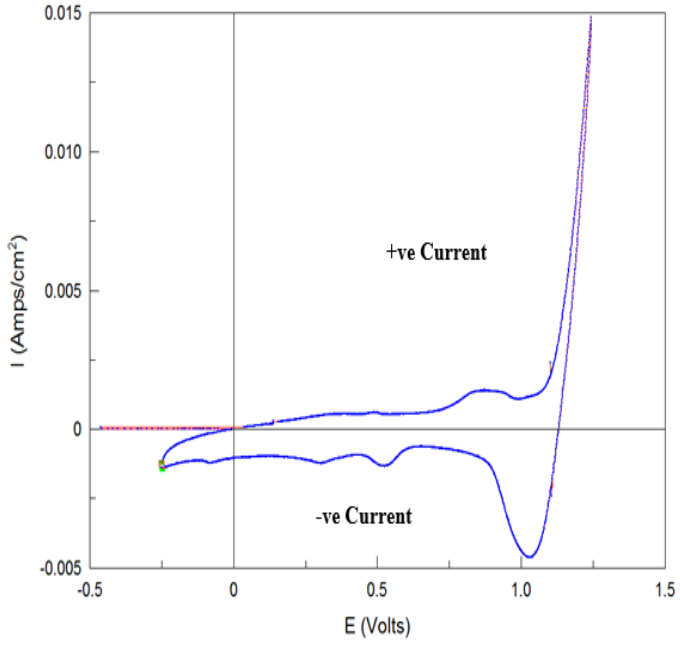

(f)

Figure 4.8: Cyclic voltammetry curves of (a) 30 ppm $AuCl_3$ in 0.1 M HCl, (b) 60 ppm $AuCl_3$ in 0.1 M HCl, (c) 30 ppm $AuCl_3$ in 0.5 M HCl, (d) 60 ppm $AuCl_3$ in 0.5 M HCl, (e) 0 ppm $AuCl_3$ in 0.1 M HCl and (f) 0 ppm $AuCl_3$ in 0.5 M HCl at room temperature.

4.1.4 Conclusions

The redox reaction of $AuCl_3$ in HCl solution of various concentrations has been electrochemically studied using cyclic voltammetry technique. The concentration of the reduced $AuCl_4^-$ ion was determined using the Nernst equation. The results showed that anodic and cathodic peaks were present in the solution containing $AuCl_3$ of various concentrations, while no peaks were generated in HCl solution in the absence of $AuCl_3$. The measured E_{pc} in the tested solutions was the same showing evidence that the reduction potentials are independent of the concentration. However, the reduction current varied with the concentration of solution, affirming the dependency of current on concentration. This study has interesting implications to

determine the electrochemical parameters of gold reduction during leaching and adsorption processes with more accurate results obtained for specific process.

4.2 Electrochemical Study of Redox Reaction during the Adsorption of Gold

4.2.1 Introduction

This section covers the cyclic voltammetry study of the bio adsorption of gold metal. However, research works on the use of signals generated by cyclic voltammetry technique in the study of reduction of silver iodide [140], and interplay between redox properties adsorption and self assembly process of porphins on gold surfaces [141] have been published, non has established the electrochemical study of bio adsorption of gold. The present work investigated the use of pre-treated cedar wood bark to adsorb and precipitate gold from acidic solution. The process was further studied using cyclic voltammetry technique, where formation of peaks was adopted to determine the oxidation and reduction at pre-adsorption, adsorption and precipitation stages. The specific objective of investigating the adsorption process by electrochemical study, and subsequent instrumental detection of gold flakes on the prepared bioadsorbent was achieved.

4.2.2 Experimental procedure

2 sets of 200 mL of working solution were prepared and subjected to cyclic voltammetry (CV) measurement using potentiostat/galvanostat with a set up as described in section 4.2.2.2. After the CV measurement, each of the working solution was mixed with D-AD adsorbent at a solid/liquid ratio of 1.5 mg/mL and the mixture was further subjected to CV measurement. Then the 2 sets of the heterogeneous mixture were shaking at 298 K and 200 rpm. After 24 h, one of the sets was subjected to CV measurement, and the other was left in the shaker for 96 h and then the final CV measurement was taken.

4.2.3 Results and discussion

4.2.3.1 Cyclic voltammetry measurement of Au(III) adsorption/reduction

The curve for the D-AD adsorbent mixture with the test solution before adsorption indicates a clear redox response because of direct electron transfer between the adsorbent and Au(III) solution, as well as a direct electrochemical reaction in a heterogeneous mixture. The kinetics study in terms of electrochemical reaction depends largely on the current flow. In Figure 4.9, the potential applied generated current and cyclic movement from point **A** and follow the arrow until it reaches the peak of the current at the positive zone. A cycle is complete when the potential is reduced, and the cyclic movement returns to the starting point **A**. The current peaks formed at the oxidation and reduction zones are well pronounced in the CV measurement of Au(III) solution without adsorbent as shown in Figure 4.9a, and anodic and cathodic current peaks have a ratio of 1, making the reaction at this point reversible. However, when the adsorbent was introduced and mixed before shaking for adsorption as presented in Figure 4.9b, the current peak at the oxidation (anodic) zone was higher than that of the reduction (cathodic) zone. This could be explained to be responsible for the spontaneous redox reaction at the beginning of the adsorption process corroborated with the negative value of ΔG^o. Figure 4.9c depicts the CV measurement after adsorption for 24 h. The anodic current peak was observed to be lower than that of the cathodic current peak, and this could be interpreted as reduction in kinetics of the process. The adsorption favors reduction process as confirmed by the reduction of the gold (III) chloride to gold (III) after the adsorption for 24 h. Figure 4.9d shows a pair of small redox peaks indicating direct but slow electron (current) transfer and could also be described as an irreversible process (the ratio of anodic current peak to that of cathodic is not equal to 1). Figure 4.9d can be compared to Figure 4.9e which represents the CV of HCl without $AuCl_3$ (analyte). The two

figures are very similar, indicating that the Au(III) has really been depleted during adsorption as shown in Figure 4.9d.

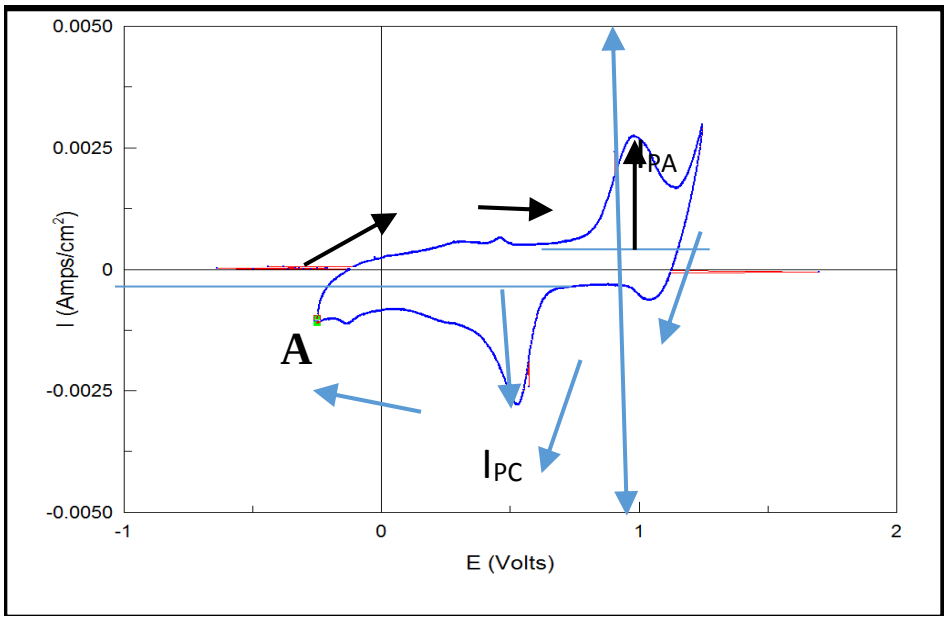

(a)

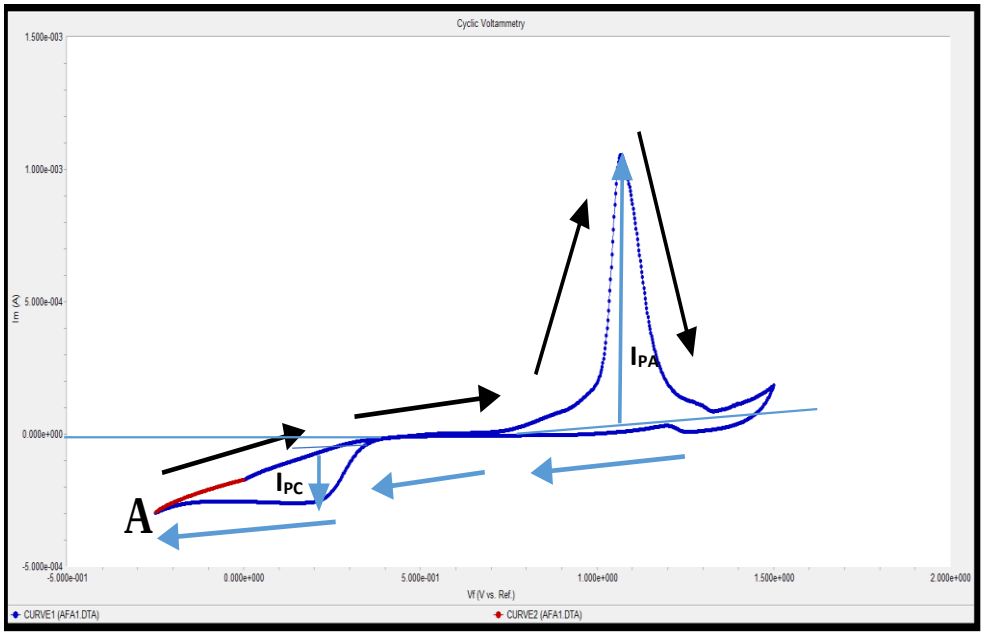

(b)

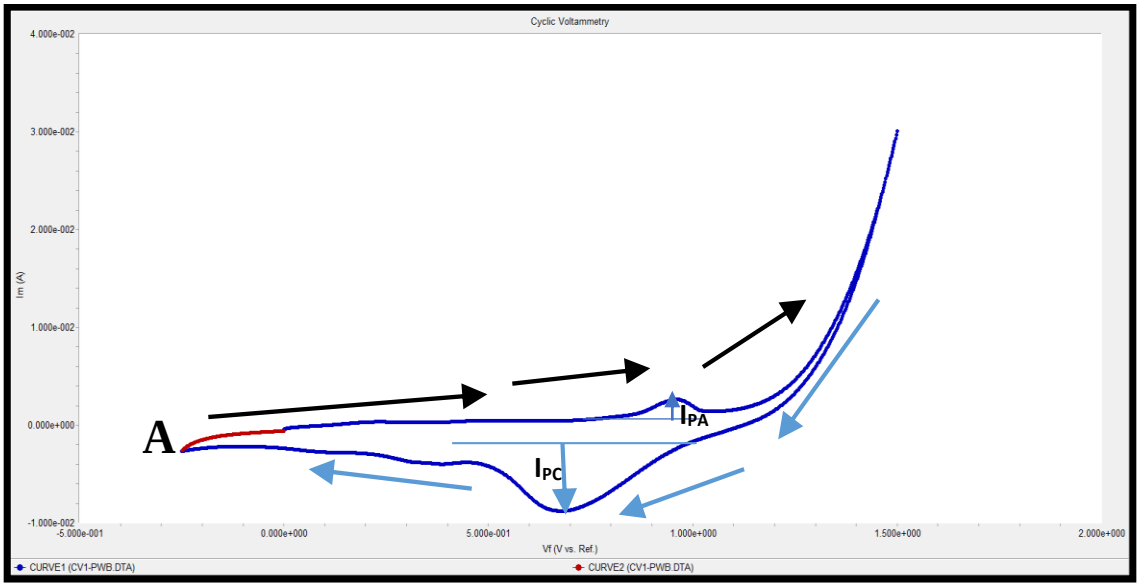
Cyclic Voltammetry
4.000e-002
3.000e-002
2.000e-002
1.000e-002
0.000e+000
-1.000e-002
Im (A)
-5.000e-001
0.000e+000
5.000e-001
1.000e+000
1.500e+000
2.000e+000
Vf (V vs. Ref.)
A
IPA
IPC
CURVE1 (CV1-PWB.DTA)
CURVE2 (CV1-PWB.DTA)

(c)

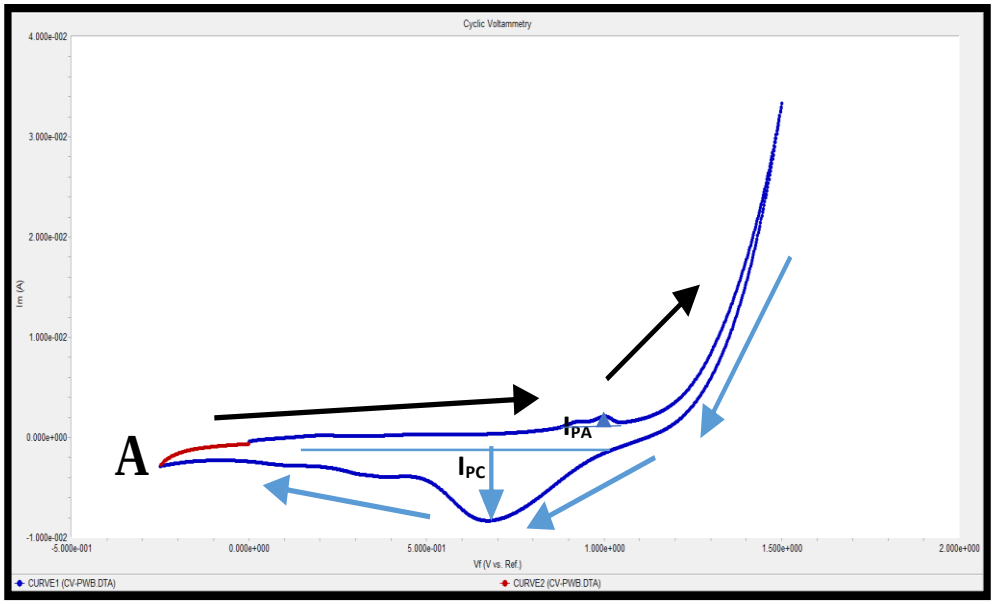
Cyclic Voltammetry
4.000e-002
3.000e-002
2.000e-002
1.000e-002
0.000e+000
-1.000e-002
Im (A)
-5.000e-001
0.000e+000
5.000e-001
1.000e+000
1.500e+000
2.000e+000
Vf (V vs. Ref.)
A
IPA
IPC
CURVE1 (CV-PWB.DTA)
CURVE2 (CV-PWB.DTA)

(d)

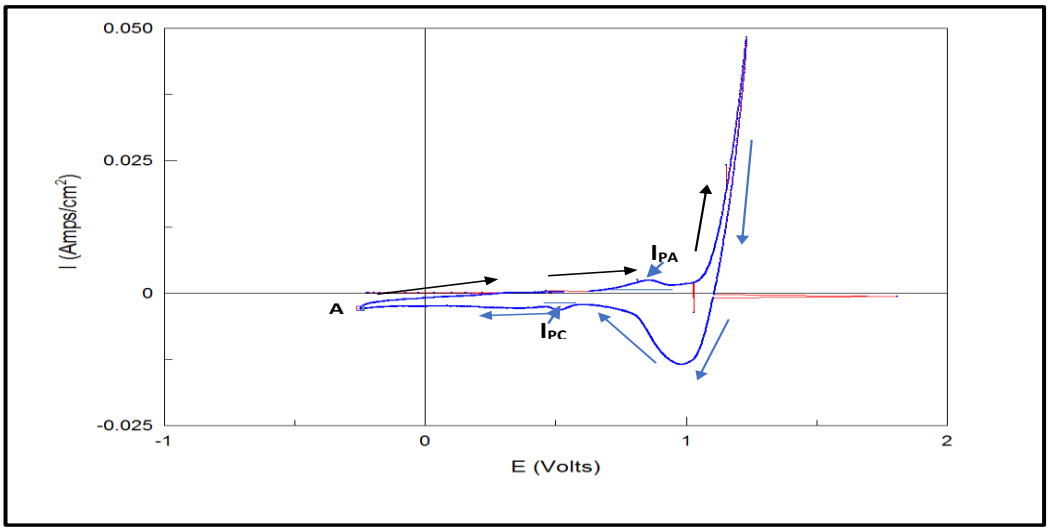

(e)

Figure 4.9: CV curves of (a) Au(III) solution without adsorbent, (b) heterogeneous mixture of D-AD and Au(III) solution before adsorption, (c) heterogeneous mixture of D-AD and Au(III) solution after adsorption for 24 h, (d) heterogeneous mixture of D-AD and Au(III) solution after adsorption for 96 h and (e) HCl without $AuCl_3$. WE: glassy carbon; RE: SCE; CE: Pt wire.

4.2.4 Conclusions

The cyclic voltammetry (CV) technique employed to study bio adsorption of gold showed the spontaneous reaction at the beginning of the adsorption, and slow redox reaction during adsorption. Using the CV results, it was confirmed that the process was irreversible after the adsorption process.

CHAPTER FIVE

THE ADSORPTION STUDY OF GOLD ON PRE-TREATED WOOD BARK IN ACIDIC AND BASIC MEDIA

Authors: Afolabi F. Ayeni, Shafiq Alam, and Georges J. Kipouros

Status of the paper: the paper is currently undergoing revision by Profs S. Alam and G. J. Kipouros. The paper is yet to be published due to some sensitive information contain there-in.

C**ontribution of the Ph.D. candidate**

I designed the experimental plan in collaboration with Profs S. Alam and G. J. Kipouros. All the specimen preparation and experimental work was performed by me. I performed all of the data analysis and wrote the first draft of the manuscript.

Contribution of this chapter to the overall study

The preparation of cedar wood bark into adsorbents using various concentration of acid solutions and subsequent adsorption test of the adsorbents in gold solution are contained in this chapter. The outcome of the test confirmed the development of a suitable bioadsorbent from wood bark for the extraction of gold, which is the first specific objective of this research work.

Notes on editing for the thesis:

To improve the flow of the thesis, the section of acknowledgements has been removed.

Abstract

This paper presents the research findings on the potential use of cedar wood bark as a source of biomass for the biosorption of gold (III) ions in solutions. Cedar wood bark was pre-treated with different concentrations of H_2SO_4 to prepare three efficient biosorbents, dilute air-dried (D-AD), concentrated not-washed-oven-dried (CNW-OD) and concentrated washed-air-dried (CW-AD) that were used to recover gold from gold (III) solutions. After testing the prepared adsorbents by initial one-point adsorption in prepared gold (III) solutions of hydrochloric acid (HCl), sodium thiourea (CH_4N_2NaS) and sodium thiosulfate ($Na_2S_2O_3$) lixiviant, the D-AD adsorbed about 99.996 % of the Au(III) in the acidic chloride solution, which was the highest adsorption capacity obtained when compared to the basic solutions. The FTIR characterization of the pre-treated wood bark before and after adsorption of gold ions in both the acidic and basic solutions confirm the interaction of the hydroxyl group with the gold ions and subsequent reduction of the ions and oxidation of the hydroxyl functional group to carbonyl functional group.

5.1 Introduction

The demand for gold in the global market has jolted researchers into their recovery from either ore or waste products of consumer electronics (urban mining). Given the scale of global demand for gold to store values, it is important to consider whether adequate resources of gold minerals are present in the earth's crust and technically available to meet our future needs; where increase recycling (or secondary recovery), improved material efficiency and demand management will play important roles. Technological progress in exploration, mining and processing minerals has been the key driver that has enabled supply to keep up with demand. This has generated interest in the discovery of more hydrometallurgical processes such as leaching process and adsorbent for gold adsorption. Recent research shows several techniques, such as, electrodialysis, chemical

precipitation, ion exchange, adsorption, being employed for the removal of gold from consumer electronics, wastewater or tailings [165]. Currently, gold mining industry produces the metal by leaching with cyanide (CN), followed by activated carbon as the main adsorbent for precious metals recovery. However, this method results into poisonous waste generation as cyanide counter ion is mostly used in the leaching process. High cost of activated carbon and huge energy input are other major setbacks of this method. Recently, biosorption process (biohydrometallurgy), which is the use of biomass-based materials as adsorbents for precious and base metal capture, have shown much promise in gold recovery from aqueous solutions. The adsorption process takes advantage of the physiochemical interaction between organic functional groups on biopolymers and charged metal ions. Common functional groups of the organic materials are amines, hydroxyls and carboxylic acids. Several biopolymers such as chitosan, wheat straw, tannins, lignin, and alfalfa [133, 166, and 9] have shown potential as biosorbents in the recovery of gold and other metals from aqueous solutions. For instance, wood bark, which is the biosorbent that was used in this research, is cellulose that is the most abundant naturally occurring polymers in the world, and to our knowledge, the adsorption capacity of metals using this abundant biomass is yet to be reported. Apart from being environmentally friendly, cedar wood bark is much available especially in North America, inexpensive and highly sustainable. The main objective of this paper is to present the potential of pre-treated cedar wood bark as an adsorbent in the recovery of gold from its solutions.

5.2 Experimental

5.2.1 Chemicals and instrumentations

The working solutions were prepared in glassware from laboratory grade gold (III) chloride (Acros Organics Company, New Jersey, USA) with analytical grade hydrochloric acid (HCl),

sodium thiourea (CH_4N_2NaS), sodium thiosulfate ($Na_2S_2O_3$) and de-ionized water. The wood bark was obtained commercially from a store in Saskatoon, Saskatchewan, Canada. Analytical grade sulfuric acid was purchased from Fischer Scientific for the Pre-treatment. Inductively coupled plasma optical emission spectrophotometer (ICP-OES) was used to analyze the metal concentration in the prepared samples. VWR shaker and Fischer Isotemp stirrer were used for the shaking of the solution with adsorbent and preparation of adsorbent respectively. VarioEl V4.01 CHNS elemental analyzer (Elementar Analysensyteme GmbH) and Fourier Transform Infrared-Attenuated Total Reflection Spectroscopy (Vertex 70 FTIR-ATR, Bruker Optics Inc., Billerica, MA, USA) were used for the analysis of the original cedar wood bark and biosorbent.

5.2.2 Preparation of the adsorbent

Three biosorbents, dilute -air dried (D-AD), concentrated not washed-oven dried (CNW-OD) and concentrated washed-air dried (CW-AD) were prepared from cedar wood bark biomass at different experimental conditions. The cedar wood bark used for this study was purchased from a store in Saskatoon. The cedar wood bark was believed not to have been treated with any chemicals because of its rot resistant, insect and water repellant property [138]. The wood bark was crushed and grinded to a particle size of 250 µm. The D-AD adsorbent was prepared with dilute acid (H_2SO_4) and the wood bark, mixed at ratio 10:1 in a 1000 mL beaker and placed on the Fischer Isotemp stirrer at a temperature of about 423 K (150^{o}C) and stirring speed of 350 rpm for 2 h. The temperature of the mixture was measured to be about 403 K (130^{o}C) using a thermometer. This elevated temperature for the experiment might have been achieved due to the affinity of H_2SO_4 for water (also very hygroscopic), low vapor pressure and high boiling point of about 610 K (337^{o}C) [167]. The mixture was filtered using Buckner filtration unit, and the residue was air dried at a room temperature of 298 K (25^{o}C) for 48 h. The CNW-OD and CW-

AD adsorbents were prepared with concentrated acid (H_2SO_4) and the wood bark, the procedure was followed except for the stirring temperature at 298 K (25^{o}C). The CNW-OD was not washed after filtration and it was oven dried at 338 K (65^{o}C) for 24 h, while the CW-AD was washed with deionized water after filtration and air dried for 48 h. Also used as adsorbent was the cedar wood bark as received.

5.2.3 Initial one-point adsorption

This was done to verify the capacity of the three prepared adsorbents and the original wood bark on the adsorption of gold (III) from the three solutions. Since this idea is novel, some assumptions were made on the ratio of adsorbent to solution, the concentration of gold solutions, temperature, stirring speed and time. About 20:1 g/L of gold (III) chloride in the three lixiviants (0.5 M HCl, 0.5 M CH_4N_2NaS and 0.5 M $Na_2S_2O_3$), 298 K (25^{o}C), stirring speed of 200 rpm for 24 h were wildly guessed as experimental conditions respectively. The adsorbent/solution ratio was chosen to enable the adsorption process reached equilibrium within a short period of time. Each mixture of adsorbent and test solutions at this experimental condition was run using an orbital shaking incubator (VWR, Model 1570, Cornelius, Oregon, USA) for 24 h. Samples were filtered, and the residue determined using ICP-OES. The percentage of gold adsorbed was calculated using equation (2.3) [17]. The test was repeated thrice to minimize experimental error.

$$\%\ \text{adsorbed} = \frac{C_i - C_f}{C_i} \times 100$$

From the test, the most effective adsorbent and lixiviant were chosen.

5.2.4 Characterization of the wood bark

The elemental and FTIR analyses of the original cedar wood bark and preferred biosorbent were carried out using VarioEl V4.01 CHNS elemental analyzer (Elementar Analysensyteme GmbH) and Fourier Transform Infrared-Attenuated Total Reflection Spectroscopy (Vertex 70 FT-IR-ATR, Bruker Optics Inc., Billerica, MA, USA) respectively.

5.2.5 Adsorption tests

The adsorption tests carried out were solid/liquid ratio and effect of lixiviant concentration on adsorption of gold. The tests were repeated thrice to minimize experimental error.

5.2.5.1 Solid/liquid (S/L) ratio

After determining the adsorbent and solution for the research, solid/liquid ratio test was carried out to optimize the process. This was done by varying the ratio of the adsorbent to solution in the order of 0, 0.5, 1, 1.5, 2, 2.5, 4 mg/mL. The same experimental condition and procedure in initial one-point adsorption save ratio was used. Equation (2.3) was used to calculate the percentage of adsorption. The optimum S/L ratio was determined (after this ratio no significant increase in adsorption capacity was noticed).

5.2.5.2 Effect of lixiviant concentration on adsorption

The effect of lixiviant concentration on adsorption of Au(III) ion by the adsorbent was determined. Molarity of the lixiviant was varied thus; 0.1, 0.5, 1, 2, 3, 4 and 5 M. Using the optimum S/L ratio, the mixtures of the adsorbent and gold (III) chloride in various lixiviant concentrations were run using the shaking incubator at 298 K (25^{o}C) and stirring speed of 200 rpm for 24 h.

5.3. Results and Discussion

5.3.1 ICP-OES analysis of test solutions

The average assays of Au metal in the solution of various lixiviant were 105, 114 and 101 ppm for HCl, CH_4N_2NaS and $Na_2S_2O_3$ respectively.

5.3.2 Initial one-point adsorption

The initial one-point adsorption was very important in this study, especially in a novel one like this, because it was used to predict the adsorption capacity of each prepared adsorbent in gold solution prepared with various lixiviants (hydrochloric acid, ammonium thiosulfate and sodium thiourea). Figure 5.1 shows the percentage adsorption of original wood bark and the adsorbents in the gold solutions. The percentage of adsorption was plotted against the adsorbents. It is depicted in the figure that diluted air dried (D-AD) adsorbent in gold solution of HCl has the best adsorption capacity of about 99.996%. In comparison, it is evident that hydrochloric acid is more effective than other lixiviants for gold (III) adsorption using wood bark adsorbents. It is noteworthy that the presence of sulfur in other lixiviants might have been responsible for low adsorption capacity of Au ions by the adsorbent, because of the competitive sorption of Au ions, since sulfur has great affinity for gold.

The experimental error was about ± 5%.

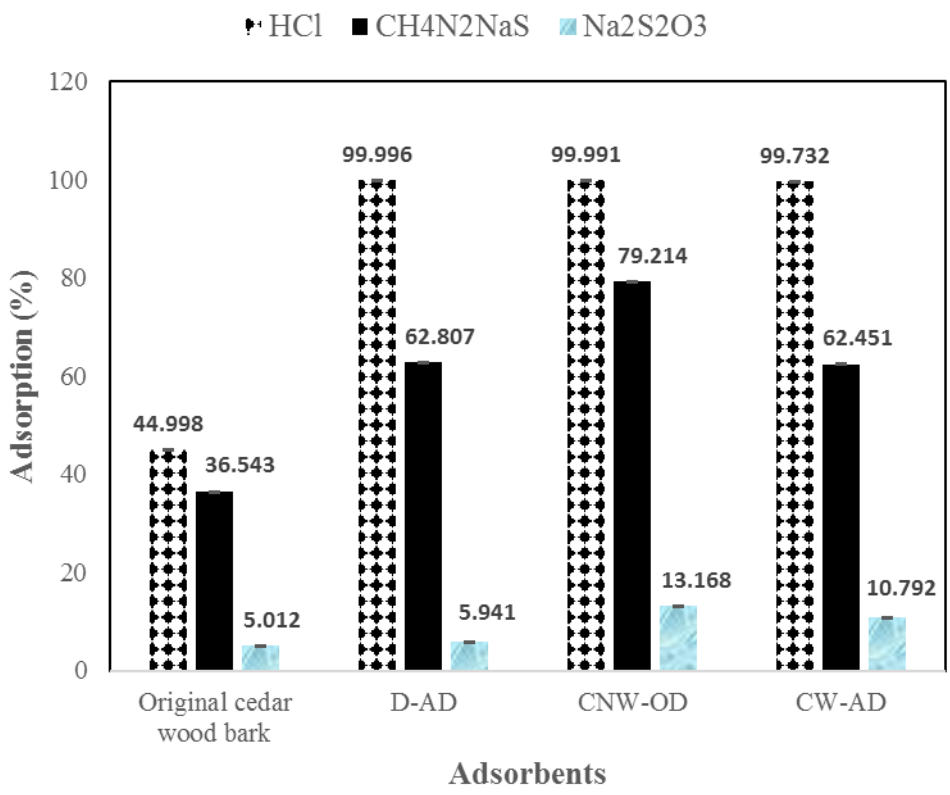

Percentage error: 5% .

Figure 5.1: Initial one-point adsorption plot of percentage adsorption in various Au(III) solutions vs adsorbents at a temperature of 25^{o}C, S/L ratio of 20:1 mg/mL, stirring speed of 200 rpm for 24 h. 105 ppm of Au in 0.5 M HCl, 114 ppm of Au in 0.5 M CH_4N_2NaS, and 101 ppm of Au in 0.5 M $Na_2S_2O_3$.

Although, CNW-OD and CW-AD in the same solution have 99.991 and 99.732 % adsorption capacity respectively, this might look as a slim difference, but if tonne of solution is under consideration, huge difference can be made in terms of recovery. Another consideration for choosing D-AD over others for the adsorption study was that the waste from the process would have less negative impact on the environment, less corrosion on application and cost effective because of low consumption of reagent [105].

5.3.3 Elemental CHNS analysis of the adsorbent

Table 5.1 shows CHNS results obtained from the wood bark prior and after pre-treatment with dilute H_2SO_4. The composition of sulfur in the wood bark prior to Pre-treatment was low and below 1% of the total mass, indicating that this biomass (wood bark) practically could not be used in its original form, for the recovery of gold, because sulfur has been reported to have great influence in the adsorption of gold. However, in comparison with the original wood bark, the Pre-treatment of the wood bark with sulfuric acid resulted in increase in the composition of sulfur from 0.037 % to 4.878, and decrease in carbon, hydrogen and nitrogen. The higher sulfur content introduced by the Pre-treatment was responsible for the cross-linking bonds between the natural polymeric chains (of the wood bark) according to Torget *et al*. concept [168]. Hence, the high sulfur content favors the recovery of gold. The wood bark used in the adsorption test is resinous [137], and resin has been reported to exhibit high affinity for gold [169].

Table 5.1: Elemental CHNS analysis of wood bark prior (to) and after pre-treatment.

Wood bark samples	Elemental analysis (% wt./wt.)			
	C	H	N	S
Before Pre-treatment	50.98	6.311	0.275	0.037
After Pre-treatment	44.06	5.652	0.188	4.878

5.3.4 FTIR spectrum for functional group determination

For the understanding of the difference between the composition of the original wood bark and that of pre-treated wood bark (D-AD), Fourier transform infrared spectroscopy (FTIR) was performed. The FTIR spectra of original wood bark and pre-treated wood bark are observed as shown in Figure 5.2 (a, b, c and d for comparison), which shows full spectra (4000 to 400 cm^{-1}). In Figure 5.2, the peaks appearing at 3397 cm^{-1} are attributed to the stretching frequency of hydroxyl, hydrogen bonded (O-H) groups of alcohols and phenol, while those at 2917 and 2850 cm^{-1} are stretching frequencies for carbon-hydrogen (C-H) bond. From these FTIR fingerprints, the peaks at 1633 and 1578 are assigned to secondary amine (NH), and those at 1155, 1135, 1025 and 1083 cm^{-1} are assigned to the general stretching of thiocarbonyl groups (C=S). The peak 1674 cm^{-1} is attributed to the presence of carbonyl (C=O) group. Comparing Figures 5.2a, 5.2b, 5.2c and 5.2d it is observed that carbonyl group becomes stronger with sharper peak (1674 cm^{-1}) in Figures 5.2b, 5.2c and 5.2d, and the difference in these peaks could be due to the cross-linking between the polymeric chains by the increase in sulfur composition of the pre-treated wood bark.

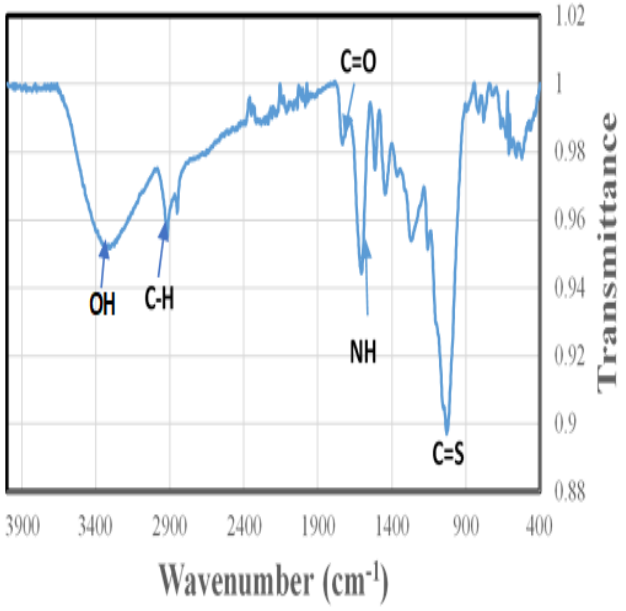
C=O
OH
C-H
NH
C=S
1.02
1
0.98
0.96
0.94
0.92
0.9
0.88
Transmittance
3900
3400
2900
2400
1900
1400
900
400
Wavenumber (cm-1)

(a)

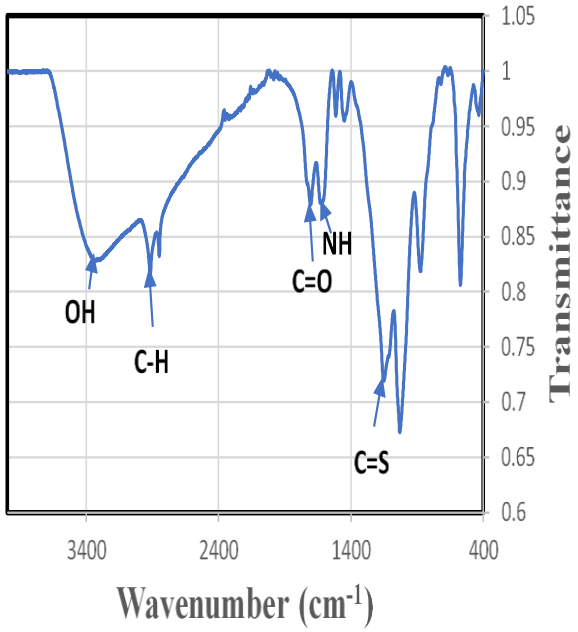
OH
C-H
NH
C=O
C=S
1.05
1
0.95
0.9
0.85
0.8
0.75
0.7
0.65
0.6
Transmittance
3400
2400
1400
400
Wavenumber (cm-1)

(b)

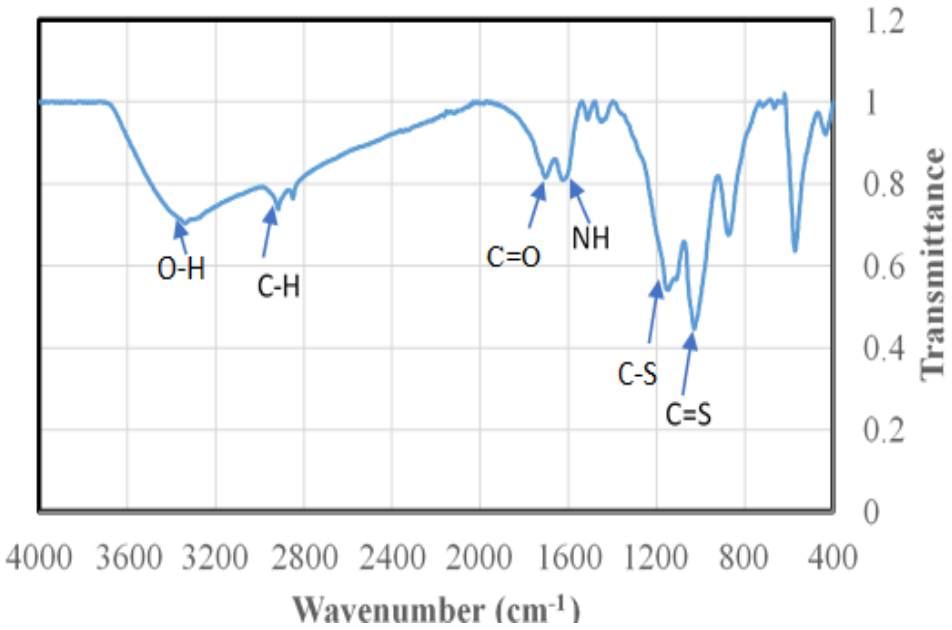
O-H
C-H
C=O
NH
C-S
C=S
1.2
1
0.8
0.6
0.4
0.2
0
Transmittance
4000
3600
3200
2800
2400
2000
1600
1200
800
400
Wavenumber (cm-1)

(c)

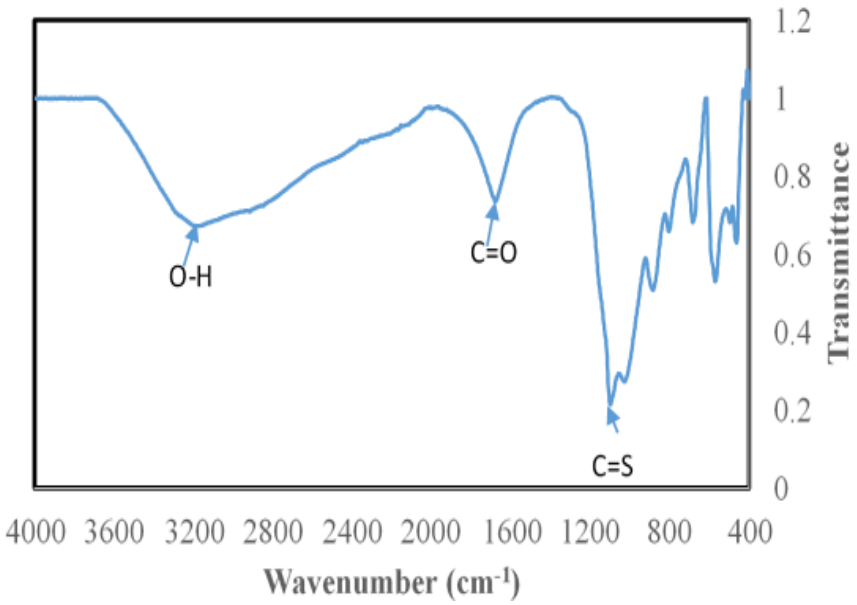

(d)

Figure 5.2: FTIR spectra for (a) original wood bark, (b) pre-treated wood bark (D-AD adsorbent), (c) pre-treated wood bark (CW-AD) and (d) pre-treated wood bark (CNW-OD).

From Figure 5.2d, there is no presence of C-H bond (2917 and 2815 cm^{-1}) which might have been due to the breaking down of this bond by the concentrated sulfuric acid [169, 170, 171, and 172].

5.3.5 Adsorption study

The solid/liquid (S/L) ratio was determined and the outcome is presented in Figure 5.3. The Figure shows that at S/L of 0 mg/mL there was 105 ppm of Au(III) in the solution, and as the ratio increased the concentration of Au(III) reduced until 1.5 mg/mL, where the concentration of Au(III) that remained in the solution did not have any significant difference as the ratio increased

to 4 mg/mL. Hence the choice of 1.5 mg/mL as an optimum and moderate S/L ratio, because after this point there was no considerable or significant increase in the gold (III) adsorbed.

The adsorption test of Au(III) on D-AD adsorbent at different concentrations of the HCl medium is depicted in Figure 4.4. From the figure, quantitative adsorption of Au(III) was observed at the lower HCl concentration and this was found to be reducing as the HCl concentration increased. This decrease in adsorption with increase in HCl had been attributed to the competitive sorption of chloride ions with the chloroaurate anion during the electrostatic interaction of the anionic species of Au(III) with oxonium centre of the adsorbent [168].

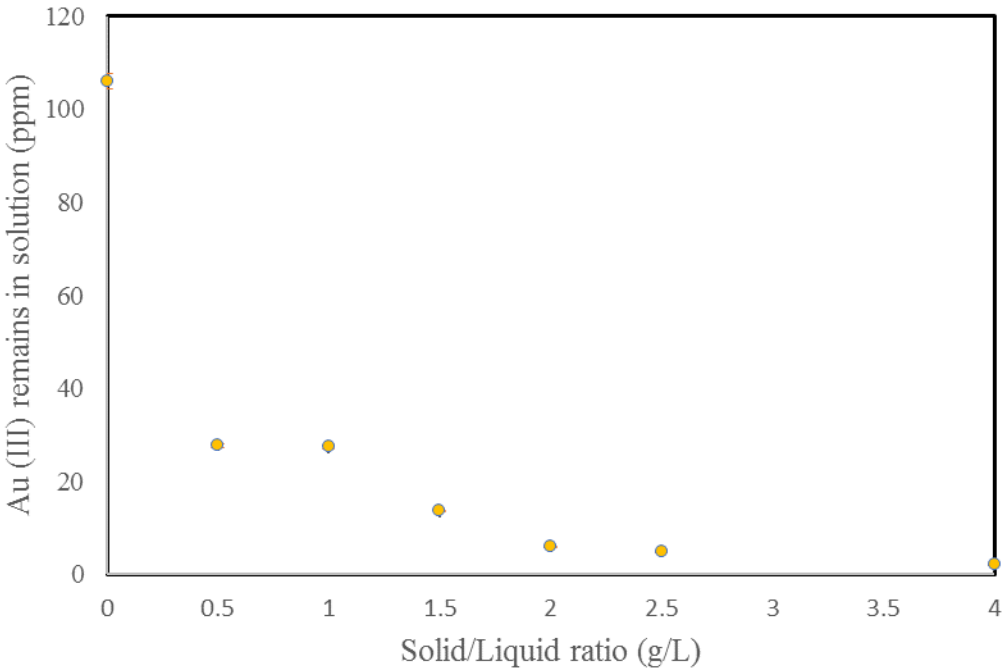

Percentage error: 5%

Figure 5.3: Concentration of Au(III) in solution under different loading conditions, 105 ppm of Au in 0.5 M HCl at 25^{o}C, stirring speed of 200 rpm for 24 h.

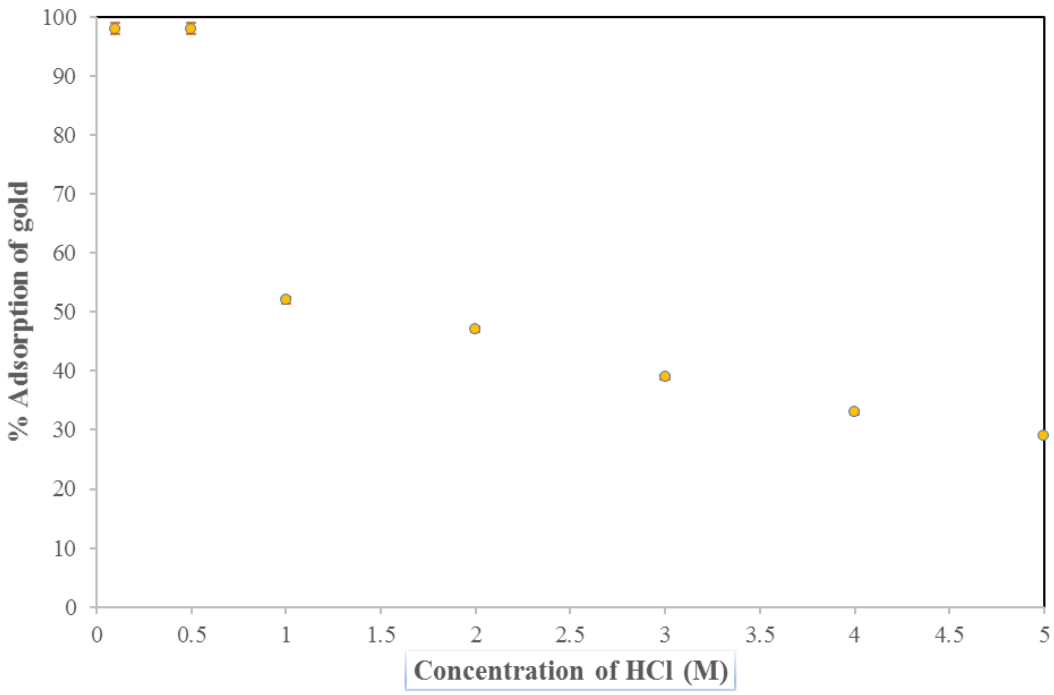

Percentage error: 5%

Figure 5.4: Effect of HCl concentration on percentage adsorption of Au(III) at S/L ratio of 1.5, shaking speed of 200 rpm, at 25^{o}C for 24 h.

5.4 Conclusions

This study has presented the potential use of cedar wood bark as a source of biomass for the biosorption of gold (III) ions from acidic chloride solution. Initial one-point adsorption has shown that 99.996 % of gold ion was obtained by using D-AD adsorbent in chloride solution. The research has proven that pre-treated wood bark adsorbed gold ions better in acidic than basic media. The FTIR characterization of the pre-treated wood bark before and after adsorption confirmed the interaction of the hydroxyl group with the chloroaurate ions and oxidation of the hydroxyl functional group to carbonyl functional group.

CHAPTER SIX

THE KINETIC AND THERMODYNAMIC STUDY OF GOLD BIOSORPTION FROM ACIDIC CHLORIDE SOLUTION- WOOD BARK AS A POTENTIAL BIO-ADSORBENT

Authors: Afolabi F. Ayeni, Shafiq Alam, Georges J. Kipouros

Status of the paper: the paper is currently undergoing revision by Profs S. Alam and G. J. Kipouros. The publication of this paper is kept on hold due to sensitive information contain there-in.

Contribution of the Ph.D. candidate

I designed the experimental plan in collaboration with Profs S. Alam and G. J. Kipouros. All the specimen preparation and experimental work was performed by me. I performed all of the data analysis and wrote the first draft of the manuscript.

Contribution of the chapter to the overall study

The chapter in conjunction with chapter five discusses the specific objectives two and three of the research work.

Notes on editing for the thesis:

To improve the flow of the thesis, elements that repeat what is discussed elsewhere have been removed. The introduction, portions of the experimental have been edited out, keeping only the information regarding batch adsorption kinetic test discussed in the manuscript. Elemental

CHNS analysis and FTIR Spectrum for functional group determination are sections edited from results and discussion. The acknowledgements section has been edited.

Abstract

This paper presents the evaluation of adsorption kinetics and thermodynamics of Au(III) onto pre-treated wood bark adsorbent in a chloride solution at different temperatures of 298, 303 and 313 K. Solution of $AuCl_3$ was prepared in 0.5 M HCl and analyzed by inductively coupled plasma optical emission spectrophotometer (ICP-OES). Pre-treatment of the wood bark was achieved by impregnating the wood bark with dilute H_2SO_4. The elemental CHNS analysis of the wood bark before and after pre-treatment shows an increase in the sulfur and oxygen contents from 0.037 and 42.397 % to 4.878 and 45.22 % respectively. This results in the cross-linking of the functional group and improved oxidation during adsorption process. The FTIR characterization of the adsorbent prior to and after adsorption indicates that the hydroxyl group oxidizes to carbonyl group. Heterogeneous mixtures of the solution and adsorbent were prepared and shaken at different temperature of 298, 303 and 313 K, and samples were taken at intervals. For the kinetic study, pseudo-second order model has correlation coefficients of 0.988, 0.996 and 0.998 at 298, 303 and 313 K respectively, while the pseudo-first order model has correlation coefficients of 0.91, 0.77 and 0.62 at the three different temperatures. Hence, the adsorption process follows the pseudo-second order model. The activation energy calculated from the pseudo-second order rate constant indicates that the process is chemisorption with a value of 59.86 kJ/mol. To determine the diffusion control of the adsorption, both intraparticle and liquid film rate-limiting diffusion controls are tested at the three temperatures. The outcome reveals that the liquid film diffusion has the tendency of controlling the process at 298 K. After shaking the mixture for 96 hours, precipitation of gold flakes by the bioadsorbent was observed visually, and

at 5- and 20-microns magnification. The FTIR and XRD tests also confirmed precipitation of gold.

6.1 Experimental

6.1.1 Batch adsorption kinetic test

The adsorption kinetic experiments were performed by shaking about 200 mL of gold chloride solution mixed with the bioadsorbent at a predetermined solid/liquid ratio of 1.5. The heterogeneous mixtures were shaking at three different temperatures of 298 K, 303 K and 313 K, at a speed of 200 rpm for 96 h. The tests were performed in a 300 mL Erlenmeyer flask and the various temperatures were maintained throughout the experiments. About 10 mL of the mixture samples were taken at different time intervals using micro-pipette. Each sampled mixture was filtered, and the filtrate was taken for analysis of residual metal concentration in the solution using ICP-OES. The amount of metal adsorbed at each time interval was calculated using the relationship of initial concentration and at time, t, to the quantity of metal adsorbed q_t as represented by equation 2.1 in chapter 2. The pseudo-first order and pseudo-second order kinetic equation [98, 170, and 171], intraparticle and liquid film diffusion model [134] are determined by equations 2.7, 2.9, 2.4 and 2.5 respectively.

The activation energy was used to determine whether the adsorption process is physical or chemical. This was achieved by employing Arrhenius equation as stated in equation 2.8.

6.2 Results and Discussion

6.2.1 Kinetics of gold (III) adsorption

Figure 6.1 depicts the amount of adsorption of gold (III) at any time (t), at various temperatures of 25^{o}C, 30^{o}C and 40^{o}C. The curves generated from the data show that the rate of adsorption of gold (III) on the wood bark increases with increase in temperature. The initial increase from 25^{o}C to 30^{o}C (5^{o}C increase) really had significant impact on the rate of adsorption. The adsorption process was very slow at 25^{o}C to the extent that quantitative adsorption (at equilibrium) was not achieved until about 48 h, while within 24 h, the quantitative adsorption (at equilibrium) was achieved at elevated temperatures of 30^{o}C and 40^{o}C. The percentage experimental error was about ±2%.

The adsorption kinetics of gold (III) on the wood bark was evaluated using the pseudo-first order, pseudo-second order, Intraparticle and liquid film diffusion models. These models were tested to interpret the data obtained from the kinetic experiment and the pseudo models are depicted in Figures 6.2 and 6.3, respectively.

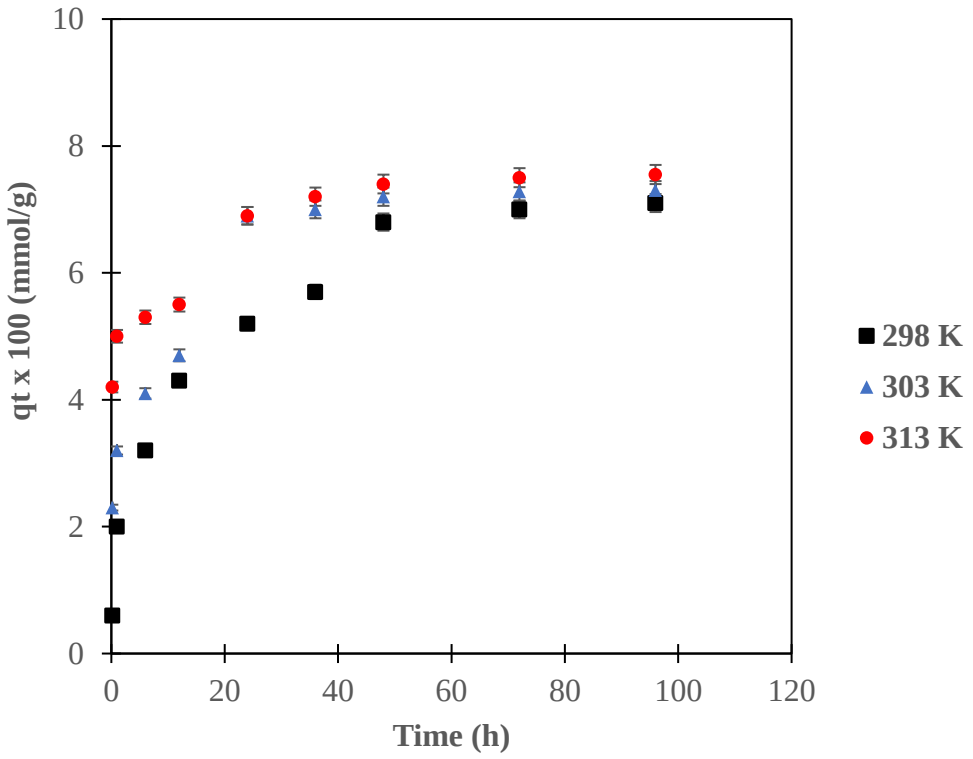

Percentage error: 2%

Figure 6.1: Experimental plot of adsorption of Au(III) on D-AD adsorbent versus shaking time at different temperatures of 25°C, 30°C and 40°C for 105 ppm $AuCl_3$ (0.5 M HCl).

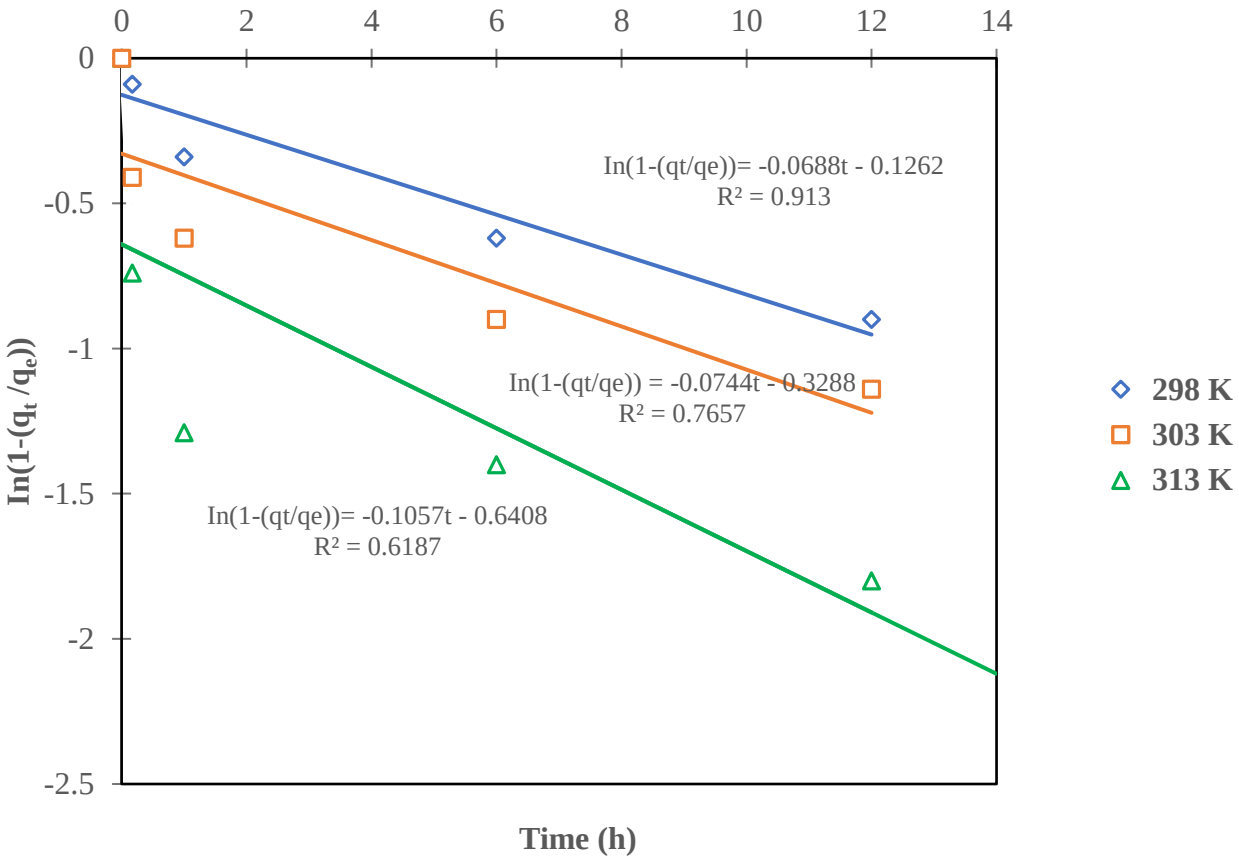

Figure 6.2: Pseudo-first order kinetic model for the adsorption of Au(III) on D-AD adsorbent at different temperatures of 25°C, 30°C and 40°C for 105 ppm $AuCl_3$ (0.5 M HCl).

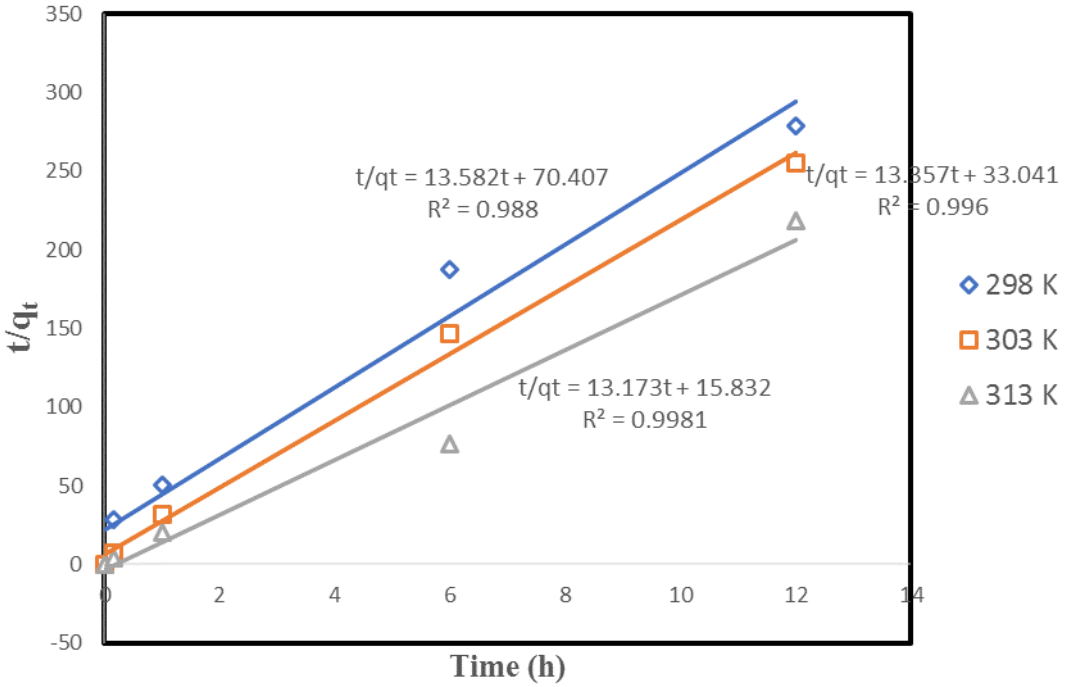

Figure 6.3: Pseudo-second order kinetic model for the adsorption of Au(III) on D-AD adsorbent at different temperatures of 25°C, 30°C and 40°C for 105 ppm $AuCl_3$ (0.5 M HCl).

Table 6.1 shows the comparison of the coefficient of determination obtained for pseudo-first order and pseudo-second order models at different temperatures of 25°C, 30°C and 40°C. The values obtained for the pseudo-second order model is consistent for the three temperatures, and higher than that of the pseudo-first order model. This indicates that the adsorption process followed the pseudo-second order model.

Table 6.1: Adsorption rate constants and coefficient of determination for the pseudo-first order and pseudo-second order kinetic models at different temperatures.

Temperatures (K)	Pseudo-first order rate constant (k_1) (h^{-1})	Determination coefficient (R_1^2)	Pseudo-second order rate constant (k_2) (h^{-1})	Determination coefficient (R_2^2)
298	0.16	0.91	2.62	0.988
303	0.17	0.77	5.4	0.996
313	0.23	0.62	11	0.998

6.2.2 Activation energy for adsorption of Au(III)

The activation energy could be used to determine whether the process is physical or chemical. The natural log of rate constant obtained from the pseudo-second order model, $In(k_{2})$, was plotted against the inverse of temperatures (1/T) in line with equation (2.9) as presented in Figure 6.4. The coefficient of determination obtained from the Arrhenius plot was 0.9997, and the slope was used to calculate the activation energy. The activation energy (E_a) value obtained for adsorption of Au(III) on the wood bark as calculated from the slope of the straight line was 59.86 kJ/mol [134]. This is much higher than the activation energy required for physical adsorption which is not greater than 4.2 kJ/mol, because the forces involved in physical adsorption are always weak. The activation energy for chemical sorption is between the range of 8.4 and 83.7 kJ/mol [169], because the forces involved are usually stronger than that of the physical adsorption. In this

present work, the significant high value for activation energy, and the increase in rate of reaction with temperature suggests that the adsorption of Au(III) on the wood bark is an activated chemisorption process. Chemical adsorption of Au(III) with biomass such as lignin and lysine has been earlier reported by Adhikari *et al.* and Parajuli *et al.* [7, 170].

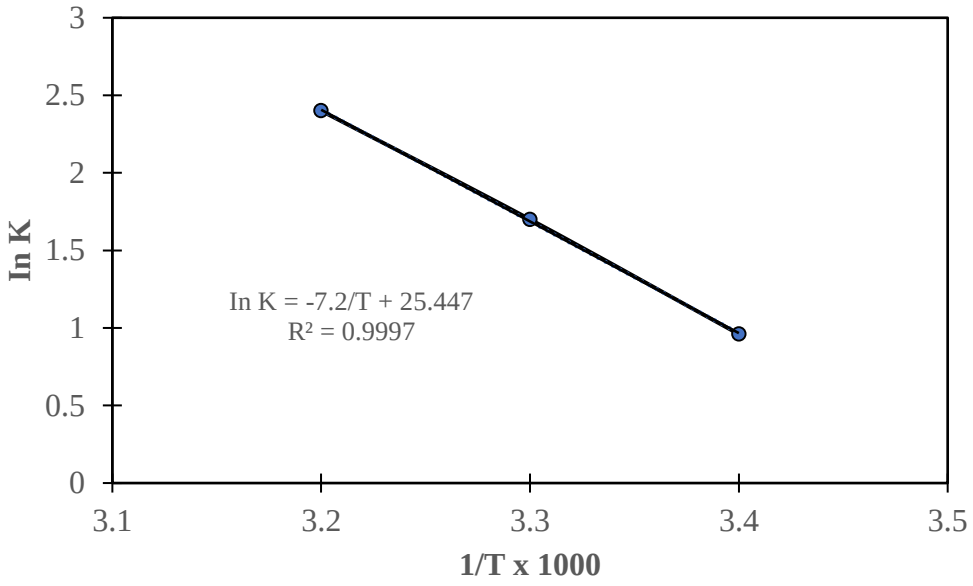

Figure 6.4: Arrhenius plot for the pseudo-second order rate constants of the Au(III) adsorbed on wood bark at 25°C, 30°C and 40°C for 105 ppm $AuCl_3$ (0.5 M HCl).

6.2.3 Diffusion control

The adsorption data of the kinetic study were processed to find out the diffusion control, and the intraparticle and liquid diffusion control were considered. In Figure 6.5, the intercepts obtained vary from 0.48 to 4.33 and the straight line did not pass through the origin, this indicated that the intraparticle diffusion might not be solely responsible for the rate controlling step of the process [134].

However, Figure 6.6 depicts the intercepts obtained from liquid film diffusion which varies from 0.19 to 0.96, this indicates that the liquid film diffusion is very close to the rate controlling step of the process, even though the straight line does not pass through the origin. In comparison, the liquid film diffusion might be inferred to be responsible for the process control of Au(III) adsorption with wood bark at a temperature of 298 K which has an intercept of 0.19 (≅ 0). The determination coefficients R^2, of the two diffusion control models are higher than 0.5, as shown in Table 6.2.

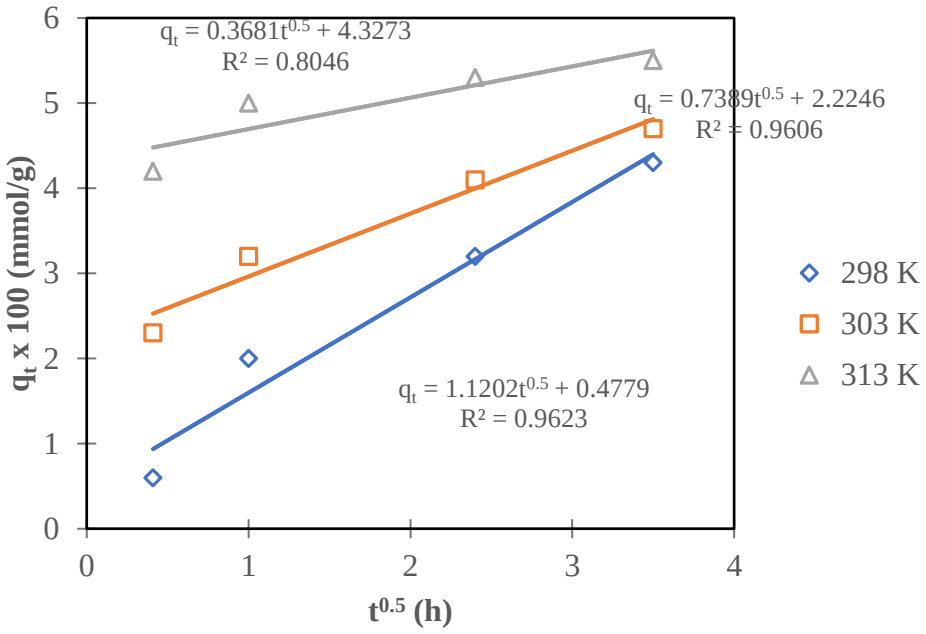

Figure 6.5: Intraparticle diffusion model for the adsorption of Au(III) at temperatures of 25°C, 30°C, and 40°C, at 250 µm adsorbent particle size.

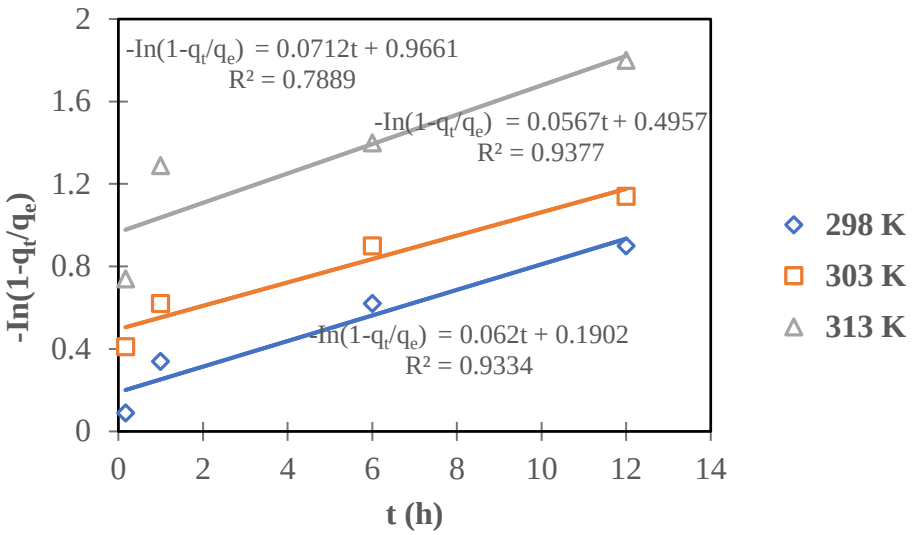

Figure 6.6: Liquid film diffusion model for the adsorption of Au(III) at temperatures of 25°C, 30°C, and 40°C.

Table 6.2: Intraparticle and liquid film diffusion rate constants for Au(III) onto D-AD adsorbent at temperature of 298, 303 and 313 K and particle size of 250 µm.

Temperature (K)	Intraparticle diffusion			Liquid film diffusion		
	K_{id} (mg/g $h^{0.5}$)	Intercepts	R^2	K_{fd} (h^{-1})	Intercepts	R^2
298	1.12	0.48	0.96	0.06	0.19	0.93
303	0.74	2.23	0.96	0.06	0.50	0.94
313	0.37	4.33	0.80	0.07	0.97	0.79

Table 6.2 depicts the effect of temperature on the intraparticle and liquid film diffusion kinetic model of the adsorption process. The increase in temperature resulted in the increase of the intercept which could be interpreted to be an increase in the initial rate of adsorption. However, the increase in temperature led to a decrease in diffusion rate constant which might be responsible for the decrease in adsorption capacity with time as shown in Figure 6.5. For liquid film diffusion model, the increase in temperature also led to an increase in the initial rate of adsorption as evident in the increase of the intercept, while the increase temperature has little or no effect on the adsorption capacity with time as shown in Figure 6.6

6.2.4 Adsorption isotherms

The adsorption test data were tested with two of the most widely used isotherm models in hydrometallurgical study, the Freundlich and Langmuir isotherm models. The Freundlich isotherm is based on multiple layers with uniform energy, while Langmuir isotherm explains the monolayer adsorption on active sites of the adsorbent. Freundlich and Langmuir models are presented in Figures 6.7 and 6.8 respectively and the corresponding parameters (isotherm constants) along with the determination coefficients are listed in Table 6.3. The R^2 value of Freundlich isotherm model is higher than that of Langmuir, hence the adsorption of Au(III) follows Freundlich multilayer adsorption with a constant value of 1, 103 mg/g.

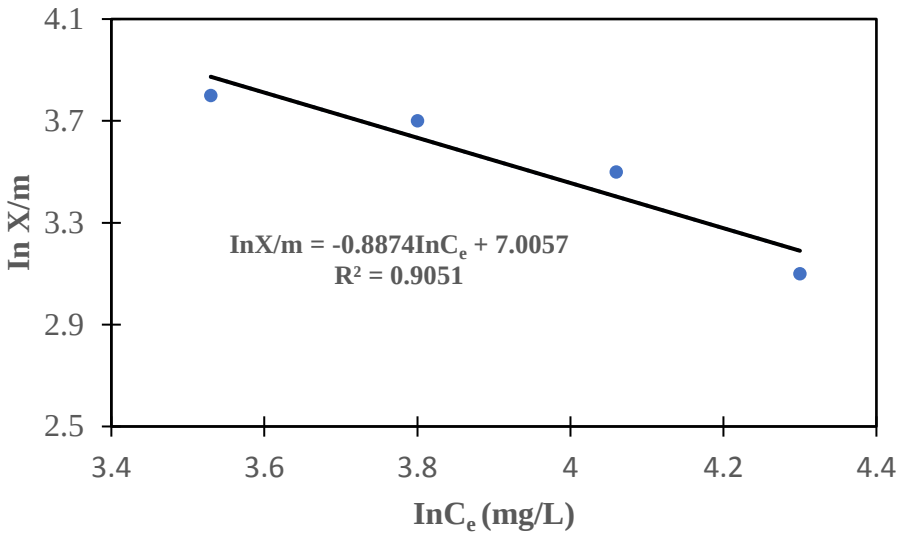

Figure 6.7: Freundlich adsorption isotherm at 303 K (30°C), 1.5 S/L ratios, contact time 12 h.

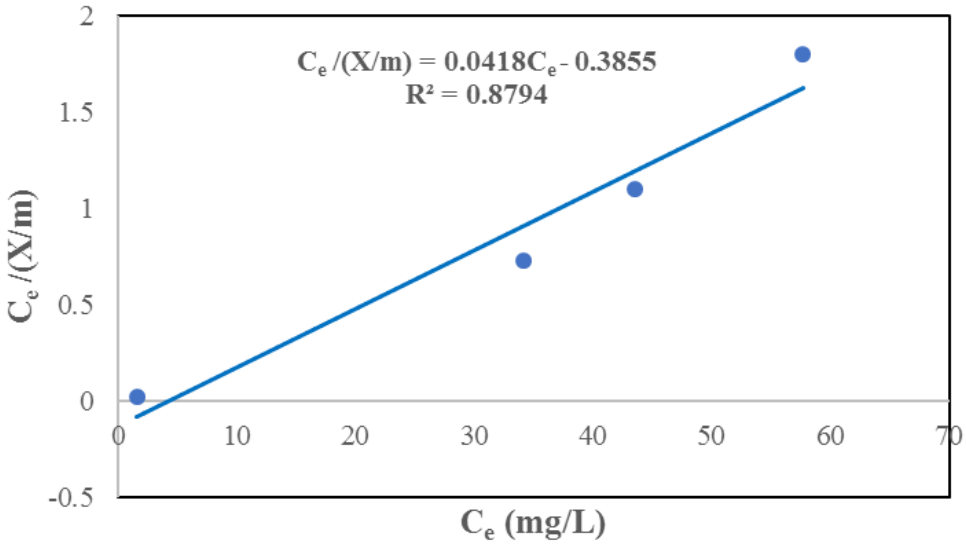

Figure 6.8: Langmuir adsorption isotherm at 303 K (30°C), 1.5 S/L ratio, contact time 12 h.

Table 6.3: Freundlich and Langmuir isotherm constants with determination coefficient.

	Au(III)
Freundlich	
K_F (mg/g)	1,103
N	1.13
R^2	0.9051
Langmuir	
Q_m (mg/g)	23.92
K_L	0.1
R^2	0.8794

6.2.5 Thermodynamics study of the adsorption

The influence of temperature on the adsorption of Au(III) was studied with 105 ppm initial metal concentration at 25°C (298 K), 30°C (303 K) and 40°C (313 K). The results indicate that the adsorption capacity increased with temperature and point that the adsorption is endothermic in nature. The thermodynamic parameters for the adsorption were calculated from the following equations [169]:

$$\Delta G^{o} = -RT \ln K_c \quad (6.1)$$

$$K_c = \frac{C_{Ae}}{C_e} \quad (6.2)$$

$$\log K_c = \frac{\Delta S^o}{2.30R} - \frac{\Delta H^o}{2.30RT} \quad (6.3)$$

Where R is the gas constant, K_c is the equilibrium concentration of metal on adsorbent, T is the temperature (K), C_{Ae} is the equilibrium concentration of Au(III) on D-AD adsorbent (mg/g), and C_e is the equilibrium concentration of Au(III) in the solution (ppm or mg/L).

Figure 6.9 depicts the Van't Hoff linear plot of log K_c versus 1/T. The values of ΔH^o and ΔS^o are calculated from the slope and intercept of the plot. The results are presented in Table 6.4. The negative values of ΔG^o could be attributed to the spontaneous nature of adsorption. The values of ΔG^o increase with an increase in temperature, resulting in more adsorption capacity at higher temperature. The positive value of ΔH^o indicates that the adsorption is endothermic, and the entropy term favours the adsorption process. Therefore, as the temperature increases, $T\Delta S^o$ term in the Gibbs free energy equation (6.4) would begin to predominate, and ΔG^o becomes negative value making the process to proceed. Positive and higher entropy showed that the adsorption process was irreversible within the first 12 h (Figure 6.9) on which the thermodynamic study of this process was based.

$$\Delta G^o = \Delta H^o - T\Delta S^o \quad (6.4)$$

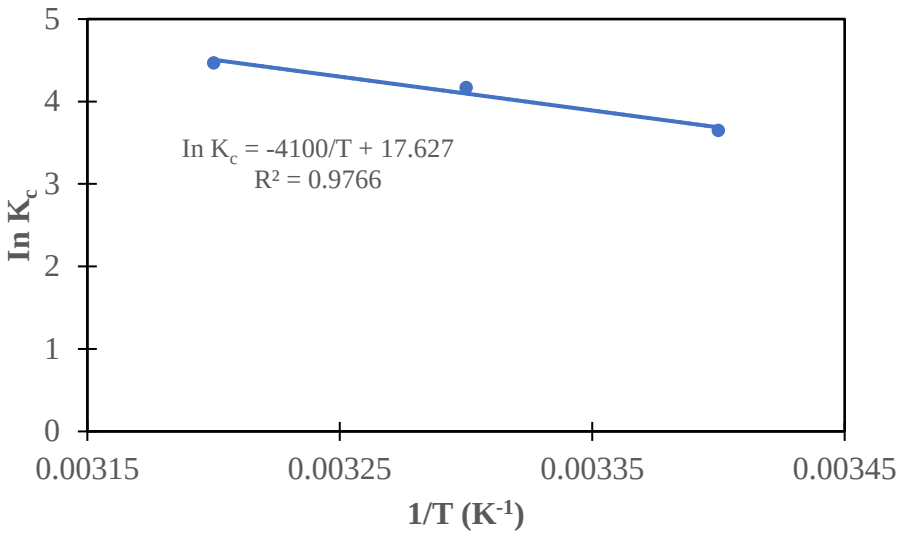

Figure 6.9: Van't Hoff plot for the adsorption of Au(III) onto D-AD adsorbent. Experimental conditions: 105 ppm Au(III) ion concentration; temperature: 25°C (298 K), 30°C (303 K) and 40°C (313 K); contact time: 12 h.

Table 6.4: Thermodynamic parameters for the adsorption of Au(III) on the D-AD adsorbent.

Temp (K)	ΔG^0 (kJ/mol)	ΔH^0 (kJ/mol)	ΔS^0 (J/mol/K)	R^2
298	-20.1			
303	-21.7	78.3	330	0.9766
313	-25.1			

6.2.6 Reduction of Au(III) to elemental gold

Figure 6.10a shows the gold flakes residue after decantation of the equilibrium mixture of Au(III) solution and D-AD adsorbent, Figure 6.10b depicts gold flakes mixed with the adsorbent after drying at a magnification of 5 microns, while Figure 6.10c shows the 20 microns magnification of the gold in the mist of the adsorbent. The XRD spectra of the adsorbent before and after Au adsorption are shown in Figure 6.11(a and b respectively). Figure 6.11a shows a typical spectrum of cellulose at $2\theta = 20.5$ and Figure 6.11b depicts sharp peaks at $2\theta = 37.04$, 43.1, 63.55 and 76.7 which correspond to the typical values of elemental gold [169]. This confirms the reduction of Au(III) to elemental gold, and this is an evident that redox reaction has taken place. The FTIR analysis of the adsorbent before and after adsorption as shown in Figures 6.12a and 6.12b also suggested that the reduction of Au(III) to elemental Au might be due to the interaction between the hydroxyl group and the gold (III) chloride resulting into the oxidation of the hydroxyl group to carbonyl and simultaneous reduction of gold chloride to gold (III) as shown in reactions R_{10} to R_{13}. From the figures 6.12a and 6.12b, it is observed that the absorption intensity (or transmittance) of the adsorbent before adsorption is higher than that after adsorption, which indicates that the adsorbent has taken up the gold (III) leaving very little space for further adsorption as compared in Figure 6.13. The outcome of the Freundlich isotherm model which favors multilayer adsorption on the surface of the adsorbent could be used to confirm accumulation through metallic bond formation, thus leading to the formation of aggregates of metallic gold which clearly become gold flakes.

The weight difference was also used to confirm the precipitation of gold on the adsorbent. Equal volume of adsorbent before and after adsorption/precipitation was weighed. The difference of 60 mg in weight was measured.

(a)

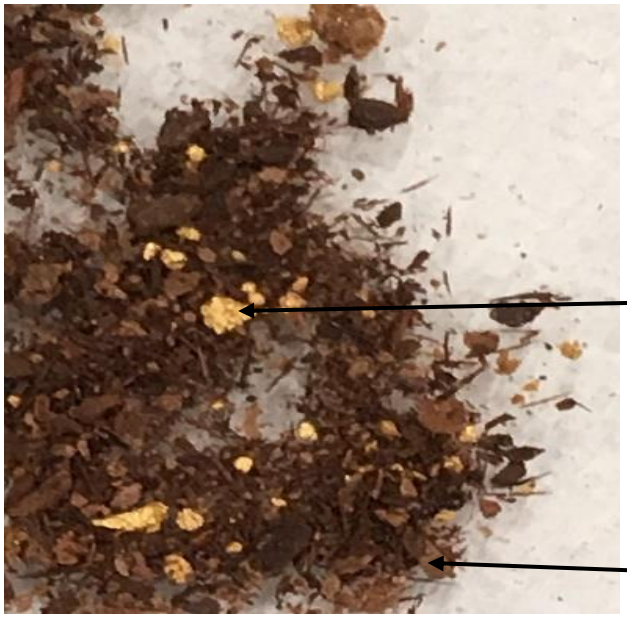

(b)

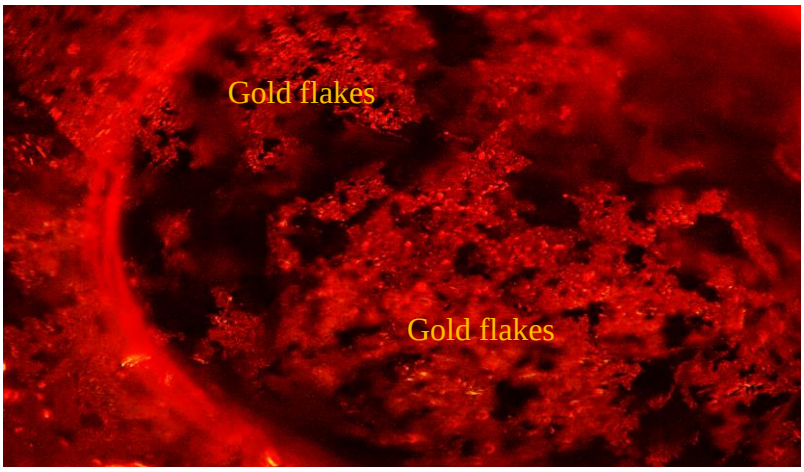

(c)

Figure 6.10: Observation of gold flakes confirmed by (a) visual, (b) magnifying app. 5 microns, (c) optical microscope 20 microns magnification.

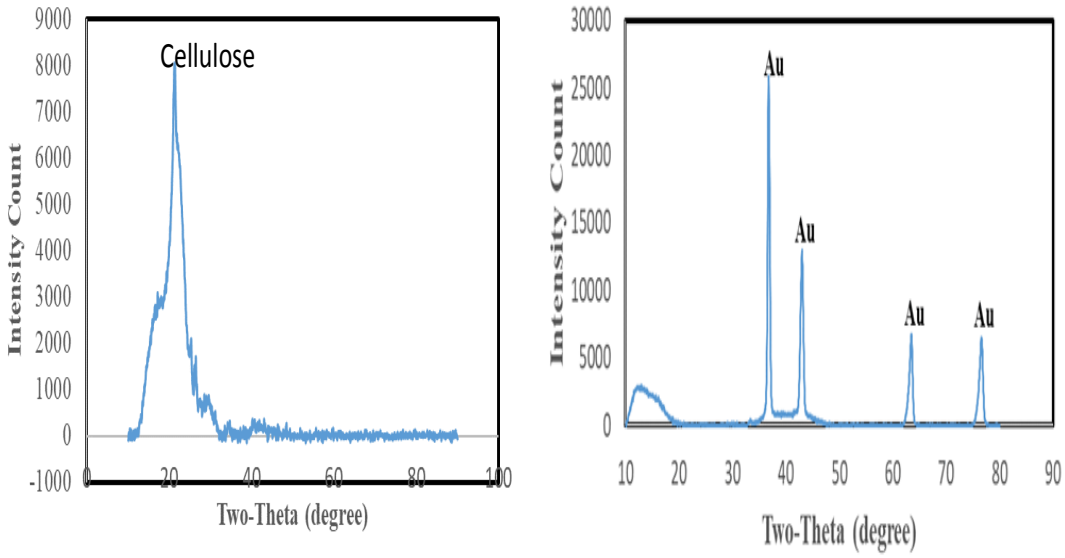

(a) (b)

Figure 6.11: XRD spectra of adsorbent (a) before adsorption and (b) after adsorption with evidence of gold precipitation at 298 K (25^{o}C), shaking speed of 200 rpm for 96 h.

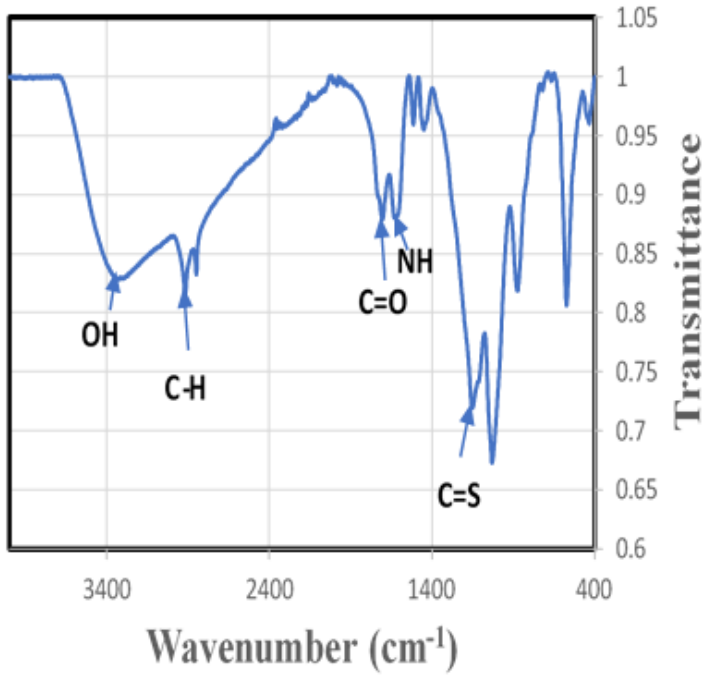

(a)

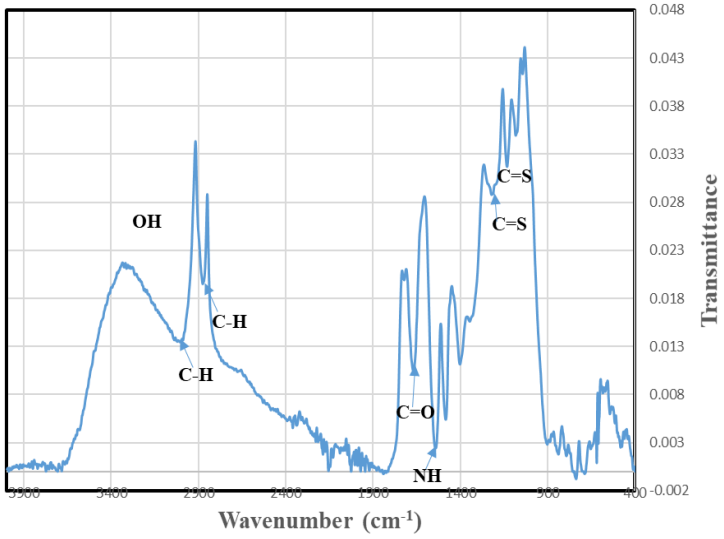

(b)

Figure 6.12: FTIR spectra of (a) adsorbent before adsorption, and (b) adsorbent after gold precipitation.

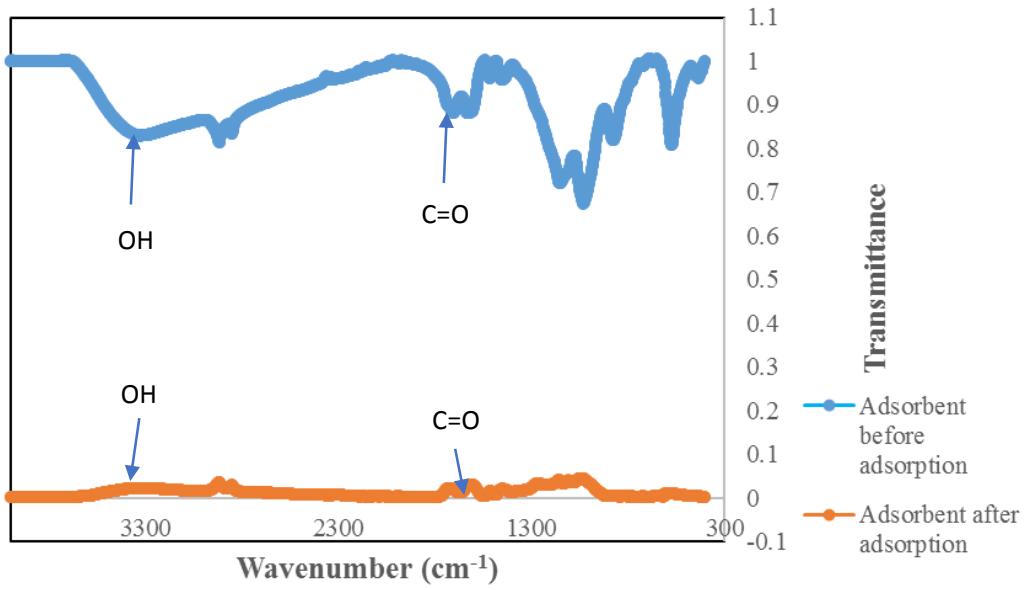

Figure 6.13: FTIR spectra comparing adsorbent before and after adsorption of gold

Redox mechanism:

$$AuCl_3 + HCl \rightarrow [AuCl_4]^-_{(s)} + H^+_{(aq)} \qquad R_{10}$$

Reduction:

$$[AuCl_4]^-_{(s)} + 3e^- \rightarrow Au(0)_{(s)} + 4Cl^-_{(aq)} \qquad R_{11}$$

Oxidation:

$$R - OH_{(s)} \rightarrow R = O_{(s)} + H^+_{(aq)} + e^- \qquad R_{12}$$

Overall redox:

$$[AuCl_4]^-_{(s)} + R - OH_{(s)} \rightarrow Au(0)_{(s)} + R = O_{(s)} + 3H^+_{(aq)} + 4Cl^-_{(aq)} \qquad R_{13}$$

6.3 Conclusions

The study evaluated the kinetics of Au(III) adsorption onto pre-treated wood bark adsorbent in a chloride solution of 0.5 M HCl at 298, 303 and 313 K. The adsorbent was found to be highly rich in resin with the presence of hydroxyl group, which has been reported to be a functional group in biomass that has affinity for Au(III). The elemental analysis of the wood bark before and after Pre-treatment established the increase in the sulfur and oxygen contents after Pre-treatment. These might have resulted in the cross-linking of the functional group and improve oxidation during the adsorption process. The FTIR characterization of the adsorbent prior to and after adsorption indicated that the hydroxyl group was oxidized to carbonyl group because of reduction of Au(III) to Au aggregate in the heterogeneous solution. For the kinetic study, pseudo-second order model has better correlation coefficient than the pseudo-first order model. The activation energy obtained suggested that the process was chemisorption considering the high E_a of 59.86 kJ/mol. For the diffusion control, liquid film has tendency of controlling the process.

The adsorbed A(III) was further reduced to Au (0) after an increase in the resident time. The change in FTIR spectra further revealed the formation of Au(0) which was attributed to the reducing functional group (hydroxyl) being oxidized to another functional group (carbonyl). FTIR, XRD, magnifying glass and optical microscope were successfully engaged to study the gold precipitates after reduction of Au (III) ions to Au(0).

CHAPTER SEVEN

SUMMARY, CONCLUSIONS AND RECOMMENDATIONS

7.1 Summary

Cedar wood bark was pre-treated with different concentration of H_2SO_4 to prepare three efficient biosorbents, D-AD, CNW-OD and CW-AD, that could be used to recover gold from gold (III) solutions. After testing the prepared adsorbents through initial one-point adsorption in prepared gold (III) solutions of HCl, CH_4N_2NaS and $Na_2S_2O_3$ lixiviants, the dilute air dried (D-AD) adsorbed about 99.997 % of the Au(III) in HCl. The outcome of the performance of the D-AD adsorbent in the gold acid solution achieved the first specific research objective of developing a bioadsorbent for the extraction of gold from solution. The second specific objective was achieved with the characterization of the D-AD adsorbent using Elemental analysis, and FTIR techniques. Adsorption test was performed in various concentration of acidic lixiviant (HCl) and it was found that 0.5 M HCl concentration gave the highest percentage adsorption of 99.99%. When the test for loading ratio of the adsorbent to lixiviant was performed, the loading (Solid/Liquid) ratio of 1.5 gave optimum gold (III) adsorption. All tests were repeated thrice to minimize error. A pseudo-second order kinetic model clearly favored the kinetic studies conducted at various temperature. The kinetic model helped in the estimation of the activation energy to be 59.86 kJ/mol making the process chemisorption. Liquid film diffusion control was found to have the tendency of controlling the rate-limitation of the process at 25^oC (298 K). The adsorption of Au(III) ion on the D-AD adsorbent at 30^oC (303 K) followed the Freundlich multilayer adsorption. The rate of adsorption increased with temperature making the process an endothermic in nature, resulting in entropy term favoring the reaction. The rate of adsorption

obtained at 298 K, 303 K and 313 K after 96 h was 7.1 x 10^{-2} mmol/g, 7.5 x 10^{-2} mmol/g and 7.9 x 10^{-2} mmol/g respectively (Figure 6.1), and these were indications that the adsorption of gold on bioadsorbent was determined. The fourth specific research objective was achieved by the electrochemical study of the adsorption via cyclic voltammetry (CV) technique. The CV peaks showed the spontaneous reaction at the beginning of the adsorption, and slow redox reaction during adsorption. Using the CV results, it was confirmed that the process was irreversible at the time of measurement.

The adsorbed Au(III) was further reduced to Au (0) after an increase in the resident time to 96 h. The formation of Au (0) flakes was attributed to the reducing functional group (hydroxyl) being oxidized to another functional group (carbonyl.

This study presented the efficacy of cedar wood bark as a potential biosorbent for the recovery of gold from acidic chloride media.

7.2 Conclusions

This study has presented the potential use of cedar wood bark as a source of biomass for the biosorption of gold (III) ions from acidic chloride solution. The FTIR characterization of the pre-treated wood bark before and after adsorption confirmed the interaction of the hydroxyl group with the chloroaurate ions and subsequent reduction of the ions to Au(0) and oxidation of the hydroxyl functional group to carbonyl functional group. The kinetic studies of the adsorption followed pseudo-second order chemisorption with activation energy of 59. 86 kJ mol^{-1}. The adsorption process followed the Freundlich isotherm with multilayer adsorption, which might have been responsible for the precipitation of gold on the surface of the wood bark. The thermodynamics study suggested that increase in temperature favored the process to proceed. CV

was successfully used to study the redox reaction of tested solution, and the adsorption process. At the point of adsorption, the oxidation reaction peak started diminishing while the reduction peak became sharper, indicating that the process is an adsorption process coupled with reduction process. FTIR, XRD, and optical microscope were engaged to study the gold precipitates after reduction of Au(III) ions to Au(0). For the FTIR and XRD study, the spectra of the adsorbent before and after adsorption were compared and the presence of gold was clearly shown. Magnifying glass clearly depicts the grains of gold in the adsorbent and the optical microscope features indicated the presence of gold aggregates in the mist of the wood bark adsorbent.

7.3 Recommendations

The positive results obtained from this project is an indication to build on its success in the future works. Hence, the following highlighted recommendations are made:

- The wood bark adsorbent should be tested in a real leached solution of gold
- The resident time of adsorption could be increased to improve the thermodynamics study of the process at equilibrium
- The use of cedar wood bark for adsorption of gold in cyanide solution could be investigated
- Wood barks from other tree species should be prepared and tested as adsorbents with various particle sizes and agitation speeds.

7.4 Contributions to Knowledge Development

This study provided information on the composition of bioadsorbent generated from cedar wood bark and established the percentage adsorption, adsorption capacity, adsorption kinetics and thermodynamics of the process in respect to gold adsorption in a benign environment.

REFERENCES

1. Wang, J., Chen, C. (2009), Biosorbents for Heavy Metals Removal and their Future Biotechnology Advances**,** Vol. 27, No. 2, 195 – 226.

2. Mack, C., Wilhelm, B., Duncan, J. R., Burgess, J. E. (2007)**,** Biosorption of Precious Metals, Biotechnology Advances**,** 25 (3), 264 – 271.

3. Kratochvil, D., Volesky, B. (1998), Advances in the Biosorption of Heavy Metals, Trends in Biotechnology**,** 16 (7), 291 – 300.

4. Barakat, M. A., Mahmoud, M. H. H. (2004), Recovery of Platinum from Spent Catalyst, Hydrometallurgy, 72, 179 – 184.

5. Jeffrey, M. I. (2001), Kinetic Aspects of Gold and Silver Leaching in Ammonia–Thiosulfate Solutions, Hydrometallurgy 60, 7 – 16.

6. Feng, D and Van Deventer, J. S. J. (2001), Preg-Robbing Phenomena in the Thiosulphate Leaching of Gold Ores, Minerals Engineering, 14 (11), 1387 – 1402.

7. Adhikari, B. B., Gurung, M., Alam, S., Tolnai, B., Inoue, K. (2013), Kraft Mill Lignin – A Potential Source of Bio-Adsorbents for Gold Recovery from Acidic Chloride Solution, Chemical Engineering Journal, 231, 190 – 197.

8. Kim, Y. H., Ogata, T. and Nakano, Y. (2007), Kinetic Analysis of Palladium (II) Adsorption Process on Crosslinked-Tanin Gel Based on Redox Reaction Models, Water Res. 41, 3043 – 3050.

9. Gamez, G., Gardea-Torresdey, J. L. and Tiemann, K. J. (2003), Recovery of Gold (III) from Multi-Elemental Solutions by Alfalfa Biomass, Adv. Environ. Res., 7, 563 – 571.

10. Ramesh, A., Hasegawa, H., Sugimoto, W., Maki, T., Ueda, K. (2008), Adsorption of Gold (III), Platinum (IV) and Palladium (II) onto Glycine Modified Crosslinked Chitosan Resin, Bioresource Technology 99, 3801–3809.

11. Won, S. W., Maob, J., Kwak, I. S., Sathishkumar, M., Yun, Y. S. (2010), Platinum Recovery from ICP Wastewater by A Combined Method of Biosorption and Incineration, Bioresource Technology 101, 1135–1140.

12. http://sciencentes.org/printable-periodic-table/, accessed on October 11, 2018.

13. Morf, L. S., Gloor, R., Haag, O., Haupt, M., Skutan, S., Lorenzo, F. D., Böni, D. (2013), Precious Metals and Rare Earth Elements in Municipal Solid Waste – Sources and Fate in A Swiss Incineration Plant, Waste Manage., 33, 634 – 644.

14. Muchova, L., Bakker, E., Rem, P. (2009), Precious Metals in Municipal Solid Waste Incineration Bottom Ash, Water Air Soil Pollut. Focus, 9, 107–116.

15. Huismann, J., Magalini, F., Kuehr, R., Maurer, C., Ogilvoe, S., Poll, J., Delgado, C., Artim, E., Szlezak, J., Stevels, A. (2007), 2008 Review of Directive 2002/96 on Waste Electrical and Electronic Equipment (WEEE) Final Report, ENV.G.4/ETU/2006/0032, United Nations University, Bonn, Germany.

16. Cui, J., Zhang, L. (2008), Metallurgical Recovery of Metals from Electronic Waste: A Review, J. Hazard. Mater., 158, 228–256.

17. Park, Y. J., Fray, D. J. (2009), Recovery of High Purity Precious Metals from Printed Circuit Boards, J. Hazard. Mater., 164, 1152–1158.

18. Wang, X., Gaustad, G. (2012), Prioritizing Material Recovery for End-Of-Life Printed Circuit Boards, Waste Manage., 32, 1903–1913

19. Das, N., (2010), Recovery of Precious Metals through Biosorption – A Review, Hydrometallurgy, 103, 180–189.

20. https://metgold.net/gold-nuggets/, accessed on October 20, 2018.

21. https://en.wikipedia.org/wiki/Gold, accessed on November 20, 2019.

22. World Gold Council, Gold Supply – Mining & Recycling", accessed on November 12, 2018.

23. U.S. Geological Survey, Mineral Commodity Summaries, January 2016" (PDF), USGS, 2016, accessed on November 30, 2018.

24. Mandaro, L. (17 January 2008), "China now world's largest gold producer; foreign miners at door", Market Watch, accessed on September 10, 2018.

25. Beinhoff, C., Removal of Barriers to the Abatement of Global Mercury Pollution from Artisanal Gold Mining, accessed on December 02, 2018.

26. https://commons.wikimedia.org/wiki/File:Gold_-_world_production_trend.svg, accessed on November 21, 2018.

27. O'Connell, R. (2007), Gold Mine Production Costs up by 17% in 2006 while Output Fell, archived from the Original on 6 October 2014, accessed on November 3, 2018

28. Noyes, R. (1993), Pollution Prevention Technology Handbook, William Andrew, 342.

29. Pletcher, D., Walsh, F. (1990), Industrial Electrochemistry, Springer, 244.

30. Marczenko, Z., María, B. (2000), Separation, Preconcentration, and Spectrophotometry in Inorganic Analysis, Elsevier, 210.

31. Soos, A. (2011), Gold Mining Boom Increasing Mercury Pollution Risk, Advanced Media Solutions, Inc. Oilprice.com, accessed on September 30, 2018.

32. Country Wise Gold Demand, accessed on October 21, 2018.

33. Harjani, A., It's official: China overtakes India as top Consumer of Gold, accessed on August 28, 2018.

34. Abdul-Wahab, S. A., Ameer, M., F. (2011), The Environmental Impact of Gold Mines: Pollution by Heavy Metals, Central European Journal of Engineering, 2 (2), 304–313.

35. Summit declaration, Peoples' Gold summit, San Juan Ridge, California in June 1999, Scribd.com (2012), accessed May 14, 2018.

36. Death of a River, BBC News (15 February 2000), accessed on July 28, 2018.

37. Cyanide spill second only to Chernobyl, Abc.net.au. 11 February 2000, accessed on December 4, 2017.

38. "Pollution from Artisanal Gold Mining, Blacksmith Institute Report 2012, accessed on August 20, 2018.

39. U.S. Geological Survey, Mineral Commodity Summaries, USGS, 2017, accessed on May 29, 2018.

40. Gold Demand Trends, accessed on November 30, 2017.

41. www.goldbroker.com/charts/gold-price/cad, accessed on November 3, 2018.

42. Norgate, T., Haque, N. (2012), Using Life Cycle Assessment to Evaluate Some Environmental Impacts of Gold, Journal of Cleaner Production, 29–30.

43. Shepard, K., McNeill, R. J., Merchant, C. (2004), Encyclopedia of World Environmental History, 3, 597.

44. Kean, W. F., Kean, I. R. (2008), Clinical Pharmacology of Gold, Inflammo-pharmacology, 16 (3), 112–25.

45. Mortier, T. (May 2006), An Experimental Study on the Preparation of Gold Nanoparticles and their Properties, PhD thesis, University of Leuven.

46. Richards, D. G., McMillin, D. L., Mein, E. A., Nelson, C. (2002), Gold and its Relationship to Neurological/Glandular Condition, The International Journal of Neuroscie-nce, 112 (1), 31–53.

47. Bozzola, J. J., Russell, L. D. (1999), Electron Microscopy: Principles and Techniques for Biologist, Jones & Bartlett Learning, 65.

48. The Demand for Gold by Industry, Gold Bulletin, accessed on June 12, 2018.

49. Wills, B. A. (1988), Mineral Processing Technology 5th Edition, Pergamon Press, 8 – 45.

50. Wilson, R. J., El-Raheim, F. H. (2003), The Application of Mineral Processing Techniques for the Recovery of Metal from Post-Consumer Wastes, Journal of Mineral Engineering, 7(8), 85 – 96.

51. Ajaka, E. O. (2009), Recovering Fine Iron Minerals from Itakpe Iron Ore Process Tailing, ARPN Journal of Engineering and Applied Sciences, 4(9), 56-70.

52. Sutherland, D. N., Maria, B. (2002), Guiding Process Developments by Using Automated Mineralogical Analysis, Mineral Processing Plant Design, Practice and Control Proceedings, 270.

53. Gupta, A., Yan, D. S. (2006), Flotation, Mineral Processing Design and Operation, Elsevier Science, Amsterdam, 555 – 603.

54. El-Raheim, F. H. (2005), Some Aspects on Albite Grinding and Liberation, The European Journal of Mineral Processing and Environmental Protection, 5(2), 18 – 21.

55. Gottlieb, P., Kolvo, H. (2000), Applications of Automated Process Mineralogy Proceedings ICAM 2000, Gottingen Germany, 1, 13 – 16.

56. Gu, Y., Gu, K. (1998), Measuring and Modelling Mineral Liberation with the JKMRC/Philips MLA, Proceeding of Minerals Processing ’98 Conference, Cape Town.

57. Sutherland, D. N., Amankwa, R. K. (1991), Application of Automated Quantitative Mineralogy in Mineral Processing, Mineral Engineering International Journal, 4, 753 – 762.

58. Fillippoud, P., Grammah, .J (2010), Recovery of Metal Values from Copper-Arsenic Minerals and other related Resources, Journal of Mineral Processing and Extractive Metallurgy Review, 28(4), 247 – 298.

59. Wills, B. A., Napier-Munn, T. J. (2006), Will’s Mineral Processing Technology, Seventh Edition, Elsevier Science and Technology Books, ISBN: 0750644508.

60. Brent, H. (2000), Metallurgy Survey, Kirk-Othmer Encyclopedia of Chemical Technology, Wiley-VCH, Weinheim.

61. Adalbert, L. (2005), "Copper" in Ullmann's Encyclopedia of Industrial Chemistry, Wiley-VCH, Weinheim.

62. Habashi, F. (2009), Recent Trends in Extractive Metallurgy, Journal of Mining and Metallurgy, Section B: Metallurgy, 45, 1 – 13.

63. Oliva, P. C., AngeloMark, P. W. (2016), Coal Combustion from Power Plant Industry in Misamis Orienta, Philippines: A Potential Groundwater Contamination and Heavy Metal Detection, Asian Journal of Microbiology, Biotechnology and Environmental Sciences, 18(1), 55 – 59.

64. Hedjazi, F. and Monhemius, J. A. (2014), Copper – Gold Ore Processing with Ion Exchange and SART Technology, Minerals Engineering, ScienceDirect, 64, 120 – 125.

65. Alam, S. (2016), Thermodynamics and Kinetics of Hydrometallurgy Process, CHE 369 Lecture Notes 3, Department of Chemical and Biological Engineering, University of Saskatchewan, Saskatoon, Canada, 4 – 14.

66. Foo, K. Y, Hameed, B. H. (2010), Insights into the modelling of adsorption isotherm systems, Chemical engineering journal, 156 (1), 2 – 10.

67. Ho, Y. S., Ng, J. C. Y., McKay, G. (2000), Kinetics of Pollutant Sorption by Biosorbents: Review. Sep Purif Methods, 29, 189–232.

68. Weber, W. J. and Morris, J. C. (1963), Kinetic of Adsorption of Carbon from Solutions, Journal of Sanit. Eng. Div. Am. Soc. Civ. Eng. 89, 33 – 50.

69. Boyd, G. E., Adamson, A. W. and Myers, L. S. (1949), The Exchange Adsorption of Ions from Aqueous Solutions by Organic Zeolites 11 Kinetics, J. Am. Chem. Soc. 67, 2839 – 2844.

70. Keller, J. U., Staudt, R. (2005), Gas Adsorption Equilibria: Experimental Methods and Adsorption Isotherms, Springer, New York.

71. Ruthven, D. M. (1984), Principles of Adsorption and Adsorption Processes, Wiley, New York.

72. Vithanage, M., Mayakaduwa, S. S., Herath, I., Ok, Y. S., Mohan, D. (2016), Kinetics, Thermodynamics and Mechanistic Studies of Carbofuran Removal using Biochars from Tea Waste and Rice Husks, Chemosphere, 150, 781–9.

73. Zhou, L., Pan, S., Chen, X., Zha, Y., Zou, B., Jin, M. (2014), Kinetics and Thermodynamics Studies of Pentachlorophenol Adsorption on Covalently Functionalized Fe_3O_4 @ SiO_2–Mwcnts Core–Shell Magnetic Microspheres. Chem Eng J, 257, 10–19.

74. Sedlacek, Z. (1975), Isosteric Adsorption Heats in Correlation with Activation Energy of Diffusion, Chemical Papers 29 (3), 344 – 349.

75. Kyzas, G. Z., Kostoglou, M., Lazaridis, N. K., Lambropoulou, D. A., Bikiaris, D. N. (2013), Environmentally Friendly Technology for the Removal of Pharmaceutical Contaminants from Wastewaters using Modified Chitosan Adsorbents, Chem Eng J, 222, 248–58 .

76. Slimani, R., Anouzla, A., Abrouki, Y. (2011), Removal of a Cationic Dye -Methylene Blue- from Aqueous Media by the use of Animal Bone Meal as a New Low Cost Adsorbent, J Mater Environ Sci, 2, 77–87.

77. Regti, A., Laamari, M. R., Stiriba, S. E., El Haddad, M. (2017), Use of Response Factorial Design for Process Optimization of Basic Dye Adsorption onto Activated Carbon Derived from Persea Species, Microchem J, 130, 129–36.

78. Alberti, G., Amendola, V., Pesavento, M., Biesuz, R. (2012), Beyond the Synthesis of Novel Solid Phases: Review on Modelling of Sorption Phenomena, Coord Chem Rev, 256, 28–45.

79. Copper, Technology & Competitiveness, Diane Publishing, 1988, 142 – 143.

80. Lamphien, M., Laari, A., Turunen, I. (2015), Kinetic Model for Direct Leaching of Zinc Sulfide Concentrates at High Slurry and Solute Concentration, Hydrometallurgy 153, 160 – 169.

81. Kipouros, G. J. (2012), Group Presentation on the Thermodynamics and Kinetics of Hydrometallurgy Processing, Dalhousie University, 15 – 19.

82. Liu, Y., Wang, Z. W. (2008), Uncertainty of Preset-Order Kinetic Equations in Description of Biosorption Data. Bioresource Technology, 99, 3309–12.

83. Lin, C. I., Wang, L. H. (2008), Rate Equations and Isotherms for Two Adsorption Models, J Chin Inst Chem Eng, 39, 579–85.

84. Liu, Y., Yang, S. F., Xu, H., Woon, K. H., Lin, Y. M., Tay, J. H. (2003), Biosorption Kinetics of Cadmium(II) on Aerobic Granular Sludge, Process Biochem, 38, 997–1001.

85. Ho, Y. S. (2006), Review of Second order Models for Adsorption Systems, J Hazard Mater, 136, 681–9.

86. Liu, Y., Liu, Y. J. (2008), Biosorption Isotherms, Kinetics and Thermodynamics, Sep Purif Technol, 61, 229–42.

87. Plazinski, W., Rudzinski, W., Plazinska, A. (2009), Theoretical Models of Sorption Kinetics including a Surface Reaction Mechanism: a Review, Adv Colloid Interface Sci, 152, 2–13.

88. Lagergren, S. (1898), About the Theory of So-Called Adsorption of Soluble Substances, Kungliga Svenska Vetenskapsakademiens, 4, 1–39.

89. Freundlich, H. (1909), Kapillarchemie, eine Darstellung der Chemie der Kolloide und verwandter Gebiete. Akademische Verlagsgesellschaft

90. Hanaor, D. A. H., Ghadiri, M., Chrzanowski, W., Gan, Y. (2014), Scalable Surface Area Characterization by Electrokinetic Analysis of Complex Anion Adsorption, Langmuir**,** 30, 15143–15152.

91. Özer, A. (2007) Removal of Pb(II) Ions from Aqueous Solutions by Sulphuric Acid-Treated Wheat Bran. J Hazard Mater, 141, 753–61.

92. Plazinski, W., and Rudzinski, W. (2010), A Novel Two-Resistance Model for Description of the Adsorption Kinetics onto Porous Particles, Langmuir, 26, 802–8.

93. Esteghlalian, A., Hashimoto, A. G., Fenske, J. J. and Penner, M. H. (1997), Modeling and Optimization of the Dilute-Sulfuric-Acid Pre-Treatment of Corn Stover, Poplar and Switchgrass, Bioresource Technology 59, 129–136.

94. McKay, G., Otterburn, M. S. and Sweeny, A. G. (1979), The Removal of Colour from Effluent using various Adsorbents-III. Silica: Rate Process, Water Research 14, 15 – 20.

95. Abdel-Aal, E. A. (2000), Kinetics of Sulfuric Acid Leaching of Lo-Grade Zinc Silicate Ore, Hydrometallurgy 55, 247 – 254.

96. Santos, F. M. F., Pina, P. S., Porcaro, R., Oliveira, V. A., Silva, C. A., Leão, V. A. (2010), The Kinetics of Zinc Silicate Leaching in Sodium Hydroxide, Hydrometallurgy 102, 43 – 49.

97. Cheng, C. Y. and Lawson, F. (1991), The Kinetics of Leaching Chalcocite in Acidic Oxygenated Sulphate-Chloride Solutions, Hydrometallurgy 27, 249 – 268.

98. Qi, P. H. and Hiskey, J. B. (1991), Dissolution Kinetics of Gold in Iodide Solutions, Hydrometallurgy 27, 47 – 62.

99. Breuer, P. L. and Jeffrey, M. I. (2000), Thiosulfate Leaching Kinetics of Gold in the Presence of Copper and Ammonia, Minerals Engineering 13(10-11), 1071 – 1081.

100. Birloaga, I., Michelis, I., Ferella, F., Buzatu, M., Veglio, F. (2013), Study on the Influence of various Factors in the Hydrometallurgical Processing of Waste Printed Circuit Boards for Copper and Gold Recovery, Waste Management 33, 935 – 941.

101. Jeffrey, M. T., Breuer, P. L., Choo, W. L. (2001), A Kinetic Study That Compares the Leaching of Gold in the Cyanide, Thiosulfate, and Chloride Systems, Metallurgical and Materials Transactions 32(6), 979 – 986.

102. Habashi, F. (1995), Bayer's Process for Alumina Production: A Historical Perspective, Bull. Hist. Chem., 17/18, 15 – 19.

103. Marsden, J. D. and House, C. L. (2006), The Chemistry of Gold Extraction, The Society for Mining, Metallurgy, and Exploration (SME) (Second Edition), 102 – 265.

104. Nicol, M. J., Fleming, C. A., Paul, R. L., The Chemistry of Extraction of Gold, www.saimm.co.za/Conferences/ExtractmarsiveMetallurgyOfGold/0831-Chapter15.pdf, accessed on October 20, 2017.

105. Tabil, L., Adapa, P., and Kashaninejad, M. (2008), Biomass Feedstock Pre-Processing-Part 1: Pre-Treatment, Biofuel's Engineering Process Technology, 411 – 415.

106. Sun, Y. and Cheng, J. (2002), Hydrolysis of Lignocellulosic Materials for Ethanol Production: A Review, Bioresource Technology, 83(1), 1 – 11.

107. Cardona, C. A. and Sanchez, O. J. (2007), Fuel ethanol production: Process Design Trends and Integration Opportunities, Bioresource Technology, 98(12), 2415 – 2457.

108. Parveen, K. U., Diane, M. S. (2009), Methods for pretreatment of Lignocellulosic Biomass for Efficient Hydrolysis and Biofuel Production, Industrial Eng. Chem. Resources, 48(8), 3713 – 3729.

109. Wang, H., Tucker, M., Ji, Y. (2013), Recent Development in Chemical Depolymerization of Lignin: A Review, www.researchgate.net.

110. Hosea, M., Greene, B., McPherson, R., Henzel, M., Alexander, M.D., Darnall, D.W., (1986), Accumulation of Elemental Gold on the Alga *Chlorella vulgaris*, Inorganica Chimica Acta 123, 161–165.

111. Kuyucak, N., Volesky, B., (1989), Accumulation of Gold by Algal Biosorbent, Biorecovery 1, 189–204.

112. Gomes, N.C.M., Camargos, E.R.S., Dias, J.C.T., Linardi, V.R., (1998), Gold and Silver Accumulation by *Aspergillus niger* from Cyanide Containing Solution Obtained from the Gold Mining Industry, World Journal of Microbiology and Biotechnology 14, 149.

113. Matsumoto, M., Nishimura, Y., (1992), Recovery by *Aspergillus Oryzae* of Gold from Wastewater Gold Plating, Nippon Nougeikagakukaishi, 66, 1765–1770.

114. Karamuchka, V., Gadd, G.M., (1999), Interaction of *Saccharomyces cerevisiae* with Gold: Toxicity and Accumulation, BioMetals, 12, 289–294.

115. Kuyucak, N., Volesky, B., (1986), In: Rao, U.V. (Ed.), Proceedings of the 10th International Precious Metals Institute Conference, Lake Tahoe, NV, 211–216.

116. Staker, W.L., Sandberg, R.G., (1987), Bureau Mines Report. Invest 9093, 1–9.

117. Mata, Y.N., Torres, E., Blázquez, M.L., Ballester, A., González, F., Mu˜noz, J.A., (2009), Gold (III) Biosorption and Bioreduction with the Brown Alga *Fucus Vesiculosus*, Journal of Hazardous Materials, 166, 612–618.

118. Ting, Y.P., Teo, W.K., Soh, C.Y., (1995), Gold Uptake by *Chlorella Vulgaris*, Journal of Applied Phycology 7, 97–100.

119. Kuyucak, N., Volesky, B., (1990), Biosorption of Algal Biomass, In: Volesky, B. (Ed.), Biosorption of Heavy Metals, CRC Press, Boca ratonne.

120. Mullen, M.D., Wolf, D.C., Beveridge, T.J., Bailey, G.W., (1992), Sorption of Heavy Metals by the Soil Fungi *Aspergillus Niger and Mucor Rouxxi*, Soil Biology and Biochemistry 24, 129–135.

121. Townsley, C.C., Ross, I.S., (1986), Copper Uptake in *Aspergillus Niger* during Batch Growth and in Non-Growing Mycelial Suspension, Experimental Mycology 10, 281–288.

122. Pethkar, A.V., Kulkarni, S.K., Paknikar, K.M., (2001), Comparative Studies on Metal Biosorption by Two Strains of, Bioresource Technology 80, 211–215.

123. Khoo, K.H., Ting, Y.P., (2001), Biosorption of Gold by Immobilized Fungal Biomass, Biotechnology and Bioengineering Journal 8, 51–59.

124. Tsuruta, T. (2004), Biosrption and Recycling of Gold using Various Microorganisms, Journal of General and Applied Microbiology 50, 221–228.

125. Lin, Z., Wu, J., Xue, R., Yang, Y., (2005), Spectroscopic Characterization of Au_3 biosorption by Waste Biomass of *Saccharomyces Cerevisiae*, Spectrochimica Acta 61, 761–765.

126. Huiping, S., Xingang, L.I., Xiaohong, S., Jingsheng, S., Yanhong, W., Zenhua, W.U. (2007), Biosorption Equilibrium and Kinetics of Au(II1) and Cu(I1) on Magnetotactic Bacteria, Chinese Journal of Chemical Engineering 15 (6), 847–854.

127. Ishikawa, S.I., Suyama, K., Arihara, K., Itoh, M. (2002), Uptake and Recovery of Gold Ions from Electroplating Wastes Using Eggshell Membrane, Bioresource Technology 81, 201–206.

128. Gardea-Torresdey, J.L., Tiemann, K.J., Parsonsa, J.G., Gameza, G.I., Herrera, M., Jose-Yacaman, M. (2002), XAS Investigations into the Mechanism(S) of Au(III) Binding and Reduction by Alfalfa Biomass, Microchemical Journal 71, 193–204.

129. López, M.L., Parsons, J.G., Peralta Videa, J.R., Gardea-Torresdey, J.L. (2005), An XAS Study of the Binding and Reduction of Au(III) by Hop Biomass, Microchemical Journal 81, 50–56.

130. Parajuli, D., Kawakita, H., Inoue, K., Ohto, K., Kajiyama, K. (2007), Persimmon Peel Gel for the Selective Recovery of Gold, Hydrometallurgy 87, 133–139.

131. Chand, R., Wateri, T., Inoue, K., Kawakita, H., Luitel, H.N., Parajuli, D., Torikai, T., Yada, M. (2009), Selective Adsorption of Precious Metals from Hydrochloric Acid Solutions using Porous Carbon Prepared from Barley Straw and Rice Husk, Minerals Engineering 22, 1277–1282.

132. Arrascue, M.L., Garcia, H.M., Horna, O., Guibal, E. (2003), Gold Sorption on Chitosan Derivatives, Hydrometallurgy 71, 191–200.

133. Donia, A.M., Atia, A.A., Elwakeel, K.Z. (2007), Recovery of Gold (III) and Silver (I) on a Chemically Modified Chitosan with Magnetic Properties, Hydrometallurgy 87, 197–206.

134. Fujiwara, K., Ramesh, A., Maki, T., Hasegawa, H., Ueda, K. (2007), Adsorption of Platinum (IV), Palladium (II) and Gold (III) from Aqueous Solutions on l-lysine Modified Crosslinked Chitosan Resin, Journal of Hazardous Materials 146, 39–50.

135. Soleimani, M., Kaghazchi, T. (2008), Activated Hard Shell of *Apricot Stonnees*: A Promising Adsorbent, Chinese Journal of Chemical Engineering 16 (1), 112–118.

136. Tasdelen, C., Aktas, S., Acma, E., Guvenilir, Y. (2009), Gold Recovery from Dilute Gold Solutions Using DEAE-Cellulose, Hydrometallurgy 96, 253–257.

137. The Editors of Encyclopaedia Britannica, www.britannica.com/plant/cedar, accessed on April 04, 2018

138. http://indigeneousfoundations.arts.ubc.ca/cedar.pdf, accessed on September 24, 2018.

139. Shindo, T., Kudo, H., Kitabayashi, S. and Ozawa, S. (2004), Characterization of Pyrolyzed Cedar (Cryptomeria japonica D. Don) Bark using N_2 Adsorption and Diffuse Reflectance Infrared Fourier Transform Spectroscopy, Journal of Soc. Mater. Eng. Resour. Japan, 39 – 35.

140. Fourcade, F., Tzedakis, T. (2000), Study of the Mechanism of the Electrochemical Deposition of Silver from an Aqueous Silver Iodide Suspension, Journal of Electroanalytical Chemistry 493, 20 – 27.

141. Tao, Y. (2006), Adsorption and Electrochemical Activity: An In-Situ Electrochemical Scanning Tunneling Microscopy Study of Electrode Reactions and Potential-Induced Adsorption of Porphyrins, Journal of Physical Chemistry 110, 6141 – 6147.

142. Bard, A. J., Faulkner, L. R. (2000), Electrochemical Methods, Fundamentals and Applications, (2 Ed.), Wiley.

143. Nicholson, R. S., Irving, S. (1964), Theory of Stationary Electrode Polarography: Single Scan and Cyclic Methods Applied to Reversible, Irreversible, and Kinetic Systems, Analytical Chemistry, 36 (4), 706–723.

144. Heinze, J. (1984), Cyclic Voltammetry-"Electrochemical Spectroscopy": New Analytical Methods, Angewandte Chemie International Edition in the English, 23 (11), 831–847.

145. Cyclic voltammetry-wikipedia, en.wikipedia.org, accessed on October 23, 2018

146. Nicholson, R.S. (1965), Theory and Application of Cyclic Voltammetry for Measurement of Electrode Reaction Kinetics, Anal. Chem. 37 (11), 1351–355.

147. DuVall, S. D. V., McCreery, R. (1999), Control of Catechol and Hydroquinone Electron-Transfer Kinetics on Native and Modified Glassy Carbon Electrodes, Anal. Chem. 71 (20), 4594–4602.

148. Bond, A. M., Feldberg, S. (1998), Analysis of Simulated Reversible Cyclic Voltammetric Responses for a Charged Redox Species in the Absence of Added Electrolyte, J. Phys. Chem. 102 (49), 9966–9974.

149. www.academics.wellesley.edu/Appendix/experimental_error.html, accessed on November 13, 2018.

150. Romero-Gonz´alez, M. E., Williams, C. J., Gardiner, P. H. E. (2003), Spectroscopic Studies of the Biosorption of Gold (III) by Dealginated Seaweed Waste, Environmental Science and Technology 37 (18), 4163–4169.

151. Niu, H., Volesky, B. (1999), Characteristics of Gold Biosorption from Cyanide Solution, Journal of Chemical technology and Biotechnology 74, 778–784.

152. Cordery, J., Will, A. J., Atkinson, K., Wills, B. A. (1994), Extraction and Recovery of Silver from Low Grade Liquirs Using Microalgae, Minerals Engineering 7 (8), 1003–1015.

153. Kuyucak, N., Volesky, B. (1988), Biosorbents for Recovery of Metals from Industrial Solutions, Biotechnology Letters 10 (2), 137–142.

154. Darnall, D. W., Greene, B., Henzl, M. T. (1986), Selective Recovery of Gold and Other Metal Ions from An Algal Biomass, Environmental Science and Technology 20 (2), 206–208.

155. Savvaidis, K. (1998), Recovery of Gold from Thiourea Solutions Using Microorganisms, BioMetals 11, 145–151.

156. Pethkar, A. V., Paknikar, K. M. (1998), Recovery of Gold from Solutions Using *Cladosporium Cladosporioides* Biomass Beads, Journal of Biotechnology 63, 121–136.

157. Atia, A. (2005), Adsorption of Silver (I) and Gold (III) on Resins Derived from Bisthiourea and Application to Retrieval of Silver Ions from Processed Photo Films, Hydrometallurgy 80, 98–106.

158. Ogata, T., Nakano, Y. (2005), Mechanisms of Gold Recovery from Aqueous Solutions using A Novel Tannin Gel Adsorbent Synthesized from Natural Condensed Tannin, Water Research 39, 4281– 4286.

159. Ishikawa, S. I., Suyama, K., Arihara, K., Itoh, M. (2002), Uptake and Recovery of Gold Ions from Electroplating Wastes Using Eggshell Membrane, Bioresource Technology 81, 201–206.

160. Kissinger, P., William, R. H. (1996), Laboratory Techniques in Electroanalytical Chemistry, Second Edition, Revised and Expanded, *CRC.*

161. Zoski, C. G. (2007), Handbook of Electrochemistry, Elsevier Science

162. Feng, J., Gao, Q., LV, X., Epstein, I. R. (2008), Dynamic Complexity in the Electrochemical Oxidation of Thiourea, Journal of Physical Chemistry, 112, 6578 – 6585.

163. Ye, T., He, Y., Bourguet, E. (2006), Adsorption and Electrochemical Activity: An In-Situ Electrochemical Scanning Tunneling Microscopy Study of Electrode Reactions and Potential-Induced Adsorption of Porphyrins, Journal of physical chemistry, 110, 6141 – 6147.

164. Khunathai, K., Matsueda, M., Biswas, B. K., Kawakita, H., Ohto, K., Harada, H., Inoue, K., Funaoka, M., Alam, S. (2011), Adsorption Behavior of Lignophenol Compounds and their Dimethylamine Derivatives Prepared from Rice and Wheat Straws for Precious Metal Ion, Journal of Chemical Engineering of Japan 44 (10), 781 – 787.

165. Kim, Y.H., Nakano, Y. (2005), Adsorption Mechanism of Palladium by Redox within Condensed-Tannin Gel, Water Research 39 (7), 1324–1330.

166. Gurung, M., Adhikari, B. B., Kawkita, H., Ohto, K Inoue, K. and Alam, S. (2011), Recovery of Au(III) by Low Cost Adsorbent Prepared from Persimmon Tannin Extract, Chem. Eng. J. 174, 556 – 563.

167. https://www.quora.com/How-does-acid-evapourate-so-quickly, accessed on May 08, 2018

168. Torget, R., Himmel, M. E. and Grohmann, K. (1991), Dilute Sulfuric Acid Pre-treatment of Hardwood Bark, Biores. Tech. 35 (3), 239 – 246.

169. Sun, Y. and Cheng, J. (2002), Hydrolysis of Lignocellulosic Materials for Ethanol Production: A Review, Bioresource Technology 83, 1–11.

170. Parajuli, D., Kawakita, H., Inoue, K. and Funaoka, M. (2006), Recovery of Gold (III), Palladium (II), and Platinum (IV) by Aminated Lignin Derivatives, Ind. Eng. Chem. Res. 45, 6405 – 6412.

171. Ho, Y. S. and Mckay, G. (1998), The Sorption of Dye from Aqueous Solution by Peat, Chemical Engineering Journal 70, 115 – 124.

172. Ho, Y. S. and Mckay, G. (1999), Pseudo-Second order Model for Sorption Processes, Process Biochem. 34, 455 – 460.

APPENDIX A

CALIBRATION OF THE POTENTIOSTAT/GALVANOSTAT INSTRUMENT

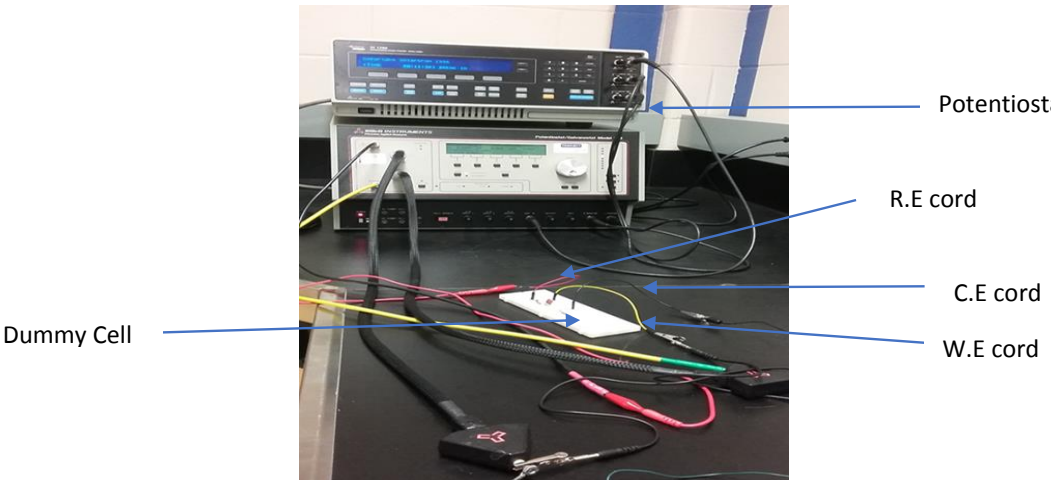

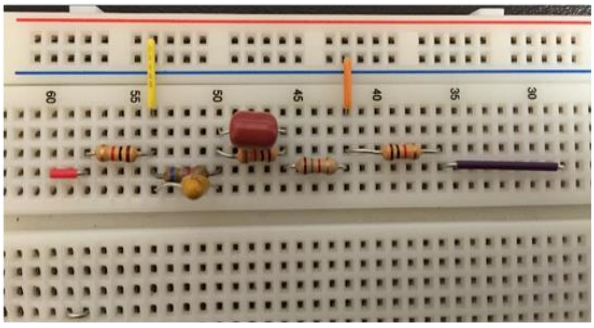

Dummy Cell

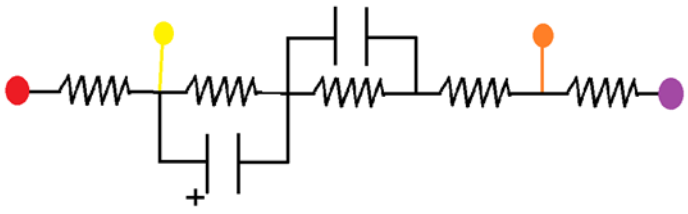

A dummy cell schematic

Picture showing the set up for the calibration of Potentiostat used for the CV measurement

APPENDIX B

CYCLIC VOLTAMMETRY (CV) INSTRUMENTAL SET UP

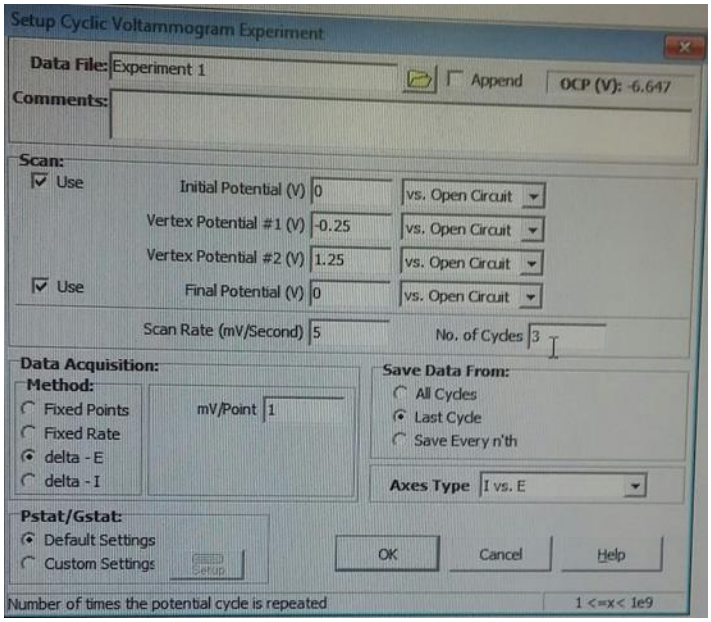

Experimental set up showing various parameter for CV measurement

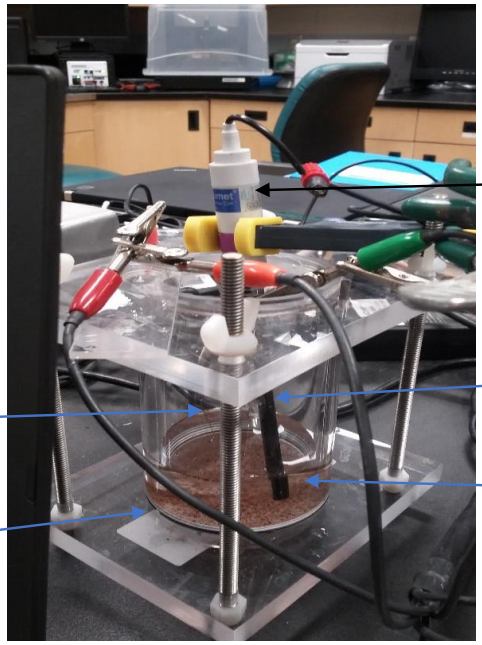

Experimental set up before adsorption with all electrodes in place

APPENDIX C

THE CEDAR WOOD BARK BIOADSORBENTS PREPARED UNDER VARIOUS EXPERIMENTAL CONDITIONS

D-AD

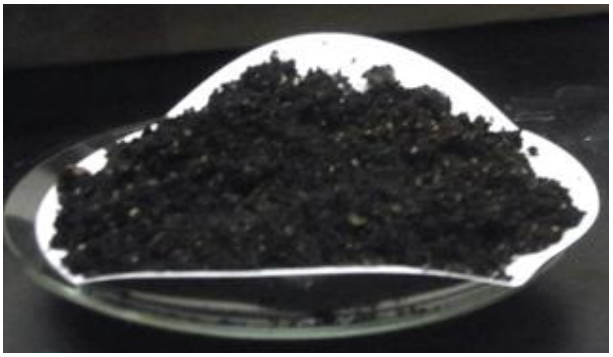

CNW-OD

CW-AD

APPENDIX D

THE ADSORPTION PROCESS USING SHAKER

Picture of arranged flasks containing samples of gold solution and bioadsorbent in a shaker

APPENDIX E

SOME SELECTED RELEVANT RAW DATA FOR THE RESEARCH

Kinetics experimental result at various temperature

SRC Geoanalytical Laboratories
125 - 15 Innovation Blvd., Saskatoon,
Saskatchewan, S7N 2X8
Tel: (306) 933-8118 Fax: (306) 933-8118 Email:
geolab@src.sk.ca

University of Saskatchewan
Attention: Dr. Shafiq Alam
Dispatch:
PO #/Project:
Samples: 14

Group #	Description	Date	Sample Type	Au Fire Assay Ppb
G-2017-2303	K1	11-16-2017	Liquid	96300
G-2017-2303	K2	11-16-2017	Liquid	81100
G-2017-2303	K3	11-16-2017	Liquid	40800
G-2017-2303	K4	11-16-2017	Liquid	27700
G-2017-2303	KE1	11-16-2017	Liquid	42800
G-2017-2303	KE2	11-16-2017	Liquid	30400
G-2017-2303	KE3	11-16-2017	Liquid	22600
G-2017-2303	KE4	11-16-2017	Liquid	1190
G-2017-2303	KM1	11-16-2017	Liquid	70800
G-2017-2303	KM2	11-16-2017	Liquid	57700
G-2017-2303	KM3	11-16-	Liquid	34200

		2017		
G-2017-2303	KM4	11-16-2017	Liquid	32800
G-2017-2303	KM4a	11-16-2017	Liquid	1070
G-2017-2303	KM4a R	11-16-2017	Repeat	1050

Result of one-point adsorption for sodium thiosulfate and S/L ratio

SRC Geoanalytical Laboratories
125 - 15 Innovation Blvd., Saskatoon,
Saskatchewan, S7N 2X8
Tel: (306) 933-8118 Fax: (306) 933-8118 Email:
geolab@src.sk.ca

University of Saskatchewan
Attention: Dr. Shafiq Alam
Dispatch:
PO #/Project:
Samples: 16

Group #	Description	Date	Sample Type	Au Fire Assay Ppb
G-2017-2143	ES 1AA	10-26-2017	Liquid	82800
G-2017-2143	ES 2AA	10-26-2017	Liquid	95000
G-2017-2143	ES 1BB	10-26-2017	Liquid	97000
G-2017-2143	ES 2BB	10-26-2017	Liquid	87700
G-2017-2143	ES 1CC	10-26-2017	Liquid	99400
G-2017-2143	ES 2CC	10-26-2017	Liquid	90100
G-2017-2143	ES 1DD	10-26-2017	Liquid	97200
G-2017-2143	ES 2DD	10-26-2017	Liquid	96600
G-2017-2143	ES 2-1	10-26-2017	Liquid	101000
G-2017-2143	ES 2-2	10-26-2017	Liquid	101000
G-2017-2143	TX 1A	10-26-2017	Liquid	27700
G-2017-2143	TX 1B	10-26-2017	Liquid	27400

G-2017-2143	TX 1C	10-26-2017	Liquid	13600
G-2017-2143	TX 2C	10-26-2017	Liquid	2030
G-2017-2143	TX 1D	10-26-2017	Liquid	6280
G-2017-2143	TX 1D R	10-26-2017	Repeat	6030

Isotherm experimental result

SRC Geoanalytical Laboratories
125 - 15 Innovation Blvd., Saskatoon,
Saskatchewan, S7N 2X8
Tel: (306) 933-8118 Fax: (306) 933-8118 Email:
geolab@src.sk.ca

University of Saskatchewan
Attention: Dr. Shafiq Alam
Dispatch:
PO #/Project:
Samples: 11

Group #	Description	Date	Sample Type	Au Fire Assay Ppb
G-2017-2488	IS11	12-20-2017	Liquid	60900
G-2017-2488	IS21	12-20-2017	Liquid	8050
G-2017-2488	IS31	12-20-2017	Liquid	48800
G-2017-2488	IS41	12-20-2017	Liquid	24700
G-2017-2488	IS51	12-20-2017	Liquid	29300
G-2017-2488	S1	12-20-2017	Liquid	225000
G-2017-2488	S2	12-20-2017	Liquid	157000
G-2017-2488	S3	12-20-2017	Liquid	332000
G-2017-2488	S4	12-20-2017	Liquid	211000
G-2017-2488	S5	12-20-2017	Liquid	359000
G-2017-2488	S5 R	12-20-2017	Repeat	357000

One point adsorption experimental result (Sodium thiourea)

SRC Geoanalytical Laboratories
125 - 15 Innovation Blvd., Saskatoon,
Saskatchewan, S7N 2X8
Tel: (306) 933-8118 Fax: (306) 933-8118 Email:
geolab@src.sk.ca

University of Saskatchewan
Attention: Dr. Shafiq Alam
Dispatch:
PO #/Project:
Samples: 11

Group #	Description	Date	Sample Type	Au Fire Assay Ppb
G-2017-2200	TH1AA	11-16-2017	Liquid	42400
G-2017-2200	TH1BB	11-16-2017	Liquid	23700
G-2017-2200	TH1CC	11-16-2017	Liquid	42800
G-2017-2200	TH1DD	11-16-2017	Liquid	18800
G-2017-2200	TH2AA	11-16-2017	Liquid	24300
G-2017-2200	TH2BB	11-16-2017	Liquid	20600
G-2017-2200	TH2CC	11-16-2017	Liquid	23800
G-2017-2200	TH2DD	11-16-2017	Liquid	14100
G-2017-2200	TH2-1	11-16-2017	Liquid	114000
G-2017-2200	TH2-2	11-16-2017	Liquid	55600
G-2017-2200	TH2-2 R	11-16-2017	Repeat	55500

One-point adsorption experimental result (HCl)

SRC Geoanalytical Laboratories
125 - 15 Innovation Blvd., Saskatoon,
Saskatchewan, S7N 2X8
Tel: (306) 933-8118 Fax: (306) 933-8118 Email:
geolab@src.sk.ca

University of Saskatchewan
Attention: Dr. Shafiq Alam
Dispatch:
PO #/Project:
Samples: 7

Group #	Description	Date	Sample Type	Au Fire Assay Ppb
G-2017-2081	ET 2.1	10-17-2017	Liquid	61300
G-2017-2081	ET 2.2	10-17-2017	Liquid	105000
G-2017-2081	ET 2A	10-17-2017	Liquid	46
G-2017-2081	ET 2AA	10-17-2017	Liquid	<2
G-2017-2081	ET 2BB	10-17-2017	Liquid	8
G-2017-2081	ET 2CC	10-17-2017	Liquid	288
G-2017-2081	ET 2.2 R	10-17-2017	Repeat	106000

Results for adsorption Vs concentration of lixiviant (HCl)

SRC Geoanalytical Laboratories
125 - 15 Innovation Blvd., Saskatoon,
Saskatchewan, S7N 2X8
Tel: (306) 933-8118 Fax: (306) 933-8118 Email:
geolab@src.sk.ca

University of Saskatchewan
Attention: Dr. Shafiq Alam
Dispatch:
PO #/Project:
Samples: 17

Group #	Description	Date	Sample Type	Au Fire Assay Ppb
G-2017-2377	E0	11-27-2017	Liquid	<2
G-2017-2377	E1	11-27-2017	Liquid	310000
G-2017-2377	E1-1	11-27-2017	Liquid	525000
G-2017-2377	E2	11-27-2017	Liquid	210000
G-2017-2377	E2-1	11-27-2017	Liquid	399000
G-2017-2377	E3	11-27-2017	Liquid	254000
G-2017-2377	E3-1	11-27-2017	Liquid	414000
G-2017-2377	E4	11-27-2017	Liquid	170000
G-2017-2377	E4-1	11-27-2017	Liquid	264000
G-2017-2377	E5	11-27-2017	Liquid	146000
G-2017-2377	E5-1	11-27-2017	Liquid	205000
G-2017-2377	IS1	11-27-2017	Liquid	421000

G-2017-2377	IS2	11-27-2017	Liquid	988000
G-2017-2377	IS3	11-27-2017	Liquid	323700
G-2017-2377	IS4	11-27-2017	Liquid	298700
G-2017-2377	IS5	11-27-2017	Liquid	444000
G-2017-2377	IS5 R	11-27-2017	Repeat	447000

Result of Kinetics and adsorption experiments using activated carbon

SRC Geoanalytical Laboratories
125 - 15 Innovation Blvd., Saskatoon,
Saskatchewan, S7N 2X8
Tel: (306) 933-8118 Fax: (306) 933-8118 Email:
geolab@src.sk.ca

University of Saskatchewan
Attention: Dr. Shafiq Alam
Dispatch:
PO #/Project:
Samples: 6

Group #	Description	Date	Sample Type	Au Fire Assay Ppb
G-2017-2419	AC1	12-04-2017	Liquid	34800
G-2017-2419	AC2	12-04-2017	Liquid	850
G-2017-2419	AC4	12-04-2017	Liquid	1700
G-2017-2419	CA	12-04-2017	Liquid	230
G-2017-2419	Pb	12-04-2017	Liquid	84
G-2017-2419	Pb R	12-04-2017	Repeat	76